MASTERARBEIT / MASTER'S THESIS

Titel der Masterarbeit / Title of the Master's Thesis

„Investigation of the influence of CD28- and CD43 costimulation on labile iron levels and microtubule polymerization in T cells"

verfasst von / submitted by

Florian Metz, BSc

angestrebter akademischer Grad / in partial fulfilment of the requirements for the degree of

Master of Science (MSc)

Wien, 2022 / Vienna, 2022

Studienkennzahl lt. Studienblatt / degree programme code as it appears on the student record sheet:	UA 066 830
Studienrichtung lt. Studienblatt / degree programme as it appears on the student record sheet:	Molecular Microbiology, Microbial Ecology and Immunobiology (Master)
Betreut von / Supervisor:	Ao.Univ.-Prof. Dr. Johannes Stöckl
Mitbetreut von / Co-Supervisor:	

Acknowledgment

I would like to thank everyone who supported me and provided me with help during the time of my thesis.

First and foremost, my gratitude goes to my supervisor Professor Johannes Stöckl, who gave me the possibility to work on this exciting project in his amazing research team and kept inspiring as well as mentoring me throughout this time.

Furthermore, I specifically want to thank Sarojinidevi Künig who made the introduction into the institute of immunology so much easier and who taught me many techniques in the lab and was always there when I needed something.

A special thanks to Pia Fritz for the great help in planning of my experiments and for the countless advices she conveyed to me.

Thank you too Claus Wenhard for the numerous FACS measurements and Petra Waidhofer-Söllner for providing me with reagents.

I also want to thank the head of the institute, Professor Wilfried Ellmeier for the chance of being part of the department.

Finally, I want to thank my Parents for always believing in me and for their unconditional support.

Abstract

Iron is crucial for numerous physiological processes in eukaryotes. The majority of iron is stably associated with enzymes, transport and storage proteins. A small fraction however is loosely bound to different low-molecular weight molecules. This so-called labile iron pool (LIP) serves multiple functions, including the appropriation of iron for incorporation into proteins involved in DNA replication. Using a calcein based method, labile iron was quantified in peripheral blood (PB) T cells and the permanent cell line Jurkat, stimulated via different activation pathways. We found elevated LIP levels in PB T cells stimulated via CD3 and via CD3 plus the costimulatory receptor CD43, compared to resting T cells. Previously, iron was hypothesized to be needed for a properly functioning microtubule cytoskeleton. To assess the effect of signal 1-stimulation and costimulation via CD28 or CD43 on microtubules of T cells, binding of anti-tubulin monoclonal antibodies (mAbs) to microtubules/tubulin was analyzed. Additionally, the effect of microtubule-stabilization on this association was evaluated. In PB T cells microtubule/tubulin binding was elevated upon CD28 costimulation and microtubule-stabilization, compared to resting cells. Furthermore, CD28 costimulation led to increased binding of the anti-tubulin mAbs upon microtubule-stabilization, compared to untreated cells. This indicates that mAbs interact better with tubulin in the polymerized form and that CD28 costimulation increases microtubule polymerization compared to the other conditions. Taken together, the results of this thesis indicate that increased LIP levels in activated T cells are not associated with enhanced tubulin polymerization and elongation.

Zusammenfassung

Eisen ist wichtig für zahlreiche physiologische Prozesse in Eukaryoten. Die Mehrheit des Eisens ist solide an Enzyme, Transport- und Speicherproteine gebunden. Ein Bruchteil ist jedoch lose mit verschiedenen niedermolekularen Molekülen assoziiert. Dieser sogenannte labile Eisen Pool (LIP) erfüllt vielzählige Funktionen, beispielsweise die Bereitstellung von Eisen für den Einbau in, für die DNA-Replikation benötigte Proteine. Hier wurde labiles Eisen durch eine auf Calcein basierende Methode in T-Zellen des peripheren Blutes (PB) sowie der permanenten Zelllinie Jurkat, die durch unterschiedliche Aktivierungspathways stimuliert wurden, quantifiziert. In CD3-stimulierten sowie in CD3- und dem costimulatorischen Rezeptor CD43 stimulierten PB T-Zellen wurden im Vergleich zu unstimulierten T-Zellen erhöhte LIP Spiegel beobachtet.

In vergangenen Jahren wurde spekuliert, dass Eisen für ein ordnungsgemäß funktionierendes Mikrotubuli-Zytoskelett benötigt wird. Um Auswirkungen von T-Zell Aktivierung via Signal 1-Stimulierung und Costimulierung durch CD28 oder CD43 auf Mikrotubuli zu analysieren, wurde die Bindung Tubulin-spezifischer monoklonaler Antikörper (mAbs) an Mikrotubuli/Tubulin quantifiziert. Zusätzlich wurde der Effekt von Mikrotubuli-Stabilisierung auf diese Bindung untersucht. Verglichen zu unstimulierten Zellen war die Mikrotubuli/Tubulin Bindung in CD28 costimulierten und Mirkotubuli-stabilisierten PB T Zellen erhöht. CD28 Costimulierung führte ausserdem zu höherer anti-tubulin mAb Bindung in Mikrotubuli-stabilisierten in Vergleich zu nicht-stabilisierten Zellen. Dies deutet auf stärkere Interaktion der mAbs mit Tubulin in seiner polymerisierten Form- sowie auf angehobene Mirkotubuli Polymerisation nach CD28 Costimulierung, im Vergleich zu alternativen Aktivierungswegen, hin. Zusammenfassend deuten die Ergebnisse dieser These darauf hin, dass Anstiege im LIP Spiegel in aktivierten T Zellen nicht mit verstärkter Tubulin Polymerisation und Elongation assoziieren.

Table of contents

1. Introduction

1.1 T lymphocytes

1.1.1 T cell development from hematopoietic stem cells

T lymphocytes represent an important part of the adaptive immune system. They originate from hematopoietic stem cells in the bone marrow which develop into common lymphoid progenitors, and subsequently into Pro-B and Pro-T cells.[1] The latter migrate through post-capillary venules over the thymic medulla into the outer cortex of the thymus.[2] In the cortex, they undergo several developmental stages, in the course of which, genetic rearrangements of the T cell receptor (TCR) take place. During these steps, they do not show CD4 or CD8 co-receptor expression on the cell surface. In the end of these so-called double negative phases, however, the precursor cells express both of them (double-positive stage) and the TCR rearrangement is completed.[3]

The next step in development is characterized by the interaction of the double-positive T cell precursors with self-peptides presented in the context of major histocompatibility complexes (MHC) on the surface of cortical thymic epithelial cells. Only progenitor cells that connect to the peptide-MHC conjugate in a weak manner, survive and keep one of the two co-receptors. Inability to bind, as well as firm binding results in clonal deletion of the cells in the cortex. Depending on whether their TCR binds to the self-peptide in the context of MHC class I or II complexes, they express CD8 or CD4, respectively.

The positively selected single-positive cells relocate into the medulla of the thymus where they are subject to further selection.[1,3]

In this negative selection process, they are exposed to self-antigens presented by medullary thymic epithelial cells and dendritic cells (DC). Developing T cells whose TCRs interact with those antigens with high affinity, usually undergo apoptotic cell death.[3,4] Thus, this process removes self-reactive T cells which may otherwise have posed damaging effects on the organism.[1] In some cases, on the other hand, high affinity interaction leads to the development of $CD4^+CD25^+$ regulatory T cells from precursor cells.[5]

The surviving, non-self-reactive T lymphocytes develop into mature cells of either the α/β or the γ/δ T cell lineages which differ in the expression of their TCR chains. Subsequently, they leave the thymus and enter blood circulation, from where they migrate into secondary lymphoid organs, such as lymph nodes and the spleen, or into the bone marrow (Figure 1).[1]
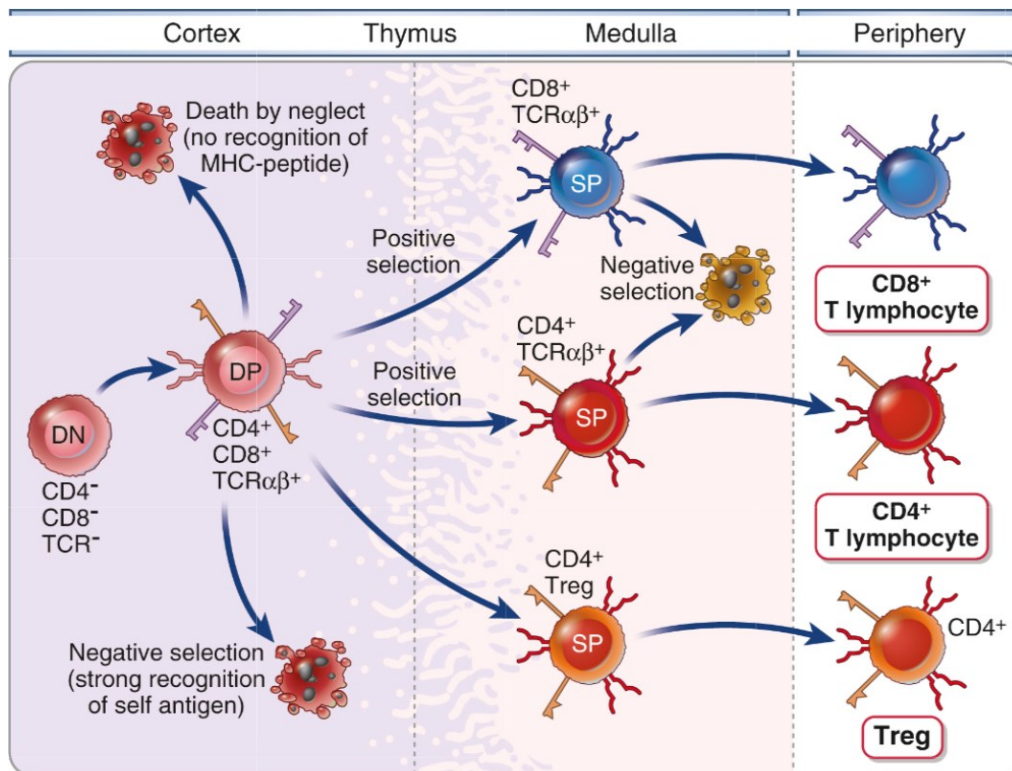
Figure 1. Maturation of hematopoietic progenitor cells into T lymphocytes in the thymus

Bone marrow derived T cell progenitors migrate into the thymus gland. Upon arrival, they lack a TCR, as well as CD4 and CD8 coreceptors, which is why they are described as double negative (DN) cells. However, once in the thymic cortex, they start expressing TCRs and both coreceptors, hence the designation double positive (DP). To sort out self-reactive and non-reactive cells, which bind presented self-antigens with high affinity or do not recognize them, respectively, DP T cells undergo positive selection in the cortex. Cells binding the peptide-MHC conjugate weakly, survive and remain expressing either the CD4 or the CD8 co-receptor. These single positive (SP) cells travel to the thymic medulla where they encounter self-antigens and are deleted or alternatively develop into regulatory T cells upon strong interaction with them. In the medulla, non-self-reactive cells differentiate into mature T lymphocytes which are released into the blood stream. (Abbas AK et al. 2017. *Philadelphia: Saunders Elsevier*. p.201)[1]

1.1.2 α/β T lymphocytes

α/β T cells comprise CD4^{+} helper T lymphocytes, CD8^{+} cytotoxic T lymphocytes (CTL), Regulatory T cells, Natural Killer T cells and Mucosa-associated invariant T cells. These different cell-classes have a wide variety of properties and functions.[1]

1.1.3 CD4+ helper T lymphocytes

The various subsets of helper T cells chiefly function through secretion of cytokines that affect several other cells. They can activate Macrophages, leading them to kill phagocytosed microbes; Attract other leukocytes like neutrophils and monocytes to the site of infection by microbes, leading to inflammation; And contribute to B cell activation, triggering their proliferation and differentiation into antibody producing plasma cells, affinity matured B cells or memory B cells. In addition, they can secrete cytokines that stimulate the proliferation of naïve CD8^{+} T cells and their differentiation into mature CTL and memory CD8^{+} T cells.[1,6]

1.1.4 CD4+ CD25+ regulatory T lymphocytes

The main role of CD4^{+} CD25^{+} regulatory T cells (CD25 being the α chain of the interleukin-2 (IL-2) receptor which is strongly expressed on their surface) is suppression of peripheral effector T cell activation and their effector functions.[1,7] In that way, they participate in the regulation of immune responses and contribute to the sustainability of self-tolerance and prevention of autoimmune diseases.[1]

1.1.5 CD8+ cytotoxic T lymphocytes

CD8+ CTL are able to detect and kill tumor cells and cells infected with intracellular microbes like viruses. Antigen presentation by infected target cells to CTL leads to their activation. This results in the release of the proteins perforin and granzyme from secretory lysosomes, called granules, into the immunological synapse. They enter the cytosol of the target cell and activate caspases, leading to cell death by apoptosis.[1,8] Alternatively, caspase-dependent apoptosis of a target cell can be induced by binding of Fas ligand, a membrane protein expressed on activated CTL, to the death receptor Fas, expressed on the surface of the target cell.[9] Additionally, they can secrete cytokines (mostly interferon-γ (IFN- γ)) that activate phagocytes like macrophages.[1]

1.2 T cell activation

Naïve (not yet having responded to an antigen) T cells get activated through the interaction of their TCR with its cognate antigen presented by antigen presenting cells (APCs) like DC in the context of MHC I or II. This is known as signal 1 of T cell activation. However, for successful activation, additional interactions of T cell surface proteins with their ligands on APCs are required.[1] These include signals by costimulators like CD28 (signal 2 of T cell activation); Adhesion molecules like LFA-1 (leukocyte function-associated antigen 1), which are necessary for stabilization of the immunological synapse formed between T cells with

APCs; And coreceptors like CD4 and CD8, which contribute to signal 1.[1,10]

This activation leads to proliferation, the production of cytokines and differentiation into effector and memory T cells.[1]

1.2.1 T cell receptor complex

1.2.2 CD3 and the ζ chain

The α/β TCR exists in a complex together with CD3 proteins and a ζ chain which are associated non-covalently with the receptor. Both of them are invariant, meaning they do not differ between T cells with varying antigen specificity. CD3 proteins are consisting of one εγ- and one εδ heterodimer of polypeptide chains and the ζ chain of a ζ ζ homodimer. All of these polypeptide chains contain ectodomains, transmembrane (TM) domains and intracellular domains. Each of the N-terminal ectodomains of the γ, δ and ε chains contains one Immunoglobulin (Ig)-like domain, side-by-side paired with the aforementioned partner of the heterodimers.[1,11] The transmembrane domains of all the chains are thought to adopt an α helical conformation.[11] They comprise a negatively charged aspartic acid residue which contributes to the interaction with the TM domains of the α and β TCR chains, in binding electrostatically to their positively charged residues.[1]

The intracellular domains of the γ, δ and ε chains contain each one intracellular Immunoreceptor tyrosine-based activation motif (ITAM), whereas the ones of the ζ chains hold three of them. This motif connects the TCR to its intracellular signal transduction machinery (Figure 2).[12]
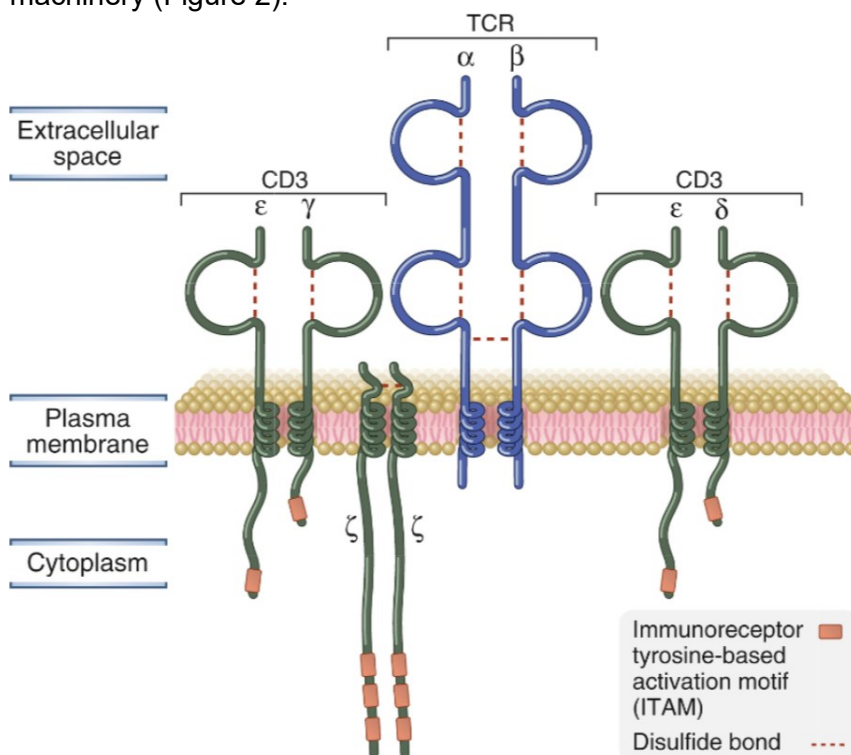

Figure 2. T cell receptor, CD3 and the ζ chain with their ITAM motifs
The α/β TCR complex comprises the receptor itself, consisting of its α and β chains, the heterodimeric CD3 proteins made up from the ε,γ and δ chains and the homodimeric ζ chain. CD3 and ζ chain are non-covalently bound to the TCR. CD3 proteins

10

contain one ITAM motif per chain, whereas each ζ chain contains three. (Abbas AK et al. 2017. *Philadelphia: Saunders Elsevier*. p.154)[1]

1.2.3 CD3 specific monoclonal antibodies OKT3 and VIT3

OKT3 is an IgG2a monoclonal antibody of murine origin, targeting the ε chain of CD3.[13] In vitro, it can stimulate T cells to enter the cell cycle and proliferate when immobilized on polystyrene plate surfaces. However, this seems mainly possible in the presence of costimulatory signals, like provided by an anti-CD28 monoclonal antibody.[14]

In vivo, OKT3 shows immune-blocking effects by lowering the expression of CD3/TCR molecules on the surface of T cells.[15,16] This makes it effective in the treatment of allograft rejections.[17]

Another anti CD3 monoclonal antibody of murine origin, also detecting the ε chain, is VIT3. It is of the IgM isotype and, according to Holter et al., does not induce T cell proliferation on its own. Upon addition of the phorbol ester 12-0-tetradecanoylphorbol-13-acetate however, it becomes an inducer of proliferation.[18]

1.2.4 CD28

CD28 is a homodimeric protein spanning the plasma membrane of T cells.[19] The extracellular region of each subunit contains a variable immunoglobulin-like domain.[1,20] A MYPPPY motif (M: Methionine, Y: Tyrosine, P: Proline) within this domain binds the costimulatory molecules CD80 (B7-1) and CD86 (B7-2) which are expressed on the surface of professional APCs, especially of activated ones which have recognized an antigen.[21] Like CD28, they also belong to the immunoglobulin superfamily.[19]

CD28 exerts an adhesive effect, enhancing the close contact between T cells and APCs.[22] The main underlying cause of this effect is thought to be the capability of CD28 to bring about rearrangements of the actin cytoskeleton which lead to stabilization of the T cell/APC conjugate and are required for signaling complexes to be recruited and organized.[23]

Thereby, CD28 signaling leads to an enhancement of signal 1-induced proliferation and differentiation of naïve T cells in a quantitative as well as a qualitative manner.[19,24]

In the presence of a TCR signal but a missing signal from CD28, naïve T cells fail to get activated and enter a state of hyporesponsiveness, called anergy. In this state, cell division, differentiation and the production of cytokines like IL-2 are hampered.[25]

1.2.5 CD4 and CD8 coreceptors

CD4 is a glycoprotein expressed on the surface of mature T helper cells.[26] It acts as a receptor for MHC class II molecules found on professional APCs like DCs and is specifically binding to their β2 domain.[1,27] CD8 on the other hand, is a surface glycoprotein expressed on

mature CTL.[26] In contrast to CD4, it is a receptor for the α3 domain of MHC class I molecules which are expressed on the surface of all nucleated cells.[28,1]

1.3 TCR signal transduction

Upon binding of the TCR to a peptide (antigen)-MHC complex, CD3 and the ζ chains are phosphorylated on their ITAMs by Lck kinases of the Src kinase family.[1] The amino acid sequence of ITAMs consists of two Tyr-X-X-Leu/Ile (Tyr: Tyrosine; X: any amino acid; Leu: Leucin and Ile: Isoleucin) repeats, separated by six to eight amino acids. Src family kinases can, upon TCR activation, phosphorylate these two tyrosine residues.[29] Lck kinases are associated with the coreceptors CD4 and CD8, which are, depending on the T cell class (CD4$^+$ T helper cells and CD8$^+$ CTL), brought into the vicinity of the TCR complex after antigen recognition.[1,30]
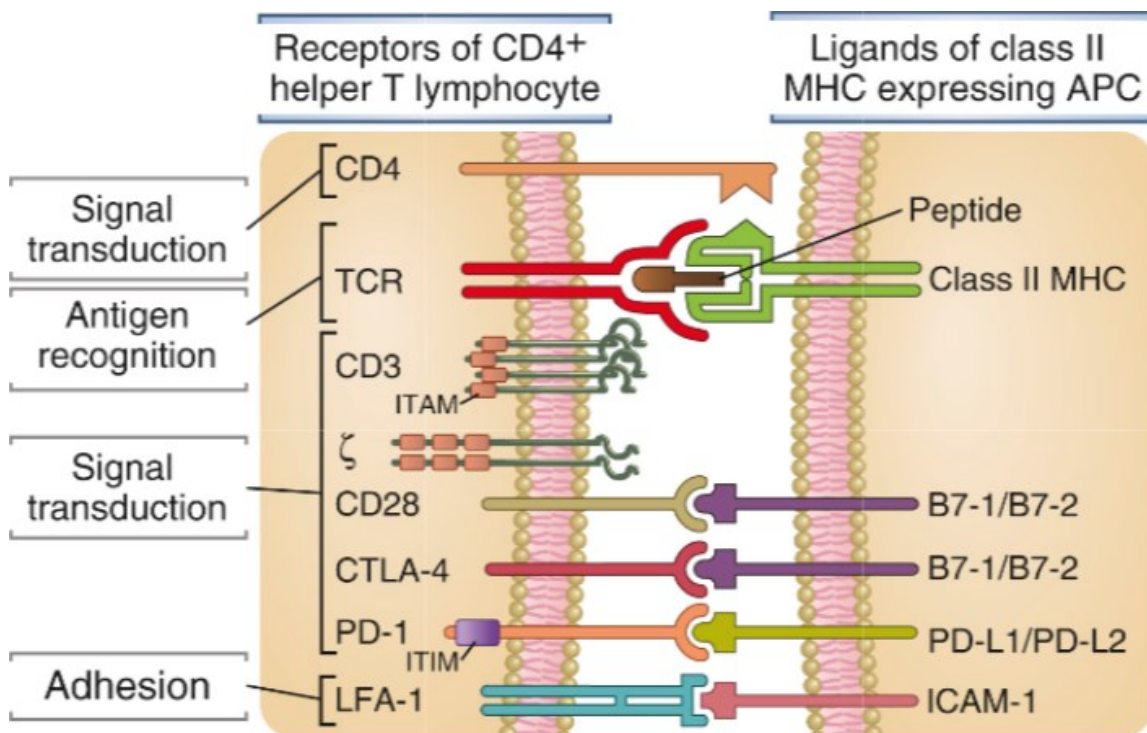
Figure 3. Receptors on T cell and their ligands on APCs

The left side depicts a CD4+ helper T lymphocyte with its receptors interacting with their dedicated ligands on APCs (on the right side) during T cell activation. The TCR recognizes and interacts with the peptide-MHC class II complex, with CD3 and the ζ chain transducing the signal. The latter two contain intracellular ITAMs which serve as binding sites for signaling molecules further down the line of the TCR signaling cascade. The CD4 coreceptor also associates with the MHC class II molecule and facilitates signaling. B7-1/B7-2 bind the CD28 costimulatory receptor on T cells to transmit signal 2 of TCR signaling. The interaction of LFA-1 on the T cell with ICAM-1 on the APC stabilizes the immunological synapse. Inhibitory receptors, such as CTLA-4 and PD-1 can attenuate signaling via their immunoreceptor tyrosine-based inhibitory receptors (ITIM). (Adapted from Abbas AK et al.

2017. *Philadelphia: Saunders Elsevier*. p.155)[1]

In case there is a TCR signal present and ligation of CD28 with CD80 or CD86 occurred, various molecules, including Lck kinases and the adapter protein growth-factor receptor bound protein-2 (Grb2), bind to multiple proline and tyrosine residues of the cytoplasmic region of CD28 and transmit activating signals.[31]

The phosphorylated ITAMs on the ζ chains are bound by the SH2 domains of the protein tyrosine kinase ZAP70, probably leading to its conformational rearrangement into a regulatory phosphorylation permitting protein. Such a phosphorylation event is mediated by Lck and results in the activation of ZAP70, which then itself phosphorylates tyrosine residues on several signaling proteins, including the adapter protein linker for the activation of T cells (LAT).[30] Phosphorylated LAT functions as a docking site for various other signaling molecules like phospholipase C γ1 (PLCγ1) and the adapter protein Grb-2, which serves as a binding site for the Ras activating guanine-nucleotide-exchange factor (GEF) SOS. SOS catalyzes the exchange of GDP for GTP on the small guanine nucleotide-binding protein Ras. Ras-GTP initiates the MAP kinase signaling cascade, eventually leading to the activation of the MAP kinase ERK by phosphorylation.[30,1] ERK, in turn, activates the transcriptional activator ELK which stimulates the expression of one of the two components of the activation protein 1 (AP-1) family of transcription factors (here referred to as AP-1), called c-Fos.[1]
The other component is c-Jun, which is activated by another MAP kinase termed c-Jun N-terminal kinase (JNK).[1]

Vav1 is a GEF, binding to the SRC homology-2-domain-containing leukocyte protein of 76 kDa (SLP76), which is also recruited to phosphorylated LAT and serves itself as an anchor for other signaling factors.[32] It converts GDP-bound Rac (another small guanine nucleotide-binding protein) to Rac-GTP, which functions in initiating a second MAP kinase pathway, eventually activating JNK.
Active AP-1 stimulates the expression of a multitude of genes, including such that are active during T cell proliferation, differentiation and apoptosis, like the *Interleukin-2* gene (promoting proliferation and differentiation into memory and effector T cells).[33,1]

After PLCγ1 is bound to LAT, it gets phosphorylated by ZAP70 and other kinases. This leads to its activation and the execution of its enzymatic function, the hydrolyzation of phosphatidylinositol 4,5-bisphosphate (PIP2), a phospholipid in the plasma membrane, into diacylglycerol (DAG) and inositol 1,4,5-triphosphate (IP3).[1]

The phospholipid DAG, often in combination with increased free intracellular calcium levels, activates the Protein kinase C (PKC) family of serine/threonine kinases, which contains multiple isoforms.[34,1] Together, these isoforms phosphorylate several targets, leading to various cellular responses. PKC-θ for instance functions as an activator of the nuclear factor κB (NF-κB), referring to a group of transcription factors representing major players in cytokine synthesis in response to antigen-stimulation of T cells (and many other cells types).[1]

IP3 binds to its receptor on the surface of the endoplasmic reticulum (ER), which acts as a Ca^{2+} channel. This interaction leads to Ca^{2+} release from the ER into the cytosol. The consequent decline in Ca^{2+} concentration in the ER is detected by the ER membrane protein STIM1, which, in response, triggers the opening of a plasma membrane Ca^{2+} channel called calcium release-activated calcium (CRAC) channel. Since this opening allows Ca^{2+} from the extracellular space to enter the cell, the result is a further increase of the cytosolic Ca^{2+} levels.[35,1] Binding to another Ca^{2+} sensor, called calmodulin, changes the sensors conformation which modulates its affinity for its binding partners and/or affects their effector functions.[36,37] One of those interaction partners is the protein serine/threonine phosphatase calcineurin which activates the nuclear factor of activated T cells (NFAT). NFAT is a transcription factor stimulating the expression of various genes encoding cytokines like IL-4, TNF and IL-2.[1]

Additionally, PIP2 is modified by the phosphoinositide 3-kinase (PI3K), which phosphorylates it on the 3' OH group of its inositol ring to produce phosphatidylinositol 3,4,5-trisphosphate (PIP3). PIP3 binds the pleckstrin homology (PH) domain of cytoplasmic proteins like the serine/threonine protein kinases 3-phosphoinositide-dependent protein kinase 1 (PDK1) and AKT. This interaction leads to a conformational change in AKT resulting in the reversal of the autoinhibited state of its activation loop.[38] That in turn allows PDK1 to phosphorylate the amino acid Threonine (T)308 in this loop and thereby activate AKT.[39] However, to get fully activated, it also has to be phosphorylated on Serine (S)473 by the mammalian/mechanistic target of rapamycin complex 2 (mTORC2). Active AKT phosphorylates a multitude of targets ultimately leading to regulation of cell survival, metabolism and proliferation.[40]

1.4 CD43

CD43 is another costimulatory receptor expressed on the surface of T cells. It has several different binding partners, including MHC-I and the intercellular adhesion molecule 1 (ICAM-1), which is expressed on APCs (also expressed on endothelial cells, T cells and B cells).[41,42,1] Its ligation with the CD43 specific mAbs 6E5 or 10G7 results in cord blood and peripheral blood T cell proliferation, in the case a TCR signal is also present. This is

independent of CD28 signaling.[43] CD43 is a transmembrane mucin consisting of a 123 amino acid long cytoplasmic C-terminal domain, a transmembrane domain of 23 amino acids and an extracellular N-terminal domain comprising 235 amino acids.[44,45] It is heavily O-glycosialylated and expresses two different types of O-glycans on T cells, being either unbranched core 1 or branched core 2 O-glycans. This leads to the existence of two CD43 isoforms with molecular weights of 115 kDa and 135 kDa, respectively.[44,46] Depending on the developmental stage T cells and their precursors are in, on their differentiation status and on whether they are activated, glycosylation varies. The 115 kDa variant is expressed on naïve peripheral T cells, immature CD4⁻CD8⁻ thymocytes and mature CD4 and CD8 single positive thymocytes. Expression of the heavier isoform, on the other hand, is found on activated T cells.[46,47]

CD43 co-stimulation was shown to regulate several target genes in a comparable way to co-stimulation by CD28, like for example the gene encoding the pro-inflammatory cytokine IL-1β. However, other genes, like the one coding for IL-2, are only very weakly expressed upon CD43 co-stimulation, whereas CD28 co-signaling leads to strong regulation of them. Another group of genes, including *uPAR* and *IL-8*, which contribute to modulation of cell motility and migration, was found to mainly be regulated by CD43.[48]

Interestingly, experiments in CD43 knockout (KO) mice revealed a suppressive role of the molecule for T cell activation, after showing enhanced proliferative responses of T cells in vitro, to several activating stimuli (including the anti-CD3 mAb 145-2C11), compared to T cells of wild-type (WT) mice.[49] Consistent with this observation, levels of antigen-specific CD8⁺ T cells in the contraction phase of the immune response to lymphocytic choriomeningitis virus infection, were shown to be elevated in CD43 KO mice compared to WT mice. This suggests CD43 to function as a negative regulator of immune responses in addition to its role in T cell activation.[50]

Like mentioned before, successful T cell activation requires stabilization of the T cell-APC conjugate. This can be achieved by adhesion via interaction between LFA-1 on T cells with ICAM-1 on APCs.[1] Additionally, T cell activation in vitro is characterized by homotypic aggregation of T cells which also interact via LFA-1 and ICAM-1.[51] Activation of CD43 via its ligation with mAbs, like 1.C1, DF-T1 MEM-59 (all binding the same or spatially proximal epitope of CD43), was shown to induce T lymphocyte clustering in an LFA-1 dependent or other adhesion receptor-dependent manner.[52] In CD43 deficient mice, on the other hand, increased T cell clustering was observed, speaking against the hypothesis that CD43 signaling enhances T cell clustering.[49]

The anti-CD43 mAbs 10G7 and 6E5 target both isoforms of human CD43. They bind different, non-overlapping epitopes on the receptor.[53]

In contrast to co-stimulation via a CD28 mAb or 6E5, 10G7 co-stimulation was not shown to enhance NFκB activation compared to CD3 stimulation alone. NFAT activation was observed to be induced by 10G7, but to a lesser extent than by 6E5 or CD28.

When looking at helper T cell cytokine production, 10G7 was found to induce IFN-γ and IL-22 in quantities comparable to CD3 alone but in lower amounts than 6E5 and CD28 mAb. Additionally, the amounts of IL-2, IL-13 and IL-4 were very low upon both, 10G7 and 6E5 co-stimulation, unlike with CD28 + CD3 stimulation.

Furthermore, the effect of CD43 co-stimulation on anti-inflammatory T cell cytokine amounts were observed. IL-10 was found to be induced by 10G7, but at lower levels than by CD28 mAb and 6E5. Interestingly, the expression of EBI3, a subunit of the inhibitory cytokine IL-35, was significantly higher upon 10G7 co-stimulation compared with the other two. Still, no inhibition of T cell proliferation was seen when supernatants of 10G7 co-stimulated PB T cells were tested for inhibitory effects in an allogeneic mixed leucocyte reaction (MLR). Contrary to T cells co-stimulated by 6E5 and CD28 mAb, 10G7 co-stimulated T cells responded only weakly with proliferation to re-stimulation with anti-CD3 mAb + 10G7, 6E5 or CD28.

In an allogeneic MLR, 10G7 co-stimulated and irradiated T cells were shown to inhibit T cell proliferation induced by DC. This effect seems to be mainly based on the formation of stable clusters of 10G7 co-stimulated T cells with DC via interaction of CD2 on T cells with CD58 on DC. Consequently, less DC are available to stimulate the allogeneic responder T cells.[43]

Many aspects of the TCR signaling pathway have been established in vitro in transformed T cell lines, like the immortalized human leukemic T cell line Jurkat.[54] This cell line was established from peripheral blood cells acquired at the time of the first relapse of a 14-year-old acute lymphoblastic leukemia patient.[55]

Besides signaling through the TCR together with CD3 and CD28, a plethora of molecules involved in the downstream transduction of their signal, were characterized using mutant subclones of this cell line. Those include IL-2 which plays a crucial role in T cell proliferation and differentiation, phosphatases including Calcineurin and kinases like Lck, PKC-θ and JNK.[56] For instance, some of the key components linking PLCγ to TCR signaling, like ZAP70, LAT and SLP-76, as well as the cytoplasmic transcription factors NFAT and NFκB and their T cell activation-dependent translocation into the nucleus in order to activate gene transcription, were identified in Jurkat cells.[56,38]

However, Jurkat cells have multiple gene expression defects. One of them results in the loss of the lipid phosphatase phosphatase and tensin homologue (PTEN). PTEN acts as a tumor suppressor whose main substrate for dephosphorylation is PIP_3. Thereby, it regulates the activation of the PI3K-AKT signaling pathway. In its absence, this pathway is constitutively active, even in the absence of TCR signals.[54,57] This may contribute to the uncontrolled proliferation and enhanced survival of Jurkat cells.[57] Due to this crucial signaling defect and its consequences, the reliability of this cell line as a model system for studying T cell biology became a subject of debate to many researchers.[54]

1.5 Microtubules

Microtubules represent an important component of the eukaryotic cytoskeleton which play a role in processes like cell division, motility, shape and intracellular transport.[58,59] They consist of repeating heterodimers of α- and β-tubulin molecules associating to form polar protofilaments. Upon lateral assembly of such protofilaments, hollow cylinders with a diameter of about 25 nm are formed.[59,60] Microtubules are highly dynamic structures which continually switch between periods of polymerization and depolymerization in a stochastic manner. This process is termed dynamic instability. It is based on the binding of GTP to both tubulin monomers and its hydrolysis to GDP.[61] The dimer encompasses two GTP-binding sites, the N (nonexchangeable)-site on α-tubulin, and the E (exchangeable)-site on β-tubulin.[60,62] Tubulin dimers are usually added to the so-called plus end of the microtubule which is capped by β-tubulin subunits. Only if the E site of the β-tubulin subunit at the cap is bound by GTP, polymerization of microtubules can occur.[60,61] During this process of growth, the α-tubulin subunit of the approaching dimer interacts with this GTP of the terminal β-tubulin subunit. This leads to hydrolysis of the GTP to GDP likely by the GTPase activity of tubulin itself.[63] Dynamic instability can be explained by the GTP cap model formulated by Mitchison and Kirschner, which states that GDP-tubulin in the body of the microtubule exhibits low stability while GTP-tubulin at the cap functions in stabilizing the structure.[58,61] A loss of the cap results in quick depolymerization of the microtubule.[58]

During cell division, microtubules represent a major component of the mitotic and meiotic spindles. Mammalian chromosomes contain monocentric kinetochores, meaning that kinetochore proteins, which are a target of microtubule binding, congregate at a single position on each chromosome. Accordingly, microtubules attach to one specific site on each chromosome. In contrast, other species like the nematode *Caenorhabditis elegans* have their kinetochores distributed across the whole surface of their chromosomes. This leads to the binding of microtubules along their entire length.[64,65]

Accordingly, spindle microtubules pull chromosomes / chromatids to the two poles at either a single point or their entire length in the course of the anaphase I of meiosis / anaphase of

mitosis, respectively.[65] This pull is achieved by depolymerization of the microtubules attached to the kinetochores, the movement of those kinetochore microtubules along other microtubules towards the poles via the microtubule-associated motor proteins dynein and kinesin, and the distancing of the poles from each other.

Prior to that, in the prometaphase / prometaphase I of mitosis / meiosis, chromosomes are moved to the equatorial plate by pushes conducted by polymerizing (on the plus end) microtubules and the action of motor proteins. In this case microtubules are not only pushing at the kinetochores.[66]

Microtubules are highly important for the intracellular transport of molecules, organelles and vesicles, since they organize their localization with the help of associated motor proteins, like dynein and kinesin. Those molecular motors can move along microtubules to transport their cargo (e.g. vesicles). Dynein is a microtubule-minus-end directed motor protein complex whereas the kinesin complex directs transport to the plus end of microtubules.[67]

Together with the actin cytoskeleton, microtubules play a major role in several aspects of T cell physiology, including their migration, interaction with APCs, activation of TCR signaling by antigen stimulation, formation of the immunological synapse and T cell activation together with their effector functions.[68]

During the migration of T cells to peripheral lymph nodes or inflamed tissues, the microtubule and actin cytoskeletons undergo coordinated rearrangements. Together with adhesion and the cell's interaction with the extracellular matrix and surrounding cells, this allows T cells to adopt modified cell shapes and motility. This, in turn enables them to migrate through different tissues or lymphoid organs where they can meet and interact with APCs or target cells.[68,67]

Binding of the cognate antigen on the encountered APC / target cell and concomitant TCR signaling results in microtubule reorganization leading to centrosome relocation toward the site of cell–cell contact.[68] The centrosome is the main microtubule organizing center in eukaryotic cells. It duplicates in the S phase of the cell cycle, so that during mitosis, the two sister centrosomes organize the correct arrangement of the spindle poles ensuring the bipolarity of the spindle. In the interphase, the centrosome participates in the control of cell adhesion, motility and polarity.[69]

In addition, strong polymerization of the actin cytoskeleton is triggered at the contact site. Accordingly, organelles like the endosomal compartment, lytic granules, mitochondria and the Golgi apparatus, which are associated with the centrosome, are directed to the contact site as well.[68]

Spreading of the T cell at the T cell – APC / target cell interface goes along with actin rearrangements, resulting in the accumulation of F(ilamentous)-actin at the periphery and the formation of a ring like structure. The central area of the contact site, on the other hand, is

almost cleared of F-actin.[32,68] Here, the microtubule-directed centrosome, together with its associated organelles, advance toward the contact site, where they release their cargo (e.g. the content of lytic granules or polarized cytokines) or rescue signaling molecules and membrane receptors.

Microtubule and actin reorganization and their orchestrated interaction also contribute to the movement of signaling microclusters within the cell-cell interface.[68] Those microclusters contain components of the TCR signaling pathway like TCR and LAT molecules assembled in separate domains already before TCR stimulation.[68,70] They congregate at the periphery of the synapse and are moved to the center upon TCR engagement, where they contribute to the formation of the immunological synapse.[71,68] This centripetal movement to the center is achieved by the interaction of microtubules with dynein motors, as well as by waves of actin polymerization. Microtubules are radially arranged from the centrosome to the periphery allowing dynein to transport microclusters along them towards the center.[72,68]

By coordinating the organization of the signaling machinery within the immunological synapse, microtubules and actin are fundamental in strengthening and maintaining TCR signaling. Contrary to this, they also play a role in the downregulation of TCR signals. Previously, upregulation of TCR signaling was observed when deceleration or impairment of the center-directed movement of microclusters was induced. This suggests regulation of TCR signal intensity by the dynamic location of the signaling microclusters.[68]

1.5.1 Taxanes

Taxanes are a class of antitumor drugs which bind microtubules with high affinity, leading to their stabilization and elongation by promotion of tubulin polymerization. In the case of spindle microtubules, this results in failure to pull chromatids to the poles of the mitotic spindle by depolymerization, ultimately causing inhibition of mitosis.

In addition, the effect of taxanes on microtubules brings about suppression of cell motility and intracellular transport. Together these implications on cells exposed to taxanes usually induce apoptotic cell death. This is utilized in adjuvant chemotherapeutic treatments of metastatic breast cancer and has also been shown to have potential in the treatment of further malignancies including ovarian cancer and non-small-cell lung cancer.[73,74]

Taxanes are highly hydrophobic, which is why lipid-based solvents are used as vehicles.

1.5.2 Paclitaxel

Paclitaxel, a widely used taxane, is usually solubilized using a non-ionic surfactant polyoxyethylated castor oil known as Cremophor EL® (CrEL), together with ethanol in a ratio of 50:50.[74]

Paclitaxel is naturally produced by endophytic fungi originally found in the pacific yew *Taxus brevifolia.* It also occurs in other members of the Taxaceae family and in a variety of other plants.[75]

It was shown to arrest cells in the late G2 or mitotic cell cycle phase, thereby inhibiting chromosome replication.

Testing different doses (0,04-4 µg/ml) of paclitaxel on the ovarian cancer cell line 1A9 showed elevated tubulin polymerization in a dose-dependent manner. This effect could not be observed in two paclitaxel-resistant sublines, derived from 1A9.[76]

Paclitaxel is a tricyclic diterpenoid compound containing a taxane ring, an oxetane ring and an ester side chain at C-13 which was shown to be required for antitumor activity.[77,78]

Paclitaxel binds to the so called taxoid site of β-tubulin, more specifically to a binding pocket in its second globular domain on the inner surface of the microtubule.[75,79] The binding pocket consists of the β-tubulin S9-S10 loop and segments of the H1, H6 and H7 helices and the S7 beta sheet.

The mechanism how paclitaxel reaches this luminal taxoid site is still not clear. As of now, the overall consensus agrees with the model proposed by Díaz and colleagues who suggested a two-step process where paclitaxel initially binds to the outside of the microtubule via the pore type I site, one of the two pore types described in microtubules.[79,80] In type I pores, β-tubulin is located at their lower fraction (when looking at the microtubule's plus-end oriented upwards) and the taxoid site near the pore.[81] In the second step the drug is detached from there quickly and subsequently enters the lumen of the microtubule where it associates with the taxoid binding site with slow kinetics.

In unassembled tubulin, on the other hand, paclitaxel is thought to bind either the type I pore site or the taxoid site.[80,79]

The resolution of the paclitaxel-β-tubulin conjugate structure is not high enough to determine the exact location of the interactions and the amino acids involved in it. However, several single amino acid mutations were detected in paclitaxel-resistant cells. Those include R284 (R=Arginine) and T276 (T=Threonine), which were shown to be significant for the binding. Further examples are A374 (A=Alanine), found in the S9-S10 loop and F272 (F=Phenylalanine), as part of the M-loop. Since both are components of the binding pocket, this suggests a contribution of them to conjugate formation. However, mutations not occurring in the binding site may also disturb the binding capability of paclitaxel since they could bring about allosteric or structural changes in β-tubulin.

Once paclitaxel is bound, its taxane ring is positioned on the N-terminal section of the M(icrotubule)-loop adjacent to the H7 core helix.[79,75]
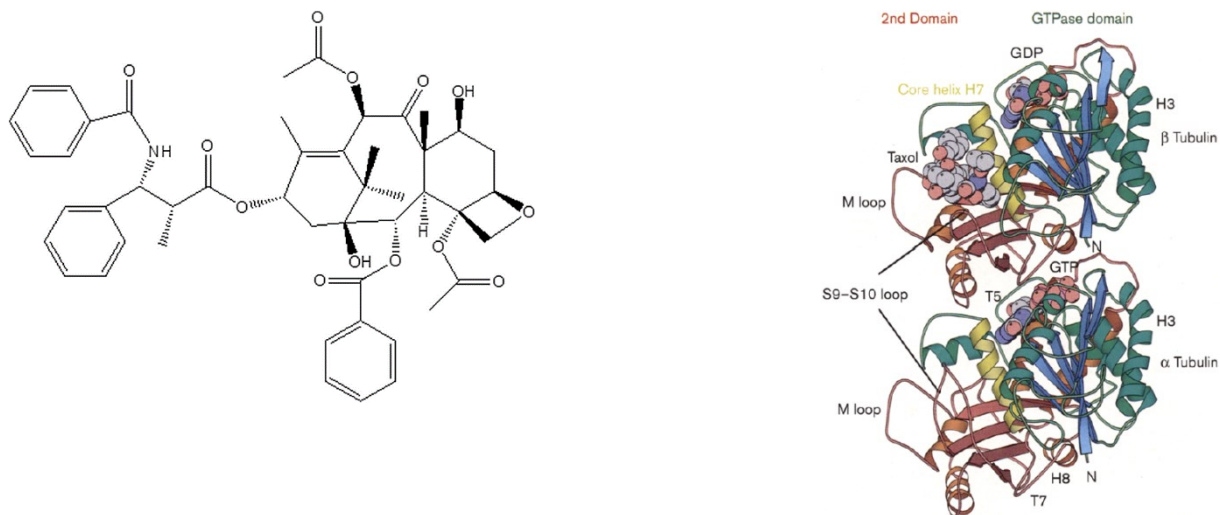
Figure 4. Structure of paclitaxel and its association with β tubulin

On the left-hand side, the structure of paclitaxel, a tricyclic diterpenoid comprising a taxane ring, an oxetane ring and an ester side chain at C-13, is depicted.[77], (Zhu L et al. 2019. *Cell Mol Biol Lett.*)[78] The right side of the figure shows a tubulin dimer with paclitaxel (=Taxol) bound to the β-subunit at the N-terminus of the M-loop, as predicted from electron crystallography.[79] (Amos LA et al. 1999. *Chem Biol.*)[75]

M-loops are crucial for the establishment of the contact between protofilaments. They interact with other M-loops on the surface of adjoining protofilaments, thereby contributing to the stabilization of microtubules. The association with paclitaxel drives the M-loop out, in the direction of neighboring protofilaments, thereby strengthening their interaction between each other and increasing microtubule stability.[79]

However, since CrEL infusion frequently leads to histamine release, hypersensitivity reactions, including anaphylaxis, are occurring regularly. CrEL also poses an efficiency-dampening effect on the treatment by restricting the penetration of tumors due to its tendency to form large polar micelles capturing paclitaxel and holding it in the plasma. This disturbs the ratio of dosage to antitumor activity of the drug, since its distribution is firstly, diminished and secondly, happening in an uneven manner. Indeed, the formation of micelles is enhanced by a concentration increase, which is why short infusion regimens with high doses of the drug result in the highest sequestration rate in the plasma. Therefore, the drug is usually administered via infusion over longer time periods.[74,82] On top of that, other cancer medications like anthracyclines can be manipulated by this effect as well when given concomitantly.[83]

Moreover, in vitro CrEL was shown to suppress endothelial transcytosis of paclitaxel, depicting another potential problem for the delivery of the drug.[82]

Even though the intensity of hypersensitivity reactions to CrEL-based paclitaxel could be decreased upon pre-administration of antihistamines such as diphenhydramine, steroids, like

the glucocorticoid dexamethasone, and H_2 receptor blockers such as cimetidine, complications and deaths in response to the drug were still reported. This led to the hunt for safer and more effective ways to deliver paclitaxel. [84,82]

1.5.3 Abraxane

Abraxane® is one of those advanced formulations, developed to circumvent these problems. In this drug, paclitaxel is packaged into human serum albumin-based nanoparticles with an average size of 130 nm, avoiding the necessity of mixing it with lipid-based solvent.[84,85] Albumin is often used as a vehicle for cancer drugs, since it helps in caveolar transcytosis of hydrophobic molecules, such as paclitaxel, through endothelial cells, which is conveyed by the gp60 albumin receptor.[85,82] Upon binding of the receptor, caveolin-1, one of the three main structural components of so called caveolae in mammalian cells, is activated. This in turn, triggers the formation of caveolae, 60-80 nm wide plasma membrane pits involved in the transport of various molecules, including albumin, across endothelial cells to the interstitial space.[84,86]

Since the nanoparticle size of about 130 nm is stabilized by the conjugation to albumin, the risk of capillary blockage is abolished.[84]

In contrast to CrEL-based paclitaxel, the pharmacokinetics of abraxane are linear and consistent, with high predictability. The reason for this probably is the absence of polyoxyethylated castor-oil.[82]

On top of the lower risk profile, abraxane administration was also shown to lead to a higher overall response rate (33%) and longer time to tumor progression (23 weeks) in an international randomized phase III trial with 454 participants with metastatic breast cancer, compared to of CrEL-based paclitaxel (19% and 16,9 weeks, respectively). The paclitaxel concentration in the abraxane-group was 48,6% higher, which was expected not to be more toxic than the standard dose of paclitaxel.[87]

In preclinical studies, higher concentrations of paclitaxel were reported within tumors when abraxane was administered as opposed to polyoxyethylated castor oil-based paclitaxel.[82,74] A possible explanation for this could be the accumulation of albumin in some tumors which is thought to be caused by the binding of albumin to secreted protein acid rich in cysteine (SPARC), which is expressed in many tumors. This association can be explained by a sequence homology of SPARC with gp60.[82] This observation, together with the increased paclitaxel dose used in abraxane, could explain its higher antitumor activity. [82,74]
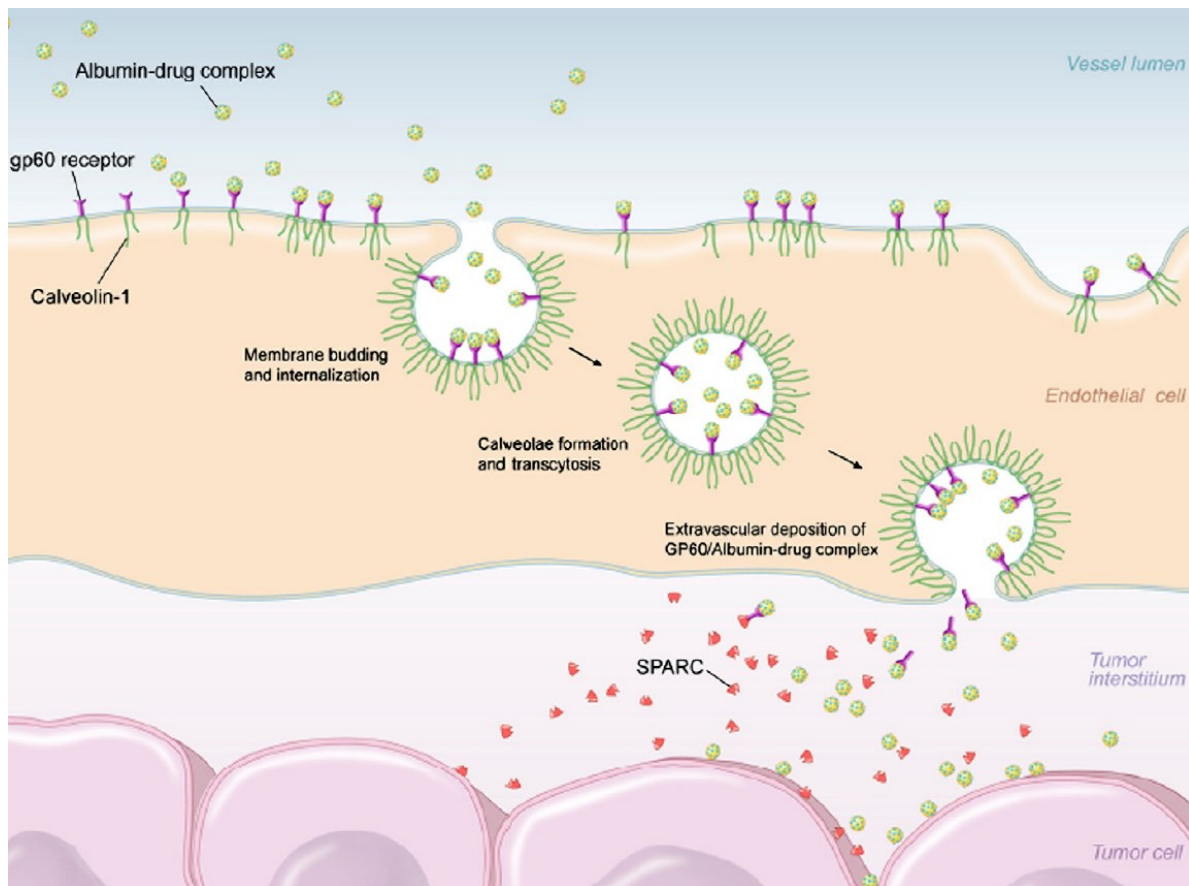
Figure 5. Transport of human serum albumin-based nanoparticles, containing drugs like paclitaxel, to the tumor interstitium

Drug-containing nanoparticles are bound by gp60 receptors on the surface of endothelial cells. Interaction of the activated receptors with caveolin-1 triggers the formation of caveolae which transport the particles across endothelial cells into the tumor interstitium. There, they associate with SPARC, a possible reason for accumulation of the drug specifically in tumors, since it is over-expressed in many of them. (Elsadek B et al. 2012. *J Control Release*.)[88]

These properties may also contribute to the responsiveness of tumors to abraxane treatment, even when resistance against CrEL-based paclitaxel was developed before, which led to relapses. This was observed in vitro in pediatric solid tumors developed from multiple rhabdomyosarcoma, osteosarcoma and neuroblastoma cell lines, as well as in vivo in rhabdomyosarcoma and neuroblastoma xenograft models.[89]

1.6 Iron

Iron is an essential component in the metabolism of most known forms of life. In mammals it is the most frequently occurring transition metal. A multitude of physiological processes,

together with the proteins and enzymes involved in them, depend on the presence of this element. This includes DNA synthesis, DNA replication, cell proliferation, erythropoiesis and the transport of oxygen. In the plasma, most Fe^{3+} ions are reversibly bound to transferrin, an abundant plasma protein, which delivers iron into the cytoplasm of cells in response to association with the transferrin receptor 1 (CD71).[90,91,92]

After binding, the complex consisting of iron-loaded transferrin and CD71 is internalized by endocytosis. Once in the endosome, metalloreductases such as members of the six-transmembrane epithelial antigen of prostate (STEAP) reduce Fe^{3+} to Fe^{2+}, which is
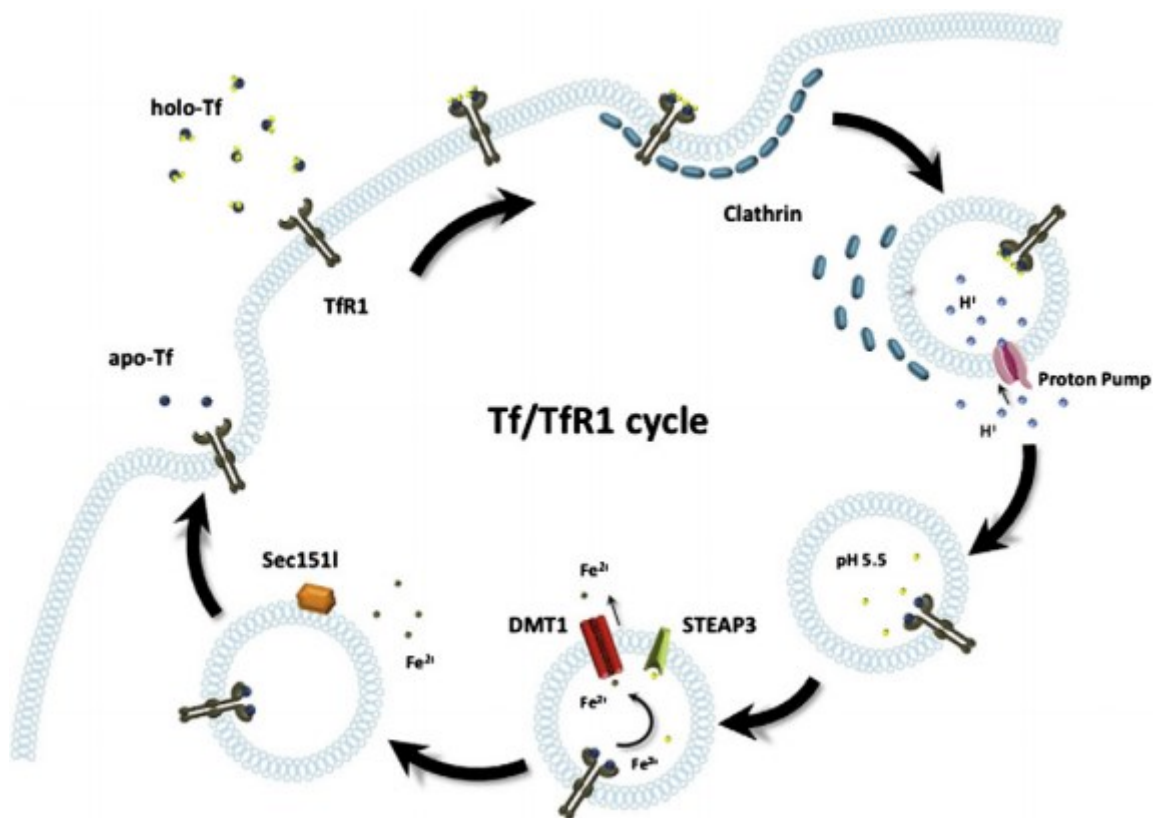
Figure 6. Uptake of iron-transferrin conjugates into the cell and the release of Fe^{2+} into the cytoplasm

Transferrin-Fe^{3+} conjugates (holo-Tf) are bound by the transferrin receptor 1 (TfR1 or CD71) at the plasma membrane, resulting in endocytosis of the whole complex by the formation of clathrin-coated pits. In the endosome, the decreased pH of 5,5 causes dissociation of Fe^{3+} from transferrin. The unbound iron molecules are reduced to Fe^{2+} by the ferric reductase STEAP3 and afterwards transported into the cytosol by the action of DMT1. The complex of TfR1 and transferrin in the non-iron bound form (apo-Tf) is finally transported back to the cell surface where apo-Tf is released from the receptor to function again in iron capturing. (Gkouvatsos K et al. 2012. *Biochim Biophys Acta*.) [93]

then carried into the cytosol by transporters like the divalent metal-ion transporter I (DMT1).[94]

The second of the two main pathways to import iron into cells is independent of transferrin and works via a ferrireductase on the cell surface which reduces Fe^{3+} to Fe^{2+} before it is taken up.[92]

In contrast to quiescent cells, where CD71 is not or only weakly expressed, activated and proliferating cells show increased expression levels. This mechanism of iron transport is crucial in many different cell types. B and T-lymphocytes are strongly dependent on it which is why it is essential for properly working adaptive immune responses. Insufficiently working transferrin / CD71-mediated uptake of iron was shown to impair immune reactions.[90] Formerly, expression levels of the microtubule-stabilizing and organizing protein CLIP-associated protein 2 were observed to be downregulated in cells upon targeting of CD71 with a blocking mAb. This led to the idea that iron is needed for a properly functioning microtubule cytoskeleton.[95]

1.6.1 Labile iron pool

The bulk of iron in biological systems is stably bound to enzymes, storage and transport proteins. However, a small proportion of iron is loosely associated to several different low-molecular weight ligands inside as well as outside of the cell.[96,97] Those can be extracellular matrix components such as glycans, membrane surface molecules like the head groups of phospholipids, ligands like siderophores and polypeptides, and organic anions (e.g. phosphates). This iron species typically does not associate with transferrin.

Together, these fractions of iron, which make up less than 5 µM of the cell's total iron concentration of 20 µM to 100 µM, are referred to as the labile iron pool (LIP) or as non-transferrin-bound iron (NTBI).[96] Cytosolic and organellar iron of this pool exists in both forms, Fe^{2+}, as well as Fe^{3+}. Depending on the particular compartment (or cytosol) and its chemical constitution and reductive capacity, their ratio can vary.[98] It is thought to serve as easily accessible iron source to be incorporated into proteins, to be used for the synthesis of enzyme cofactors like iron-sulfur or iron-heme clusters, and to present the major intersection of metabolic iron traffic in the cell, including its import into several organelles as needed.[96,99,92] Due to the loose association to its binding partners, it can engage in Fenton chemistry and thereby aid the production of reactive oxygen species (ROS) from H_2O_2. Since overabundant amounts of ROS are associated with several disorders, including chronic inflammatory, neurodegenerative and cardiovascular diseases, the levels of cellular redox-active labile iron must be carefully controlled. This is achieved by the posttranscriptional regulation of iron uptake via CD71 and iron sequestration via ferritin, a cytosolic iron-storage protein complex, by the cytosolic iron regulatory proteins (IRP) I and II.[97,92] These cytosolic iron sensing proteins are capable of binding the mRNA of ferritin and the transferrin receptor on their iron responsive elements (IREs).

In the case of iron overload, IRPs do not bind transferrin receptor mRNA which results in accessibility for RNases and, with the mRNA's degradation in lower receptor protein levels, finally leading to decreased uptake of iron. At the same time, ferritin mRNA translation is increased as a consequence of the IRPs not binding it, allowing the translation machinery to access it. This results in higher levels of the protein and therefore increased sequestration of excess iron.[100]

When iron is scarce, IRPs recognize these mRNAs and bind them, leading to stabilization and protection from RNases (CD71 mRNA) and to a block of access for the small ribosomal subunit to the ferritin mRNA. Consequently, higher numbers of CD71 are presented on the cell surface, internalizing increased amounts of iron-loaded transferrin, and lower iron-storage activity takes place due to decreased ferritin abundance.[100,101]

An additional way to maintain iron homeostasis in cells, is the export of excess iron through the membrane by the iron efflux pump ferroportin in cooperation with ferroxidases. Ferroportin as well as DMT1 are targets of IRPs too. Like with CD71 mRNA, the mRNA of DMT1 is subject to degradation by RNases when IRPs are not stabilizing it under conditions of iron overabundance. Ferroportin mRNA on the other hand, undergoes elevated translation under such circumstances, as the association of IRPs with its IRE goes down (as it is the case for ferritin mRNA).

Like with ferritin and CD71 mRNAs, the opposite is true under conditions where iron is scarce. In this case, iron efflux activity is decreased due to lower ferroportin levels and release of endosomal iron into the cytosol is increased because of the elevated DMT1 concentration.[94,100]

Both, $CD4^+$ and $CD8^+$ T cells are capable of taking up, as well as of exporting labile iron. Furthermore, ferritin concentrations in T cells were shown to be increased after the addition of labile iron, which indicates a rise in the iron-storage capacitance of these cells following the uptake of labile iron.[91,102] When stimulated via signal 1 and 2, murine $CD4^+$ and $CD8^+$ T cells as well as human $CD4^+$ PB T cells were shown to downregulate levels of the LIP.[103] Its uptake seems to be independent of DMT1 and ZIP14 (Zrt- and Irt-like protein 14 is another factor aiding the transport of Fe2+ from the endosome into the cytosol), since their mRNA and protein expression levels remain unaffected after Fe-citrate addition to the cells.[94,91,102] Accordingly, reduction of the mRNA concentrations of DMT1 and ZIP14 by 60-80% using siRNAs, does not have a significant impact on the uptake of labile iron by T cells. Considering that T lymphocytes also do not endocytose NTBI in a clathrin-dependent manner and take it up largely in the form of oligomeric ferric citrate species, particularly Fe_3Cit_3, this indicates that there may be a transporter specific for this species.

Storage and transport of labile iron out of cells was not found to differ notably between CTL and helper T cells. Their accumulating capacities allow them to withhold the metal from building up in organs, such as the liver and the spleen. Indeed, mice deficient in total T cells were shown to exhibit iron overload in the liver.[91,102,104]

Thereby, T cells seem to serve a protective barrier function guarding those organs from the toxicity arising from systemic overabundance of iron.[91,102]

This suggests that circulating T cells may contribute to the maintenance of systemic iron homeostasis.[102]

An additional characteristic feature of the LIP is its amenability to iron binding, cell permeant chelators.[97] Chelators are capable of binding labile iron with high enough affinity to ensure their specificity to the respective forms of the metal. In addition, they form complexes with the metal in a way that renders it not labile anymore and consequently non-reactive. In this conjugated form, iron ceases to contribute to the generation of ROS and thereby to pose an increased risk on cell survival via that route. These properties make chelators a viable option for the treatment of disorders of excessive iron accumulation, like systemic or regional forms of siderosis. In such therapies, appropriate administration-regimens are necessary to avoid iron deficiencies, especially over long time periods.[98]

While treatment for systemic siderosis targets iron intracellularly and in extracellular fluids, regional siderosis where iron piles up in specific cell compartments or organs while it is lacking in others, is managed by the utilization of chelators which redistribute it within the same cell or between organs. Such chelators are not only capable of binding labile iron, but also of transporting it to other cellular compartments within the cell, to other cells or to transferrin in the plasma and releasing it there.[98]

In this work, the highly hydrophobic Fe^{2+} chelator 2,2'-bipyridyl (BIP) and 2-hydroxy-1-naphthylaldehyde isonicotinoyl hydrazone (311), a tridentate aroylhydrazone ligand exhibiting high Fe^{3+} affinity, were used. [105,106]
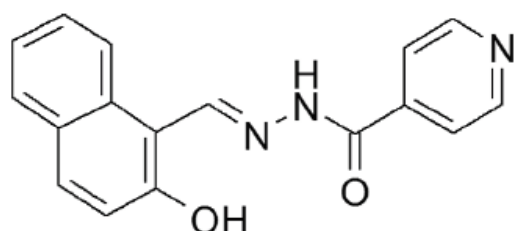
311
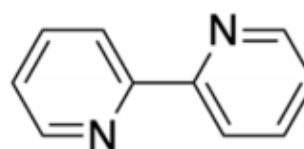
BIP

Figure 7. Structures of 2-hydroxy-1-naphthylaldehyde isonicotinoyl hydrazone (311) and 2,2'-bipyridyl (BIP)

To the left, the structural formula of the Fe^{3+} chelator 311 is shown (adapted from Lui GY et al. 2015. *Oncotarget*.)[107], while on the right side, the Fe^{2+} chelating BIP is displayed. (adapted from Constable EC et al. 2019. *Molecules*.)[108]

Another chelator used in the described experiments is the non-fluorescent molecule calcein-acetoxymethylester (AM). It binds iron via two aminotetraacetate residues which are connected to the fluorophore fluorescein.[109]

In viable cells calcein-AM is highly membrane permeable, which results from the lipophilicity of AM. However, this property is lost after its ester groups are hydrolyzed by nonspecific esterases within the cell, which gives rise to negatively charged calcein with lower membrane permeability. This results in substantial buildup of calcein inside the cell.[109,110]

In addition, the cleaved form exhibits fluorescence, emitting light with wavelengths of 520–530 nm upon exposure to light with wavelengths of 465–490 nm.[110,111]
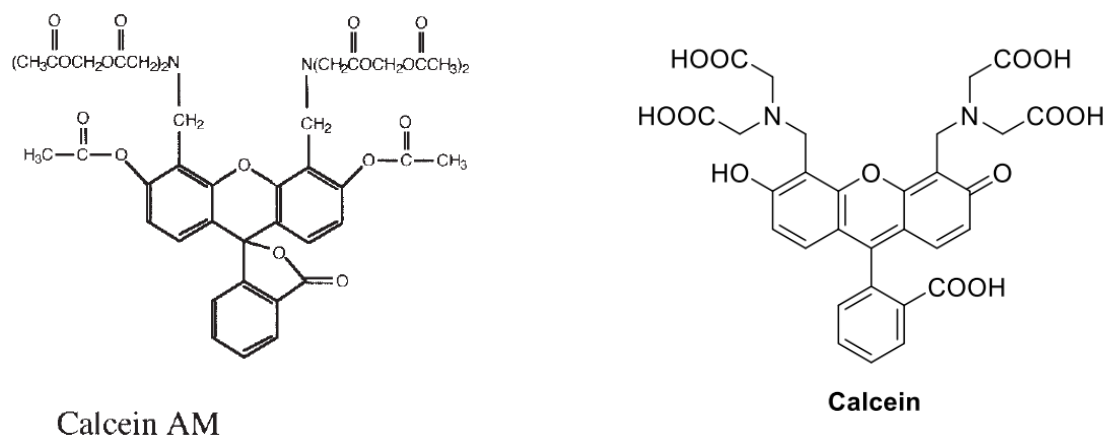
Calcein AM

Calcein

Figure 8. Structures of the fluorescent indicator calcein in its unconjugated and acetoxymethylester-linked form.

On the left side the structure of non-fluorescent calcein-acetoxymethylester (AM) is depicted (adapted from Petrat F et al. 2002. *Biol Chem*).[109] To the right, the AM was removed from the compound by cellular esterases, leaving the fluorescent calcein (adapted from Sahoo S et al. 2021. *ACS Appl Polym Mater*).[112]

Chelation of iron in the cell reversibly quenches the fluorescence of calcein. Subsequent addition of excess amounts of competing iron chelators with stronger affinities for labile iron than calcein, such as BIP and 311, can reverse the quenching of the signal if the iron previously bound by calcein indeed belongs to the LIP.[98,90] The difference in mean fluorescence intensity between cells treated with competing chelators and untreated control cells, accounts for the amount of intracellular labile iron and can be determined by flow cytometric measurements.[113,114]

This calcein-AM based method can therefore be utilized for the detection of intracellular chelatable iron.[113]

In case esterase activity in the cytosol is sufficiently high, the vast majority of calcein is present in the cytosol and the nucleus, since the ester groups are cleaved prior to passing the membranes of organelles like mitochondria or lysosomes. In such cases, calcein can only be used for determination of labile iron present in the cytosol and the nucleus.[108] Unless the administered calcein-AM concentration is too high for the esterases to cleave all of it, this is usually what happens.

Following the degradation of iron-containing cell constituents, including mitochondrial complexes and ferritin, in autophagosomes, big parts of the cellular LIP are temporarily contained in lysosomes. Even if some calcein-AM manages to enter the lysosome, it does not bind iron therein to a significant degree due to the acidic environment with a pH of 4-5. At this pH, calcein fluorescence is only quenched slightly upon external iron addition, compared to pH 7, suggesting weaker chelation. Consequently, a major fraction of labile iron is not detected by this method.[115,116]

Since calcein chelates labile iron, leading to an imbalance in the cytosolic LIP, cellular feedback mechanisms may be initiated to increase the levels again, e.g. by mobilizing some of it from ferritin. This poses a further potential problem on the reliable assessment of the LIP.[116]

2. Aims of the study

The labile iron pool consists of iron not bound to transferrin but loosely associated with different ligands of low molecular weight.[96,97] Among several of its functions, it is assumed to present an accessible iron source for the incorporation into proteins.[96]

At the same time, this iron species is prone to engage in Fenton chemistry leading to reactive oxygen species formation.[97]

In this thesis the effect of different stimulation conditions, including CD43 costimulation, on labile iron levels in T cells was investigated.

Formerly, expression levels of the microtubule stabilizing and organizing protein CLIP-associated protein 2 were observed to be downregulated in cells upon targeting of CD71 with a blocking mAb. This led to the idea that iron is needed for a properly functioning microtubule cytoskeleton.[95,117]

Here, the microtubule cytoskeleton in T cells was analyzed after stimulation via the same pathways as before.

Combining the results of these experiments, the question whether labile iron levels have an influence on the microtubule cytoskeleton was addressed.
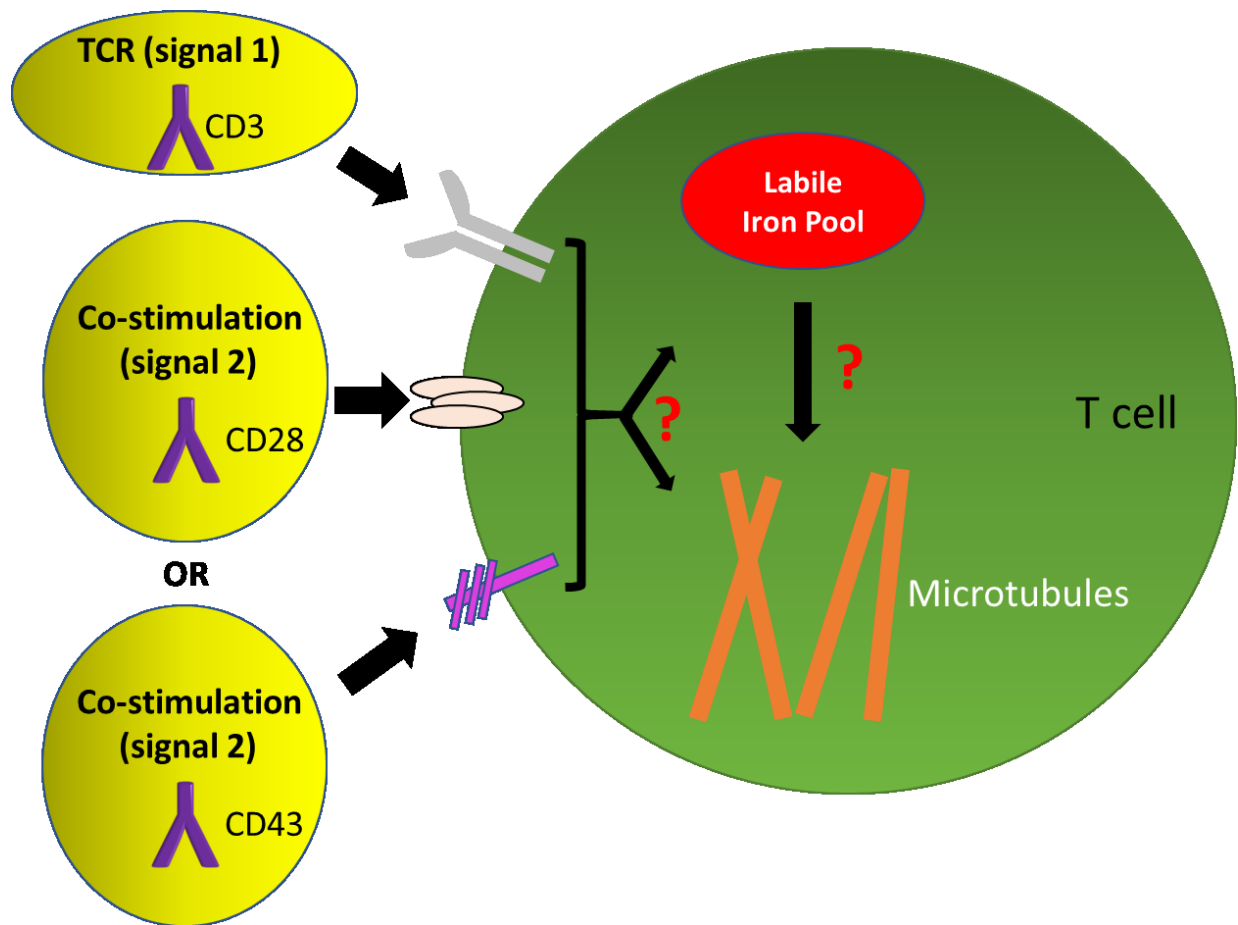
Figure 9. Overview of the aims of the study

3. Materials and Methods

3.1 Materials

3.1.1 Media, Reagents and chemicals

Material	Specifications	Producer
PBS (1x), Magnesium and Calcium free	6,7 mM PO_4	Lonza
Bovine Serum Albumin (BSA)	Used at 1% in PBS	GE Healthcare
Staining buffer	PBS (1x) / BSA (1%)	
RPMI-1640	Contains sodium bicarbonate, without Penicillin, streptomycin and L-glutamine For cell culture supplemented with • L-Glutamine (2mM) • Penicillin (100 U/ml) • Streptomycin (100 µg/ml) • FCS 10%	Sigma Life Science
Freezing Medium	• 75% RPMI supplemented • 15% FCS • 10% DMSO	
Penicillin-Streptomycin	10.000 units penicillin and 10 mg streptomycin per ml in 0,9% NaCl, sterile filtered	Sigma Life Science
L-Glutamine	200 mM, solution, sterile filtered	Gibco
Fetal Calf Serum (FCS)	Origin 500 ml Gibco/10270106	Gibco
FACS sheath fluid	• H_2O (97,8 %) • NaCl • KCl • K_3PO_4 monobasic • Na_2HPO_4 • 2-Phenoxyethanol	BD FACSFlow

	• NaF	
Abraxane	5 mg/ml	Celgene
311	10 mM, 5 mg dissolved in 1,7 ml DMSO	Sigma-Aldrich
BIP	200 mg/ml, 200 mg dissolved in 1 ml Ethanol	Sigma-Aldrich
FIX&PERM Fixation Medium		ADG (Nordic-MUbio?)
FIX&PERM Permeabilization Medium		ADG (Nordic-MUbio?)
Calcein-AM	1 mM in 50µl DMSO	BioLegend
Dimethyl sulfoxide (DMSO)	Anhydrous	BioLegend

Table 1. List of substances used in the experiments

3.1.2 Cells

Cells	Cell type	Source
Jurkat T cells	Human lymphoblast, T cell	American Tissue Culture Collection
Primary T cells 98/8934	Peripheral blood T cells	Purchased from Austrian Red Cross
Primary T cells 98/9431	Peripheral blood T cells	
Primary T cells 99/4022	Peripheral blood T cells	

Table 2. List of used cells

3.1.3 Antibodies

Specificity	Isotype	Origin	Clone	Company
α-Tubulin	IgG1	Mouse	DM1A	Sigma-Aldrich
β-tubulin	IgG	Rabbit	9F3	Cell signaling Technology
CD3	IgG2a	Mouse	OKT3	Otto Majdic, IFI, Vienna, AT
CD3	IgM	Mouse	VIT3	Otto Majdic, IFI, Vienna, AT
CD28	IgG1	Mouse	10F3	Life technologies

CD43	IgG1	Mouse	10G7	Otto Majdic, IFI, Vienna, AT
Calf intestine alkaline phosphatase – Vienna Immunology Alkaline Phosphatase (VIAP)	IgG1	Mouse	VIAP-2D5	Otto Majdic, IFI, Vienna, AT
Scavenger Receptor expressed by Endothelial cells (SREC)	IgG1	Mouse	488/9B9	Otto Majdic, IFI, Vienna, AT

Table 3. List of used antibodies

3.2 Methods

3.2.1 T cell isolation

T cells were previously isolated from up to 10^9 peripheral blood mononuclear cells (PBMNCs) using magnetic cell sorting (MACS). Different mAbs (10 µg/ml) were used to clear the PBMNC flow through of monocytes (anti-CD14 (MEM18)), granulocytes and NK cells (anti-CD16 (3G8)), B cells (anti-CD19) and monocytes, thrombocytes and myeloid progenitors (anti-CD33 (4D3)).

Resuspension of isolated PBMNCs in 750 µL MACS buffer was followed by incubation with 250 µL of antibodies conjugated to biotin for 15 min at 4°C. Unbound antibodies were removed in two washing steps using MACS buffer, succeeded by resuspension of the cells in 750 µL buffer. Subsequently, the suspension was incubated with 250 µL streptavidin MicroBeads (Miltenyi Biotec) for 15 min at 4°C. PBMNCs were then loaded onto a CS column (Miltenyi Biotec) positioned on a VarioMACS apparatus and equilibrated with 40 ml MACS buffer. 50 ml eluted and washed T cells were centrifuged for 5 minutes at 500g and resuspended. Prior to cell counting, remaining erythrocytes were removed via administration of two drops of Zap-Oglobin (Beckman Coulter).[95]

3.2.2 Culture and activation of T cells

High binding plates (Costar) were coated overnight at 4°C with the CD3 mAb OKT3 alone or in combination with CD28 mAb, with the CD3 mAb VIT3 alone or with OKT3 in combination with CD43 (10G7) mAb. All mAbs were used at a concentration of 5µg/ml and 25 µl of each were pipetted per well. Subsequently, the plates were washed twice with 1 x PBS to remove unbound mAbs, followed by the addition of 2 x 10^5 purified T cells in 200 µl RPMI-1640 medium per well. Afterwards, the plates were incubated at 37 °C, 5% CO_2. Cell were harvested after 4, 24 or 48h of incubation.

3.2.3 Freezing of T cells

Human peripheral blood and Jurkat T cells were counted at the Coulter Counter (Beckman Coulter Z2 Coulter Particle Count and Size Analyzer) and 2×10^7 cells were centrifuged at 1495 rpm for 5 min. The cell pellet was resuspended in 1 ml of freezing medium and transferred to cryotubes (Nalgen Nunc International) which were positioned in a freezing box containing isopropanol. The box was kept at -80°C overnight and stored in a liquid nitrogen container the following day.

3.2.4 Thawing of T cells

Frozen T cells were thawed at 37°C in a water bath and then dropwise resuspended in pre-warmed (37°C) RPMI 1640 medium. After two washing steps in medium and counting at the Coulter Counter, they were cultured in medium at 37°C, 5% CO_2 in T25 filter bottles (Corning) or in 96-well plates (Costar). Jurkat cells were split in a 1:10 ratio and were supplied with fresh medium every third day.

3.2.5 Evaluation of the intracellular labile iron pool

2×10^5 cells were incubated with 15 nM calcein-AM for 15 min at 37 °C, 5% CO_2 in the dark. This was followed by two washing steps using PBS/BSA (1%) and subsequent treatment with 10 µM of the Fe^{3+} chelator 311 and/or 250 µM of the Fe^{2+} chelator BIP for 2h at room temperature. After two further washing steps, the samples were examined by flow cytometry. The amount of intracellular labile iron was calculated as the difference in mean fluorescence intensity of the cells which have or have not undergone treatment with the chelator(s) (Δ MFI).

3.2.6 Flow cytometry

Intracellular staining was performed as described by Brell et al. 2020.[90] 2×10^5 cells per staining were treated with abraxane (50 ng/ml) for 2 h at 37 °C, 5% CO2. Afterwards, cells were fixed for 20 min at room temperature by the use of FIX solution and subsequently washed twice with the staining buffer PBS/BSA (1%). This was followed by permeabilization utilizing PERM solution for 20 min at room temperature. Anti-α-tubulin-FITC-Ab (0,1 µg/ml) or anti-β-tubulin -AF488-Ab (1 µg/ml) were added for 20 min together with the PERM solution. After two washing steps, samples were analyzed by flow cytometry using the FACSCalibur flow cytometer (Becton Dickinson, Franklin Lakes, NJ).

To evaluate the effect of iron chelators on microtubules of non-activated Jurkat T cells, 2×10^5 cells per staining were incubated with 10 µM of 311, 250 µM BIP or both for 3h at room temperature. This was followed by staining with anti-α-tubulin-FITC-Ab (0,1 µg/ml) or anti-β-tubulin -AF488-Ab (1 µg/ml) and flow cytometric analysis as described above.

3.2.7 Statistical analysis

For statistical analysis the GraphPad Prism software was used. Two-way ANOVA with Tukey test and multiple T tests corrected using the Holm-Sidak method were used. Significances are defined by p-values below 0.05. Significant differences are represented in the form of stars, with * describing a p-value <0.05, ** indicating p<0.01, *** designating p<0.001 and **** standing for p<0.0001.

4. Results

The intracellular labile iron pool consists of iron not associated with transferrin but with several ligands of low molecular weight.[96,97] It has various important properties including its accessibility to iron-incorporating proteins, its utilization for enzyme cofactor synthesis and its mobility between different cell organelles serving as an iron source for them as needed.[96, 99,92] In addition, it contributes to the formation of ROS, which is why it has to be controlled tightly.[97] Yarosz et al. found LIP levels to be decreasing over time of activation via CD3/CD28 stimulation in murine and human CD4$^+$ T cells. This is also the case for murine CD8$^+$ T cells. [103] In order to see how LIP levels behave in response to different activation stimuli, peripheral blood T cells were exposed to plate bound mAbs specific for different epitopes of CD3, for CD28 and CD43 for different time points. In addition, Jurkat T cells were subjected to CD3/CD28 stimulation.

Via calcein-AM staining and subsequent addition of iron chelators to the cells, LIP levels were determined.

4.1 Cultivation of Jurkat cells shows a rise in the LIP which is not observed in primary T cells

To analyze the levels of labile iron in non-activated peripheral blood and Jurkat T cells, Geo Mean fluorescence intensities (MFIs) of cells treated with calcein-AM and subsequently with or without the chelators were compared and the ∆MFI values, resembling the LIP levels, were calculated.

The most pronounced differences were observed in Jurkat cells cultivated for 48h in RPMI medium. Within this time point, 311 addition showed the highest iron levels in the LIP with a mean MFI of 373,7 compared to 213,8 in untreated cells, resembling a 1,75-fold increase. Treatment with the combination of the two chelators resulted in a value of 339,5 (1,59-fold elevation). Cells exposed to BIP showed a lower elevation with a value of 326,9 which amounts to a 1,53-fold change (Figure 11).

Among the other two time points, MFIs showed a tendency towards decreases compared to

untreated Jurkat cells in four conditions. This was the case for 311 treated cells after 4h (224,2 compared to 238 in untreated cells), BIP treated cells after 4h (202,8) and 24h (171,2 compared to 195,9 in untreated cells) and 311+BIP treated cells after 4h (192,8). In contrast to the MFI elevations after 48h of resting, these differences are not statistically significant.

In primary T cells, the differences are non-significant and less pronounced with the biggest one seen between 311 treated and untreated cells (189 vs 165,4, respectively) after 4h of cultivation. In cells cultured for 4h and 24h, treated with both chelators, lower MFIs than in untreated cells were observed. However, these differ by merely 6,5% and 5,4%, respectively (Figure 10 and Supplementary Table 4).
Interestingly, a statistically significant decrease of calcein signal intensities over time (between 4h and 48h of cultivation) was detected in primary T cells, which was not observed in Jurkat T cells (Figure 10).

4.2 CD28 costimulation leads to increased LIP levels in Jurkat cells and to trends of elevations in primary T cells

Next, cells were activated via plate bound mAbs specific for CD3 (OKT3) and CD28 for different periods of time before analyzing their LIP.
At 24h and 48h time points, there is a tendency towards a rise in the MFI in primary T cells, which is stronger upon 311 and 311+BIP treatment. After 24h, the MFIs were at 129,5 and 131,2 upon 311 and 311+BIP treatment, respectively (as opposed to 96,7 in cells not treated with chelators). After 48h, the values were 98,3 and 99,9 after 311 and 311+BIP treatment, respectively, compared to 65,2 in untreated cells (Figure 12 and Supplementary Table 5).

In Jurkat cells, MFIs show a trend towards an increase after 24h and show a significant elevation concomitantly with the highest LIP levels after 48h of stimulation. At both time points, the increase appears to be stronger when 311 was added compared to BIP. At 24h, a mean value of 166 was observed for 311 treated cells compared to 127,8 in untreated cells. Upon addition of BIP, it rose to 145,9 and administration of both chelators increased the mean value to 183.
Activation for 48h showed a 1,4-fold increase of the MFI by 124,1 (=LIP) (from 289,8 in untreated cells to 413,9) in case of 311. This was the highest observed elevation in the CD3 (OKT3)/CD28 activated cells and therefore the highest levels of iron in the LIP. When BIP was added, the MFI increased 1,3-fold, from 289,8 to 378,4 and upon addition of both chelators the ΔMFI was 105,1 with an MFI of 394,9 in treated cells (1,36-fold increase and the second highest LIP levels) (Figures 10 and 11).

As already seen under non-activating conditions, a decrease of calcein fluorescence intensities over time could be observed in primary T cells, but not in Jurkat T cells. This decrease was less pronounced than in non-activated cells and not statistically significant (Figure 12).

Comparing the quantities of iron in the LIP (ΔMFI values) between non-activated and CD3 (OKT3)/CD28 activated cells, several (not statistically significant) trends towards increases in stimulated cells could be observed (Supplementary Table 6). These occurred in primary T cells after 24h and 48h and were, with 39,4 the most marked after 24h upon addition of both chelators. After 4h, the LIP levels were lower after activation with a negative difference in the mean ΔMFI of 34,3 when 311 was added. However, such a tendency towards a decrease was not observed in the other chelator-conditions. BIP administration led to a 1,1-fold higher increase compared to untreated cells, from a ΔMFI of 6,3 in untreated cells to 19,8 and combination-treatment resulted in 1,22 times higher LIP levels / stronger elevation of the mean MFI, with a difference between ΔMFI values of 30,2 (19,5 vs. -10,7 in untreated cells) (Figure 17, supplementary table 6).

In Jurkat cells, non-significant trends of increases were observed after 4h and 24h of activation. After 4h, all conditions showed higher LIP levels (mean ΔMFI values), with the most pronounced difference seen in cells treated with both chelators followed by BIP and then 311. After 48h however, amounts of iron in the LIP (ΔMFIs) were significantly decreased after activation compared to resting cells, observable in all chelation conditions. This was most evident in 311 treated Jurkat cells with a 0,18-fold decrease in the LIP levels and a difference in ΔMFIs of 35,8 (159,9 in non-activated and 124,1 in activated cells), followed by BIP addition, where the value fell by 24,5 (113,1 in non-activated cells compared to 88,6 in activated cells) (0,146-fold decrease). When both chelators where used, iron levels in the LIP sank 0,142-fold, with the ΔMFI falling from 125,7 to 105,1 (Difference of 20,6) (Figure 13).

Figure 10. Calcein fluorescence measurements in non-activated primary and Jurkat T cells untreated or treated with 311, BIP or both chelators

Human peripheral blood/primary (=prim) and Jurkat T cells were incubated for 4h, 24h and 48h without stimulation (na=non-activated) and then stained with 15 nM calcein-AM for 15 min, followed by incubation with iron chelators (10 µM of 311 and/or 250 µM of BIP) for 2h. (A) - (C) show treatment of primary T cells with 311, BIP or the combination of both, respectively. This was compared to untreated cells. (D) – (F) show treatment of Jurkat T cells with chelators in the same order. Bar graphs show the Geo Mean fluorescence intensity (MFI) of calcein. The bars show the Geo Mean (± SEM) of 3 independent experiments.

Figure 11. Comparison of calcein MFI values between chelator treated and untreated Jurkat T cells resting or stimulated via mAbs specific for CD3 (OKT3)/CD28

Jurkat cells were resting in RPMI medium only (=non-activated (na)) (A) or incubated with plate bound CD3 (OKT3) and CD28 mAbs (B) for 4h, 24h and 48h and subsequently treated with calcein-AM for 15 min. Afterwards, they were incubated with iron chelators 311, BIP or the combination of them for 2h. Bars show fold changes of calcein Geo Mean fluorescence intensities (MFI) (± SEM) of 3 independent experiments, compared to cells not treated with chelators. Untreated cells, represented by black bars, are set to a value of 1.
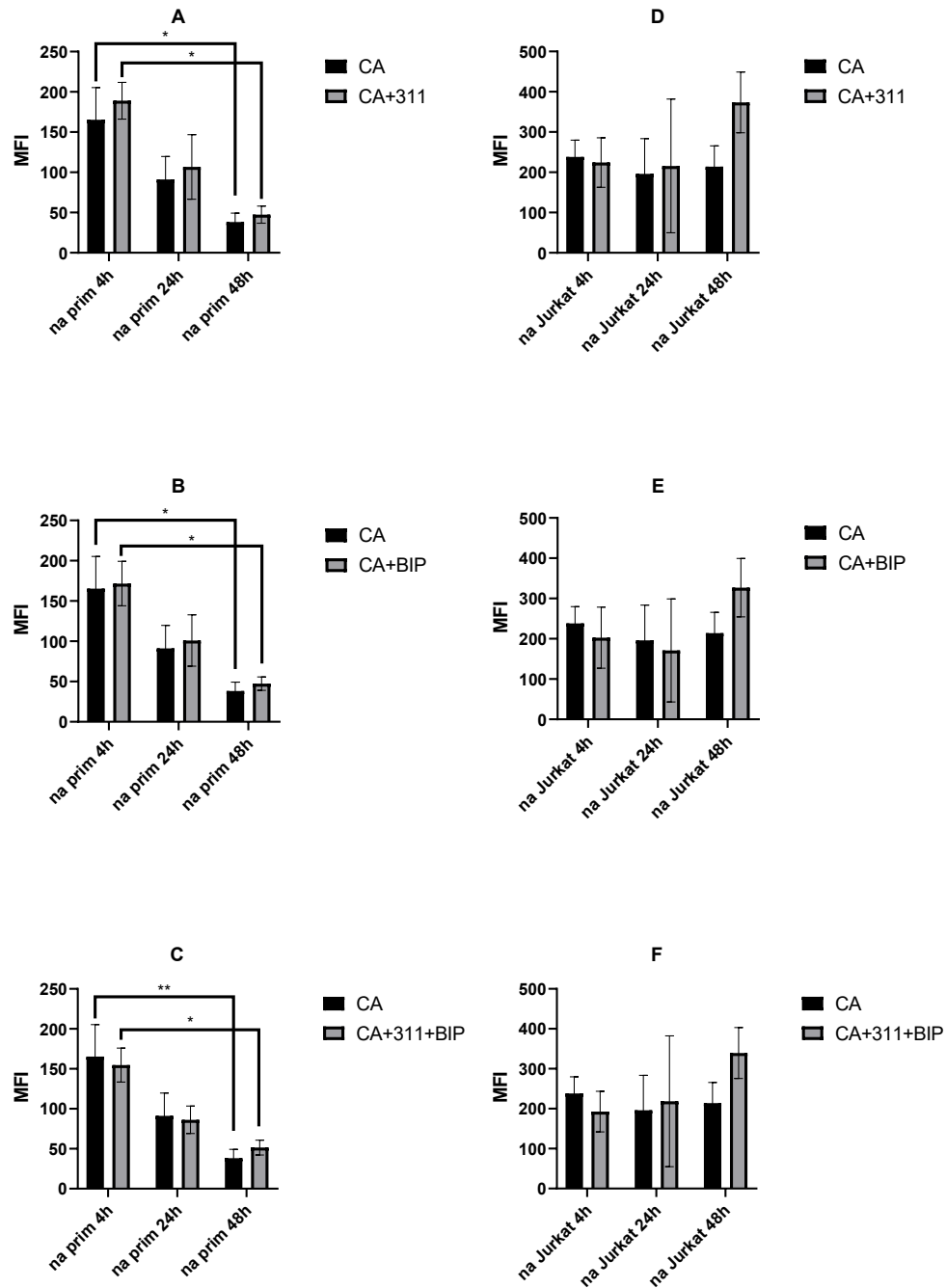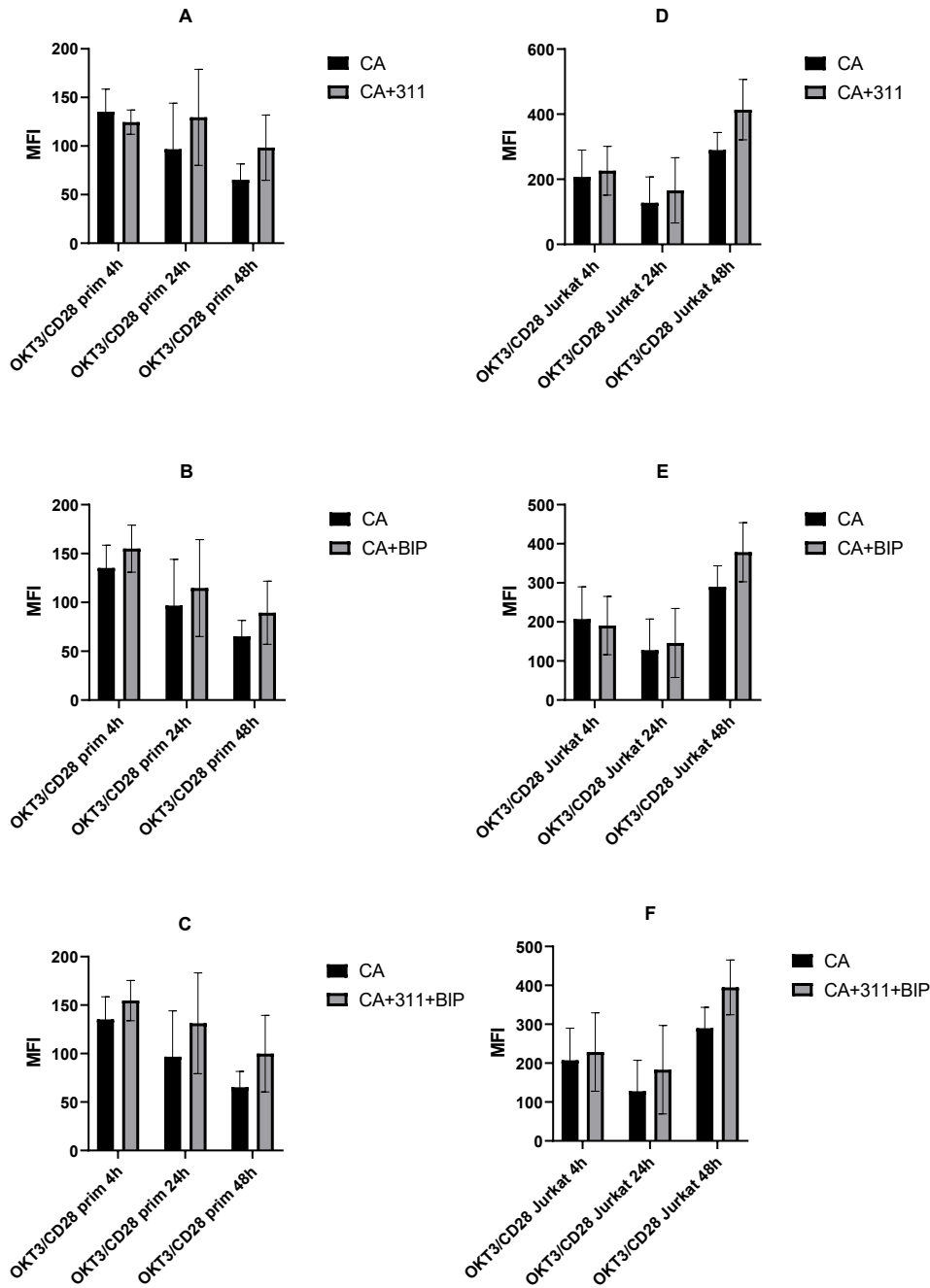
Figure 12: Calcein fluorescence measurements in CD3 (OKT3)/CD28-activated primary and Jurkat T cells untreated or treated with 311, BIP or both

Human primary (prim) and Jurkat T cells were incubated for 4h, 24h and 48h with plate bound OKT3 and CD28 mAbs and afterwards stained with 15 nM calcein-AM for 15 min, followed by incubation with iron chelators (10 µM of 311 and/or 250 µM of BIP) for 2h. (A) - (C) show treatment of primary T cells with 311, BIP or the combination of both, respectively. This was compared to untreated cells. (D) – (F) show treatment of Jurkat T cells with chelators in the same order. Bar graphs show the Geo Mean fluorescence intensity (MFI) of calcein. Bars show Geo Means (± SEM) of 3 independent experiments.
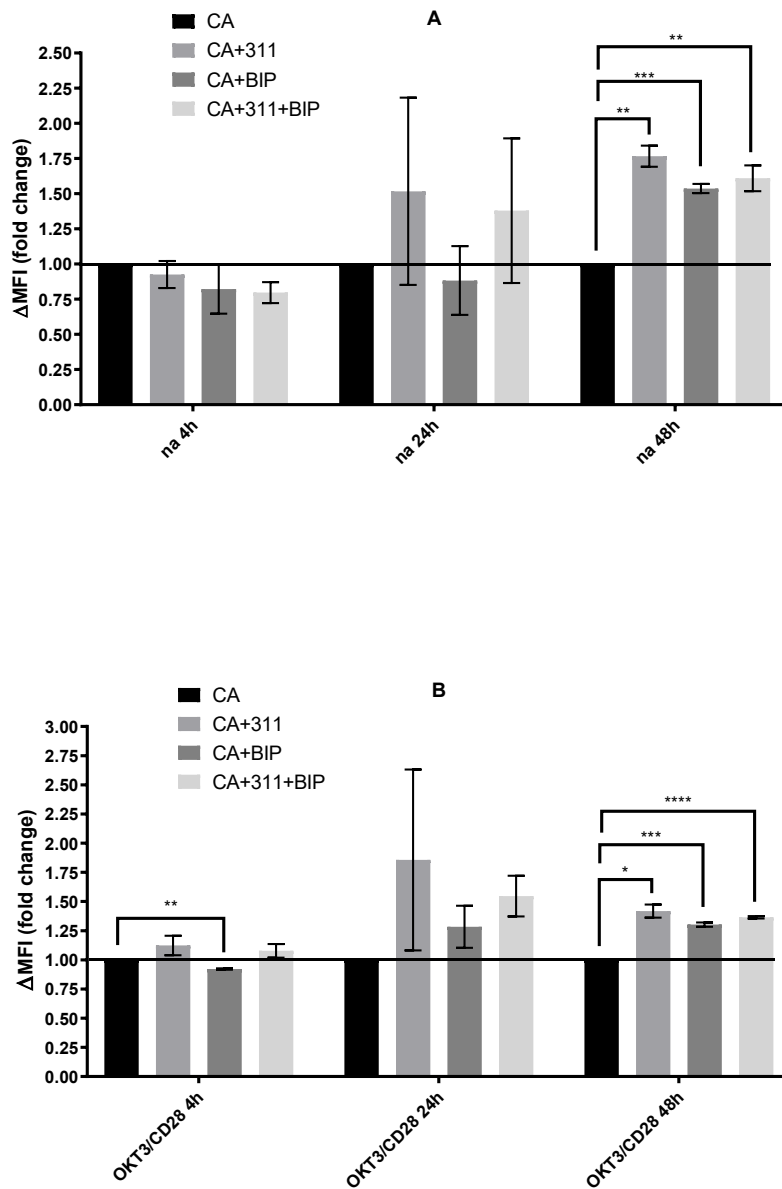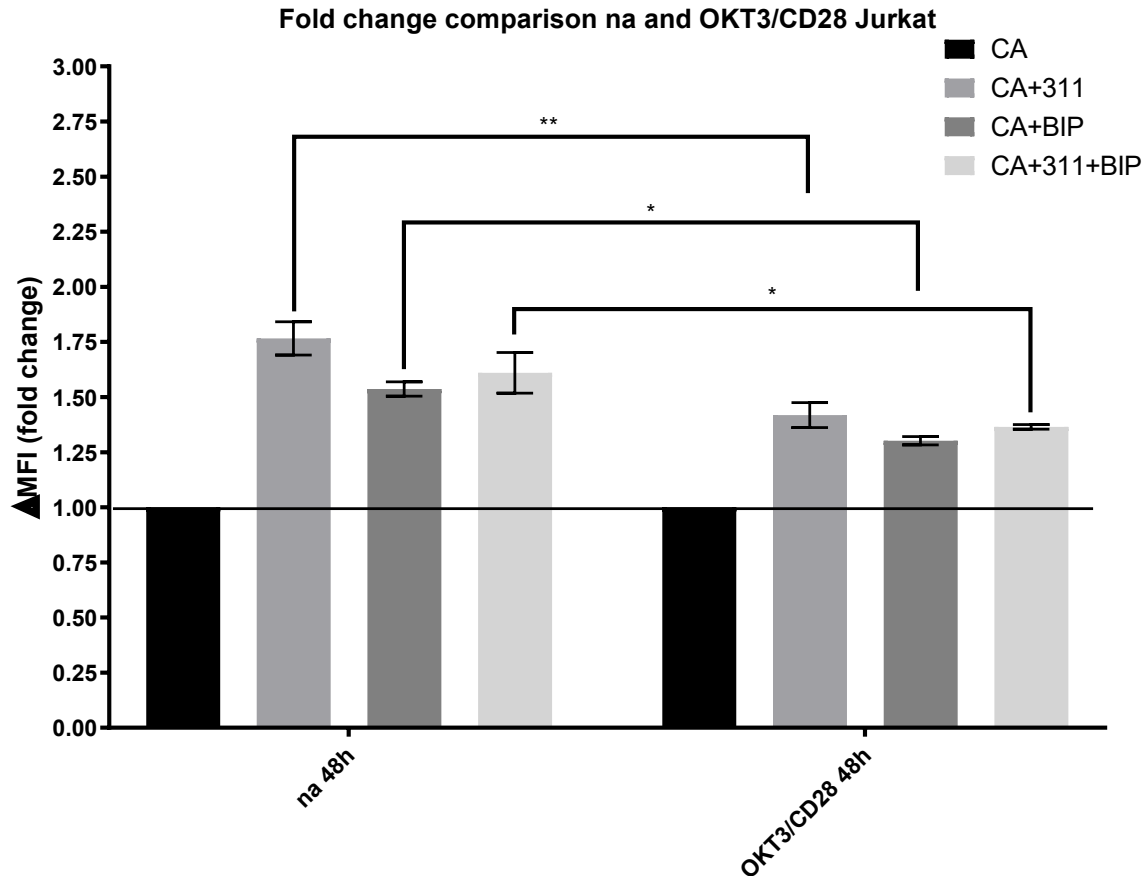
Figure 13. Comparison of calcein MFI increases upon addition of iron chelators between resting and CD3 (OKT3)/CD28 stimulated Jurkat cells

Jurkat cells were resting (na) or stimulated for 4h, 24h and 48h via plate bound mAbs targeting CD3 (OKT3) and CD28 before they were stained with calcein-AM for 15 min. Subsequently, they were incubated with the iron chelators 311, BIP or the combination of them for 2h. Bars show fold changes of calcein Geo Mean fluorescence intensities (MFI) (± SEM) of 3 independent experiments, compared to cells not exposed to chelators. Untreated cells, represented by black bars, are set to a value of 1.

4.3 CD3 (OKT3) activation of primary T cells results in increased LIP levels

Subsequently, primary T cells were stimulated only with a mAb specific for CD3 (OKT3) and analyzed for their levels of LIP. (Figure 14 and Supplementary Table 7).

Differences in the MFIs between chelator treated and untreated cells were not significant after 24h and 48h of stimulation, although tendencies towards changes could be observed. The biggest discrepancy (= highest LIP levels), being of statistical significance, occurred between cells treated with both chelators and untreated cells after stimulation for 4h. With a value of 176 in treated and 121,9 in untreated cells, the difference was 54,1 (1,44-fold

increase). This was followed by cells exposed to BIP, which showed a LIP level (mean ∆MFI) of 34,4 (156,3 in treated cells) (1,28-fold change). With a mean ∆MFI of 24,8, the difference is slightly less pronounced upon 311 treatment (1,2-fold change). The differences upon treatment with the single chelators however do not show statistical significances. After 24h and 48h of stimulation, the differences of 311 and 311+BIP treatment to untreated cells are higher compared to BIP treatment (Supplementary Table 7).

Comparing the LIP levels of 4h CD3 (OKT3) activated with 4h resting primary T cells treated with both chelators, a significant increase was observed (∆MFIs of 54,1 in activated and -10,7 in non-activated cells). BIP treated cells at this time point show a trend towards a higher difference between the LIP levels compared to treatment with 311 (1,24 times higher MFI elevation compared to untreated cells) (∆MFIs of 28,1 and 1,2, respectively).

At 24h, a rise of the mean ∆MFI of 27,9 could be observed in cells administered with both chelators. However, this elevation is not reflected in cells which have received 311 or BIP alone, where the values only differ by 9,9 and 2,5 compared to non-activated cells, respectively. At 48h, LIP levels resemble each other very closely with ∆MFI differences of 4,1 for 311, -5 for BIP and 0,9 for 311+BIP treated cells (Supplementary Table 8). Overall, these differences show no statistically significant differences, with the exception of the rise in iron quantities in the LIP at 4h in cells administered with 311 and BIP (Figure 17).

4.4 CD43 (10G7) costimulation of primary T cells brings about increased LIP levels

When looking at calcein fluorescences in primary T cells stimulated with a combination of CD3 (OKT3) and CD43 (10G7) specific monoclonal antibodies, trends of increases could be observed in cells stimulated for all three time points (Figure 15 and Supplementary Table 9). At 4h, all chelation conditions lead to increases in the mean MFIs compared to untreated cells, which were however not found to be of statistical significance. When 311 was added, an elevation of 34,8 (from 130,2 in cells only treated with calcein, to 165 in treated cells), was detected. This was followed by cells exposed to the combination of the chelators, where the MFI rose by 32,5 (from 130,2 to 162,7 in treated cells). When BIP was applied, the increase was weaker with 20,5 (150,7 in treated cells).

After 24h of stimulation, an apparent but not statistically significant rise in the signal is only observable in 311 administered cells. With a mean ∆MFI of 33,9 (from 114,2 in untreated to 148,1 in treated cells) it is higher than in the other chelation conditions where it stays relatively constant (BIP: 1,1 and 311+BIP: 4,7).

Stimulation for 48h shows the most distinct difference between calcein-only treated and calcein+chelator treated cells. Showing a mean ∆MFI (=LIP) of 41,2 (37,3 in calcein-only

treated cells and 78,5 in chelator exposed cells), this statistically significant difference is 2,1-fold when 311 was used. When both chelators were administered, the MFI was at 74,5 resulting in a delta value of 37,2 (significant 2-fold increase). Application of BIP lead to a mean increase of 20,6 (57,9 in treated cells) (1,55-fold) which was not significant (Figure 17).

Comparing the LIP levels in stimulated- to the ones in resting T cells, an elevation was observed in 311 and 311+BIP treated cells after 48h of stimulation. Upon 311 addition, the mean ΔMFI was higher by 31,9 (9,3 in non-activated cells and 41,2 in activated cells), reflecting a significant 1,6-fold higher elevation in the increase than in resting cells. Adding both chelators, a mean non-significant increase in LIP levels of 23,8 was detected (13,4 in non-activated cells compared to 37,2 in stimulated cells) (1,48-fold rise in the increase). BIP alone increased labile iron amounts by 11,3 (from 9,3 to 20,6 in resting and activated cells, respectively) (1,25-fold, non-significant increase in the elevation) (Figure 17, Supplementary Table 10).

4h of activation mainly lead to an increase compared to non-activated cells when both chelators were applied (from -10,7 to 32,5 in activated cells). 311 administered cells showed an elevation of 11,2 (ΔMFI from 23,6 to 34,8) and BIP treatment lead to a rise of 14,2 (from 6,3 to 20,5) in stimulated cells.

After 24h of stimulation, the increase in stimulated cells is, with 18,3 (15,6 in non-activated and 33,9 in activated cells) the most noticeable in 311 treated cells. However, in the other conditions the ΔMFI is only increased by 8,7 and 9,6 for BIP and 311+BIP, respectively. Differences to the rises in resting cells at the 4h and 24h time points are non-significant.

4.5 CD3 (VIT3) stimulated primary T cells show a slight trend towards increased LIP levels

Finally, primary T cells were stimulated with the CD3 specific mAb VIT3 and were analyzed for their labile iron levels by determining the differences in calcein signal intensities between untreated and chelator treated conditions (Figure 16 and Supplementary Table 11).

Under this stimulatory condition, no significant differences were found. The biggest signal difference was observed after 4h. When 311 and both chelators were added to the cells after calcein staining, the rises in the mean MFIs (labile iron amounts) of three experiments were 31,8 (from 121,5 in calcein-only treatment to 153,3 upon chelator addition) and 30,5 (152 in chelator treated cells), respectively. In BIP treated cells the elevation was, with 12,2 (133,7 in treated cells), less marked.

24h of stimulation only show a slight increase of 6,2 in the signal upon 311 utilization (107 in untreated and 113,2 in treated cells). The other chelation conditions show a slight decrease in the mean MFIs of -5,9 (from 107 in untreated to 101,1 in treated cells) and -5,5 (101,1 in

treated cells) in BIP and 311+BIP treated cells, respectively.

48h of activation goes along with an increase of the mean MFI of 18,8 in 311+BIP administered cells (43,8 in calcein-only treated and 62,6 in chelator treated cells). When applied on their own, each chelator increased the mean MFI only marginally (311: to 50,9 (ΔMFI of 7,1) and BIP: to 46,1 (ΔMFI of 2,3).

VIT3 stimulated primary T cells show similar labile iron levels as non-activated cells, with the exception of 4h of stimulation and addition of both chelators, where the mean ΔMFI is increased by 41,2 (from -10,7 in non-activated to 30,5 in stimulated cells), resembling a 1,34-fold higher increase compared to untreated cells. Treatment with each chelator alone on the other hand leads to smaller increases of 8,2 (1,1-fold elevation) and 5,9 (1,06-fold rise) for 311 and BIP respectively. At the 24h time point, LIP levels of non-activated cells are comparatively higher when each chelator was administered alone and about equal upon combination treatment (1,11-fold higher in 311 treated- and 1,17-fold higher in BIP treated cells). 48h of exposure to VIT3 show slight decreases of -2,2 for 311 (1,07-fold higher in resting cells) and -7 for BIP treated cells (1,2-fold higher in resting cells) and a weak increase of 5,4 upon combination treatment (1,06-fold increase). (Supplementary Table 12) These changes are not statistically significant.
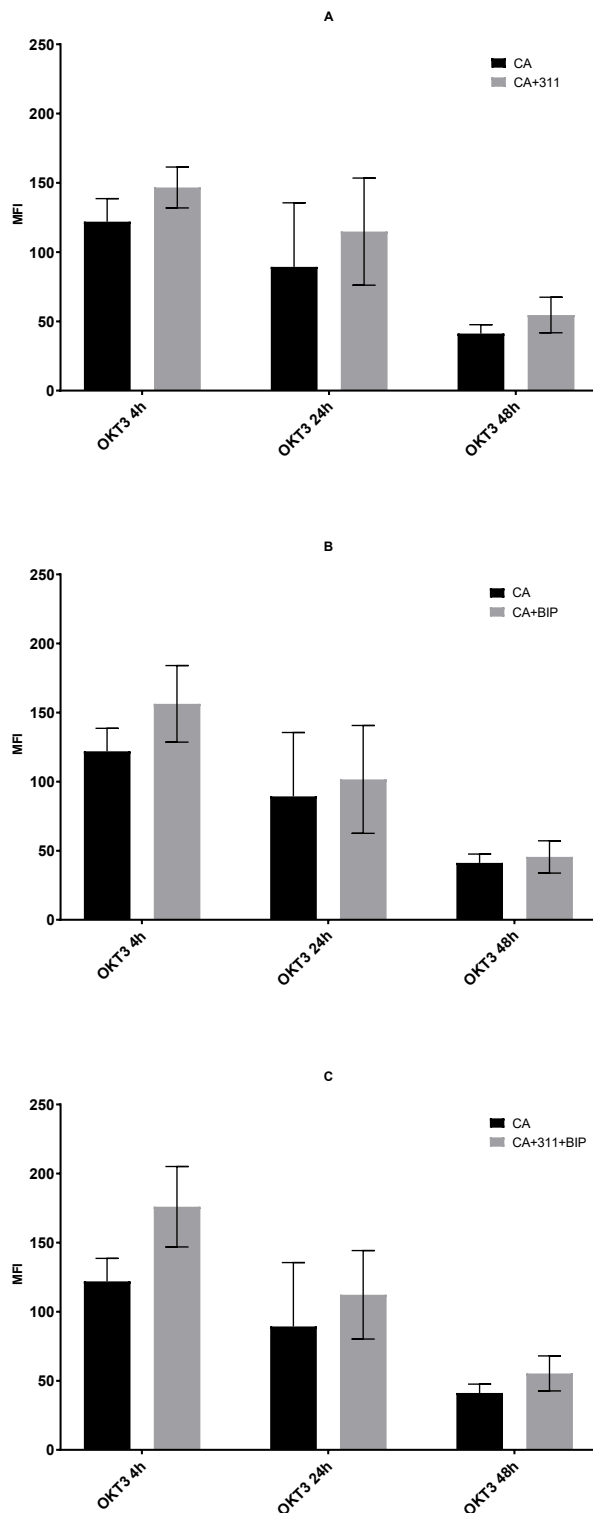
Figure 14: Calcein fluorescence measurements in CD3 (OKT3)-activated primary T cells untreated or treated with 311, BIP or both

Human peripheral blood T cells were incubated for 4h, 24h and 48h with plate bound CD3 (OKT3) mAb and subsequently stained with 15 nM calcein-AM for 15 min. Afterwards, they were incubated with iron chelators for 2h (10 µM of 311 and/or 250 µM of BIP). Bar graphs in (A) - (C) show the Geo Mean fluorescence intensities (MFI) of calcein in primary T cells administered with 311, BIP or both chelators, respectively. Black bars represent cells not treated with chelators. Bars show Geo Means (± SEM) of 3 independent experiments.
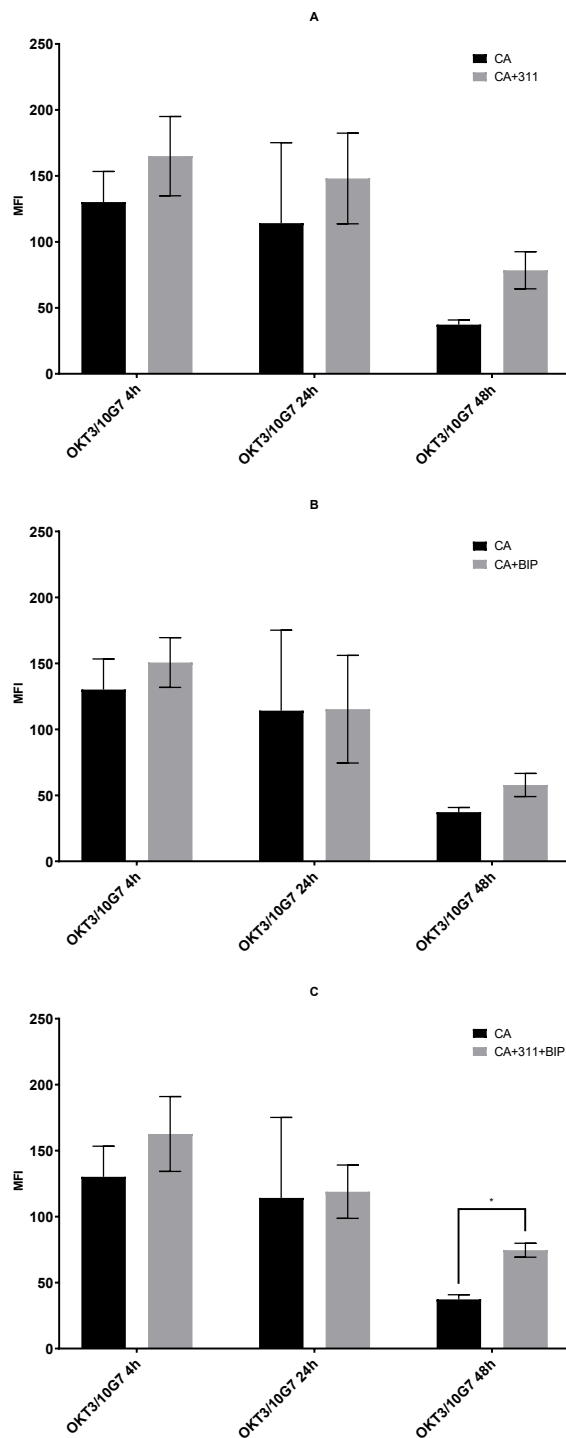
Figure 15. Calcein fluorescence measurements in CD3 (OKT3)/CD43 (10G7)-activated primary T cells untreated or treated with 311, BIP or both

Human primary T cells were stimulated with plate bound mAbs specific for CD3 (OKT3) and CD43 (10G7) for 4h, 24h and 48h and subsequently treated with 15 nM calcein-AM for 15 min. Next, they were incubated for 2h with the iron chelators 311, BIP or both of them together (10 µM of 311 and/or 250 µM of BIP). Bar graphs in (A) - (C) show calcein Geo Mean fluorescence intensities (MFI) in T cells administered with 311, BIP or both chelators, respectively. The black bars represent cells not exposed to chelators. Bars show Geo Means (± SEM) of 3 independent experiments.
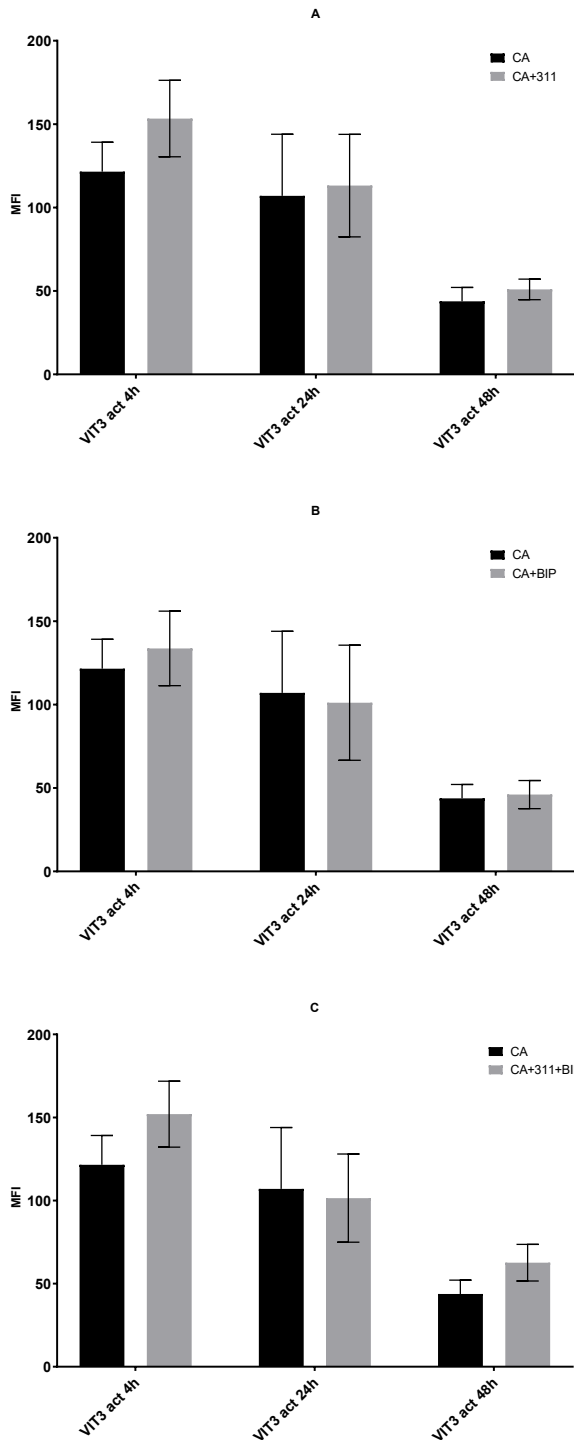
Figure 16. Measurements of calcein fluorescence in CD3 (VIT3)-stimulated primary T cells untreated or treated with 311, BIP or both

Human peripheral blood T cells were exposed to plate bound mAb specific for CD3 (VIT3) for durations of 4h, 24h and 48h, followed by addition of 15 nM calcein-AM for 15 min. Subsequently, they were incubated for 2h with the iron chelators 311, BIP or both of them together (10 µM of 311 and/or 250 µM of BIP). Bar graphs in (A) - (C) depict calcein Geo Mean fluorescence intensities (MFI) in T cells treated with 311, BIP or the combination of both chelators, respectively. Black bars represent cells only exposed to calcein but not to chelators. Bars show Geo Means (± SEM) of 3 independent experiments.
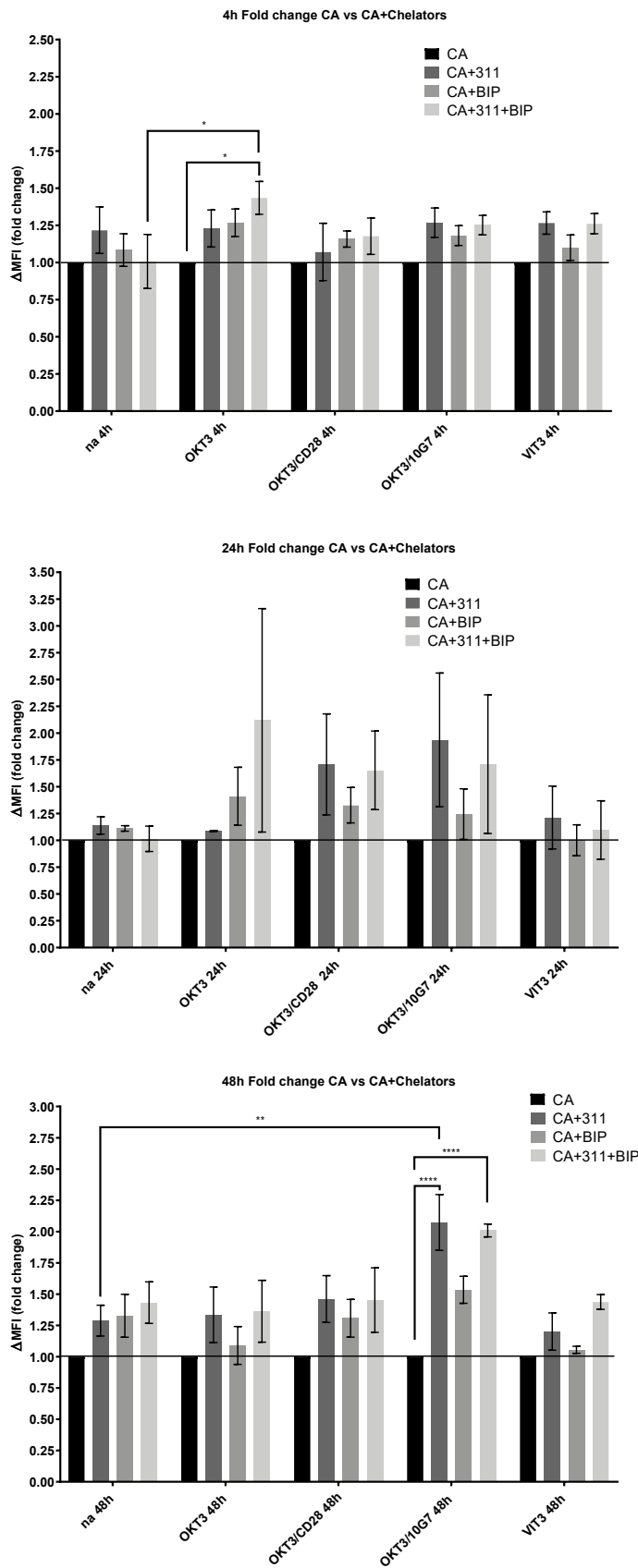
Figure 17. Comparison of calcein MFI values between chelator treated and untreated primary T cells resting or exposed to different activation stimuli

Peripheral blood T cells were incubated with plate bound mAbs specific for CD3 (OKT3 or VIT3), CD3 (OKT3) and CD28, and CD3 (OKT3) plus CD43 (10G7) for 4h, 24h and 48h and subsequently treated with calcein-AM for 15 min. This was followed up by incubation with the iron chelators 311, BIP or both of them in conjunction for 2h. Each bar shows fold changes of calcein Geo Mean fluorescence intensities (MFI) (± SEM) of 3 independent experiments, compared to cells not treated with chelators. Untreated cells, represented by black bars, are set to a value of 1.

Microtubules constitute crucial players in the regulation of cell shape and motility, as well as in intracellular transport processes and cell division.[50,51]

In addition, several aspects of T cell physiology, including their activation and effector functions, are influenced by the microtubule cytoskeleton.[60]

These regulating functions are dependent on their dynamic nature of constant switching between states of polymerization and depolymerization, which results from the binding of GTP to α- as well as β-tubulin monomers and its hydrolysis to GDP.[53]

To get an idea about the influence of various activating stimuli on the microtubule cytoskeleton in T cells, it was stained with α- or β-tubulin specific mAbs.

Abraxane is an albumin-based formulation of the tubulin polymer stabilizing/microtubule assembly promoting drug paclitaxel.[73]

The impact of the drug on the tubulin staining was assessed by incubating the cells with it prior to addition of the mAbs. Geo Mean fluorescence intensities of the, to the antibodies conjugated fluorescent dyes, were determined by flow cytometric measurements.

4.6 Abraxane treatment of resting Jurkat cells leads to a trend of increased mAb binding to tubulin compared to untreated cells

Addition of abraxane to primary T cells cultivated for three different periods of time was observed to mostly lead to trends of increases in the mean tubulin fluorescence signal intensities of three independent experiments. The biggest rise of 18,7 was seen at the 24h time point in cells stained with α-tubulin mAb (mean MFI of 36 in abraxane treated and 17,3 in untreated cells) (Figure 18 C). This was followed by an elevation of 13,5 in the mean α-tubulin mAb signal of cells resting for 4h which were exposed to abraxane (mean MFI of 36,1 in abraxane treated and 22,6 in untreated cells) (Figure 18 A). After 48h of incubation, abraxane treatment led to an increase of 9 in α- and 2,6 in β-tubulin administered cells (Figure 18 E and F). Addition of the drug to cells cultivated for 4h that were later stained with β-tubulin mAb, seemingly led to a slight decrease in the MFI compared to untreated cells (ΔMFI of -0,1 with an MFI of 12,6 in untreated and 12,5 in abraxane- treated cells) (Figure 18 B). β-tubulin staining at the 24h time point led to a mean increase of 2,9 (8,7 in untreated and 11,6 in abraxane treated cells) (Figure 18 D) (Supplementary table 13).

Interestingly, in resting Jurkat cells, mean MFI values drop upon administration of abraxane in α-tubulin stained cells after 4h of cultivation by 31,3 (203,7 in untreated and 172,3 in treated cells) (Figure 19 A) and in 48h-resting cells also stained with α-tubulin mAb by 71,5 (from 358,5 in untreated to 287 in treated cells) (Figure 19 E). At 4h, the β-tubulin stained cells, however do not show a drop in the signal, but a rise by 16,1 (55,1 in untreated compared to 71,2 in treated cells) after the drug was added (Figure 19 B). Like α-Tubulin, β-

tubulin stained cells show a decrease in the mean MFI after 48h. However, with 16 (152,3 in untreated vs. 136,3 in abraxane treated cells), this difference is smaller.

α- as well as β-tubulin stained Jurkat cells, cultivated for 24h, show signal elevations of 114,9 (270,8 in untreated vs. 385,7 upon abraxane administration) and a significant 39,6 (76,2 in untreated cells and 115,8 when the drug was applied), respectively (Figure 19 C and D) (Supplementary table 14). With exception of the latter, the mentioned changes between abraxane treated and untreated cells were not statistically significant.

4.7 Primary and Jurkat T cells costimulated via CD28 show increased tubulin binding by mAbs when treated with abraxane

When primary T cells were treated with abraxane after being stimulated with mAbs binding CD3 (OKT3) and CD28, increases in the mean MFI values compared to untreated cells could be observed.

4h of stimulation and drug treatment led to an apparent increase in the α-tubulin signal by 22,9 (51 in untreated and 73,9 in drug-treated cells) (Figure 18 A). In comparison, the increase in the mean MFI of the β-tubulin mAb was, with 3,7 (15,3 in untreated vs. 19 in cells administered with abraxane), considerably lower (Figure 18 B).

After 24h of activation, α-tubulin stained cells showed an increase from 73,3 to 149,4 when treated with abraxane (ΔMFI of 76,1) (Figure 18 C). The β-tubulin mean MFI was raised from 22,6 to 28,1 in drug administered cells, resulting in a ΔMFI of 5,5 (Figure 18 D). These trends towards rises were not significant.

At the 48h time point, abraxane addition led to a significant 3,26-fold mean increase (of three experiments) of the mean MFI by 110 (from 63,3 to 173,3) in α-tubulin stained cells (Figure 18 E) and to an almost significant (p=0,056) 1,84-fold rise of 17,3 (from 19,6 to 37) in β-tubulin stained cells (Figure 18 F) (Figure 20 and supplementary table 15).

At the same time point, the MFI of α-tubulin stained cells treated with abraxane differed significantly from the ones in resting, CD3 (OKT3) stimulated- and CD3 (VIT3) stimulated primary T cells (173,3 as opposed to 33,7 in resting-, 52,4 in OKT3-stimulated- and 49,8 in VIT3-stimulated cells) (Figure 18 E). In β-tubulin stained cells exposed to the drug, a significant increase compared to resting cells was detected (37 vs. 10,5 in resting cells) (Figure 18 F) (Figure 20).

Comparing the ΔMFI values to resting primary T cells, there were two values standing out. After 24h of stimulation with CD3 (OKT3) and CD28 and treatment with abraxane, the mean ΔMFI in α-tubulin mAb stained cells was higher than the one in resting cells by 57,4 (18,7 vs. 76,1). α-tubulin mAb stained cells stimulated for 48h, showed an elevation of 101 (9 vs. 110) when stimulated compared to resting cells. β-tubulin mAb mean ΔMFIs at this time points,

however differed by smaller degrees. After 24h, it was elevated by 2,6 (2,9 vs. 5,5) and after 48h by 14,7 (2,6 vs. 17,3) in stimulated cells. At the 4h time point, the increase was smaller, with 9,4 (13,5 vs. 22,9) for α- and 3,8 (-0,1 vs. 3,7) for β-tubulin stained, abraxane treated and stimulated cells (Supplementary table 20). Those differences were not of statistical significance.

Abraxane treatment of CD3/CD28 stimulated Jurkat cells led to increases of the mean MFI values at all three observed time points compared to untreated cells.
After 4h of stimulation, the value rose by 195,7 (221,3 in abraxane administered and 417 in untreated cells) in α-tubulin stained cells, thereby being significantly higher than in resting, drug treated cells (where they are at 172,3). Cells treated with β-tubulin mAb showed a mean elevation by 22,5 (66,8 in cells not administered with the drug and 89,3 when abraxane was added) (Figure 19 A and B).
The rise in cells stimulated for 24h was with 132,5 (361 vs. 493,5 when abraxane was added) 1,4-fold and with 67,8 (66,2 vs. 134 in abraxane treated cells) 2-fold, for α- and β-tubulin stained cells, respectively, with the latter being of statistical significance (Figure 19 C and D and Figure 20).
When stimulated for 48h, mean MFI values were shown to be elevated from 331,5 to 454,5 (ΔMFI of 123) in cells stained with α-tubulin mAbs and treated with abraxane. In β-tubulin stained cells, an elevation from 92,3 to 116,3 (ΔMFI of 24) could be observed (Figure 19 E and F and supplementary table 16). With the exception of the mentioned rise in the MFI of 24h stimulated, β-tubulin stained cells, there were no significances found in the apparent elevations after abraxane addition.

Mean ΔMFIs in Jurkat cells stimulated via CD3/CD28 were higher than in resting Jurkat cells after all time points of activation. The biggest difference of 227 (-31,3 compared to 195,5 in activated cells) was observed after 4h in cells stained for α-Tubulin. β-tubulin mAb treated, stimulated cells showed an increase of 6,4 in comparison to non-activated cells (with 16,1 in resting and 22,5 in activated cells).
With 194,5 (-71,5 in resting vs. 123 in stimulated cells) the second biggest increase was detected at the 48h time point in α-tubulin stained cells. Cells exposed to β-tubulin mAb showed a ΔMFI higher by a value of 40 (-16 vs. 24 in CD3/CD28 stimulated cells) compared to resting cells.
After 24h of stimulation, the mean increase in the MFI upon abraxane treatment was bigger by 17,6 (114,9 in resting and 132,5 in activated cells) in α-Tubulin- and by 28,2 (39,6 vs. 67,8 in stimulated cells) in β-tubulin mAb administered cells, compared to resting cells (Supplementary table 21). Here, no statistically significant differences were found.

4.8 Anti-tubulin mAbs show an inclination towards improved binding in CD3 (OKT3) stimulated, abraxane treated primary T cells, compared to untreated cells

Exposure of CD3 (OKT) stimulated primary T cells to abraxane, also led to increases in mean tubulin mAb MFI values. The biggest elevation can be observed in cells stimulated for 24h and stained with fluorescent dye conjugated mAb targeting α-Tubulin. Here an elevation of 40,1 was calculated, with a value of 55,6 when no abraxane was administered and 95,7 upon addition of the drug (Figure 18 C).

The second biggest increase was, with 33,9 (47,4 in cells not treated with abraxane and 81,3 when the drug was used), detected in α-tubulin stained cells stimulated for 4h (Figure 18 A). This was followed by α-tubulin mAb treated cells stimulated for 48h, where a rise of 20,6 (31,8 vs. 52,4 in drug treated cells) was detected, when abraxane was added (Figure 18 E). With 16,5 (13,7 without- vs. 30,2 upon abraxane treatment), the next highest change has been spotted in β -Tubulin stained cells exposed to CD3 (OKT3) mAb for 4h (Figure 18 B). β-tubulin staining in 24h and 48h stimulated cells treated with abraxane, showed mean increases of 3,2 (16,3 as opposed to 19,5) and 2,9 (15,2 compared to 18,1), respectively. (Figure 18 D and F) (Supplementary table 17). Statistically significant differences were not observed.

Comparing the rises in the mean tubulin mAb MFI values in abraxane treated, CD3 (OKT3) stimulated peripheral blood T cells to the ones in resting cells, trends towards increases (non-significant) could be observed at all time points when α- and β-tubulin were stained. The most pronounced elevation was observed at the 24h time point in α-tubulin mAb treated cells. Here, the ΔMFI was higher by 21,4 (18,7 in resting and 40,1 in CD3 (OKT3) stimulated cells) compared to resting cells. This was followed by the increase in the mean ΔMFI in α-tubulin stained cells at after 4h of stimulation, which was 20,4 (from 13,5 in resting to 33,9 in stimulated cells).

β-tubulin stained cells at the same time point show the next highest increase of 16,6 (-0,1 vs 16,5 in CD3 (OKT3) stimulated cells).

While cells stimulated for 48h and stained for α-tubulin show a rise of 11,6 (9 in resting and 20,6 in stimulated cells), β-tubulin stained cells only showed an increase of 0,3 (2,6 vs. 2,9 in stimulated cells). Likewise, β-tubulin mAb treated cells show an increase of 0,3 (2,9 vs. 3,2 when cells were stimulated) at the 24h time point (Supplementary table 22).

4.9 Abraxane treated, CD43 costimulated primary T cells display trends of rising anti-tubulin mAb binding as opposed to untreated cells

Primary T cells stimulated with a combination of mAbs specific for CD3 (OKT3) and CD43

(10G7) for 4h and 48h, were observed to show a trend towards rising mean MFI values of α- and β-tubulin specific mAb when abraxane was added to them.

At the 4h time point, MFIs were elevated by 17,4 (from 39 in untreated to 56,4 in drug treated cells) and 6,3 (14,4 without- and 20,7 with abraxane addition) for α- and β-tubulin mAbs, respectively (Figure 18 A and B).

48h of stimulation showed increases of 33,6 (65 in non-treated vs. 98,7 in drug treated cells) in the mean α-tubulin MFI and 3,7 (26,4 in untreated- compared to 30,1 in treated cells) in the mean β-tubulin MFI (Figure 18 E and F).

After 24h of stimulation, a small rise in the mean MFI from 26,5 in untreated- to 32,1 in abraxane treated, β-tubulin stained cells (ΔMFI of 5,6) was spotted. However, the value drops after drug administration in α-tubulin stained cells from 98,1 to 94 (ΔMFI of -4,1). (Figure 19 C and D) (Supplementary table 18). Changes in these values are not of statistical significance.

4h of stimulation and abraxane addition led to higher tubulin mAb mean ΔMFI values compared to non-activated cells. The α-tubulin ΔMFI increased from 13,5 to 17,4 (Difference of 3,9) and the β-tubulin stained cells showed an increase of 6,4 (-0,1 in resting and 6,3 in stimulated cells).

After 24h of stimulation, the ΔMFI in α-tubulin stained cells decreased by 22,8 (from 18,7 in resting to -4,1 upon activation). However, this apparent reduction was not observed in cells treated with β-tubulin mAb, where it increased by 2,7 (from 2,9 to 5,6 in activated cells).

At the 48h time point, elevations of 24,6 (9 vs. 33,6) and 1,1 (2,6 vs. 3,7) in the mean ΔMFIs were detected in α- and β-tubulin stained cells, respectively (Supplementary table 23). Again, no statistical significances were observed in these changes.

4.10 CD3 (VIT3) stimulated primary T cells treated with abraxane show trends towards elevated anti-tubulin mAb binding compared to untreated cells

Administration of abraxane to primary T cells stimulated via the CD3 mAb clone VIT3, led to non-significant increased mean tubulin mAb MFI values after all three time points of activation.

4h of stimulation show elevation of the values by 16,3 (44,5 vs. 60,8 in abraxane treated cells) and 5,6 (10,9 vs. 16,5) in α- and β-tubulin stained cells, respectively (Figure 18 A and B).

After 24h of stimulation, the mean value in α-tubulin mAb treated cells shows a rise of 30 (58,1 vs. 88,1) and the one in cells stained for β-tubulin was observed to show an elevation

from 15,9 to 21,4 (ΔMFI of 5,5) (Figure 18 C and D).

At the 48h time point, mean MFIs of α- and β-tubulin stained cells are elevated by 18,2 (31,6 in cells not treated with abraxane compared to 49,8 in treated cells) and 3,9 (11 vs. 14,9 when the drug was administered), respectively (Figure 18 E and F) (Supplementary table 19).

Looking at the mean ΔMFIs of CD3 (VIT3) stimulated primary T cells, non-significant increases could be detected after all three observed time points when α- as well as β-tubulin were stained, in comparison to resting T cells. At the 4h time point, the values were elevated by 2,8 (13,5 in resting and 16,3 in stimulated cells) and 5,7 (-0,1 vs. 5,6) for α- and β-tubulin mAb exposed cells, respectively.

Stimulation for 24h went hand in hand with mean rises of 11,3 (18,7 vs. 30) upon α-tubulin staining and 2,6 (2,9 vs. 5,5) in β-tubulin stained cells.

48h of stimulation showed mean increases of 9,2 (9 vs. 18,2) in α- and 1,3 (2,6 vs. 3,9) in β-tubulin mAb treated cells over resting cells (Supplementary table 24).
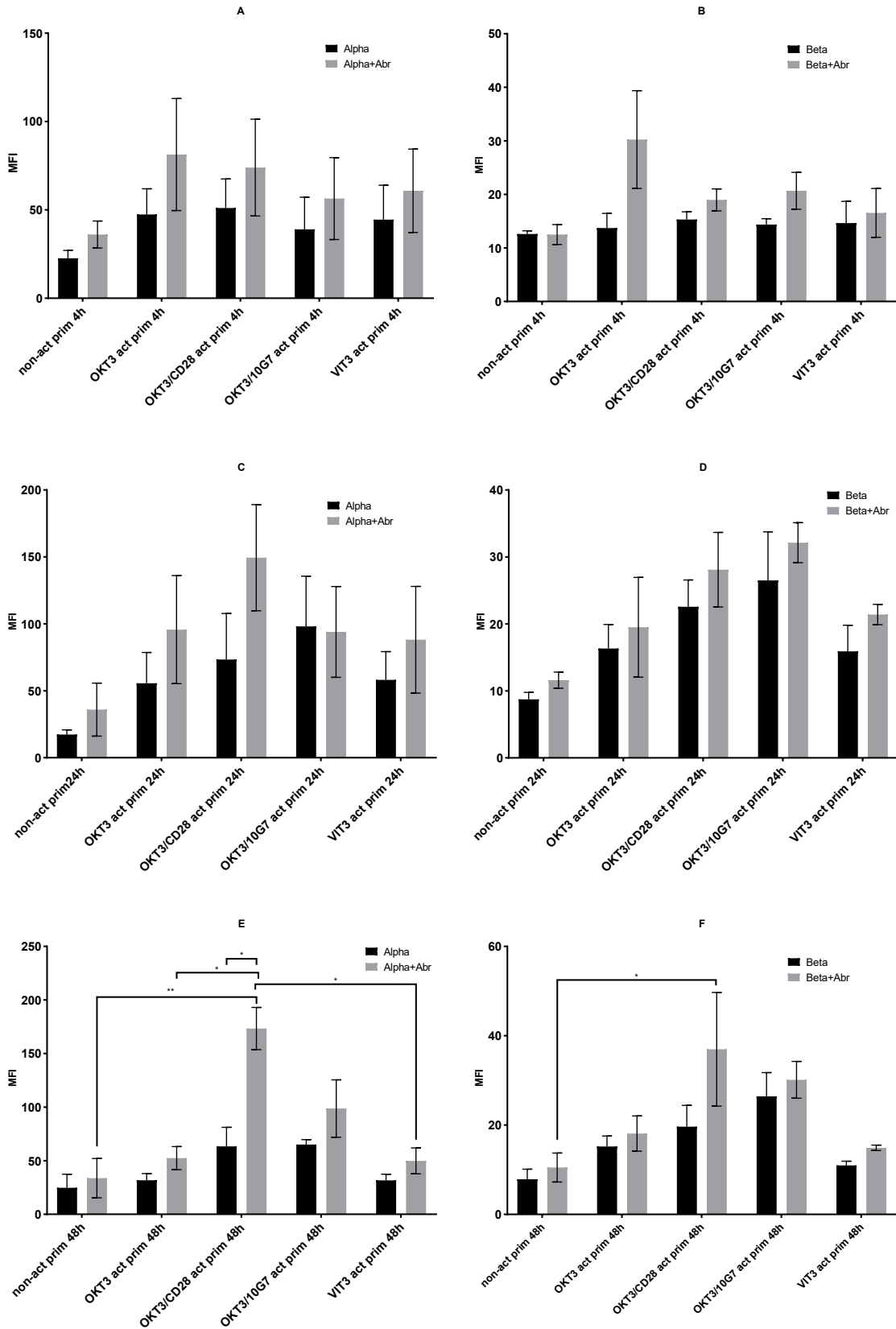
Figure 18. Tubulin mAb MFI values in primary T cells resting or activated with different stimuli and exposed to abraxane or not

Primary T cells were resting or stimulated with mAbs directed against CD3 (OKT3 or VIT3),

CD3 (OKT3) and CD28 or CD3 (OKT3) and CD43 (10G7) for 4h (A and B), 24h (C and D) and 48h (E and F), followed by treatment with abraxane for 2h. Subsequently, they were treated for 20 min with mAbs specific for α- or β-tubulin, conjugated with fluorescent dyes. Bars show Geo Mean fluorescence intensities (MFI) (± SEM) of 3 independent experiments.
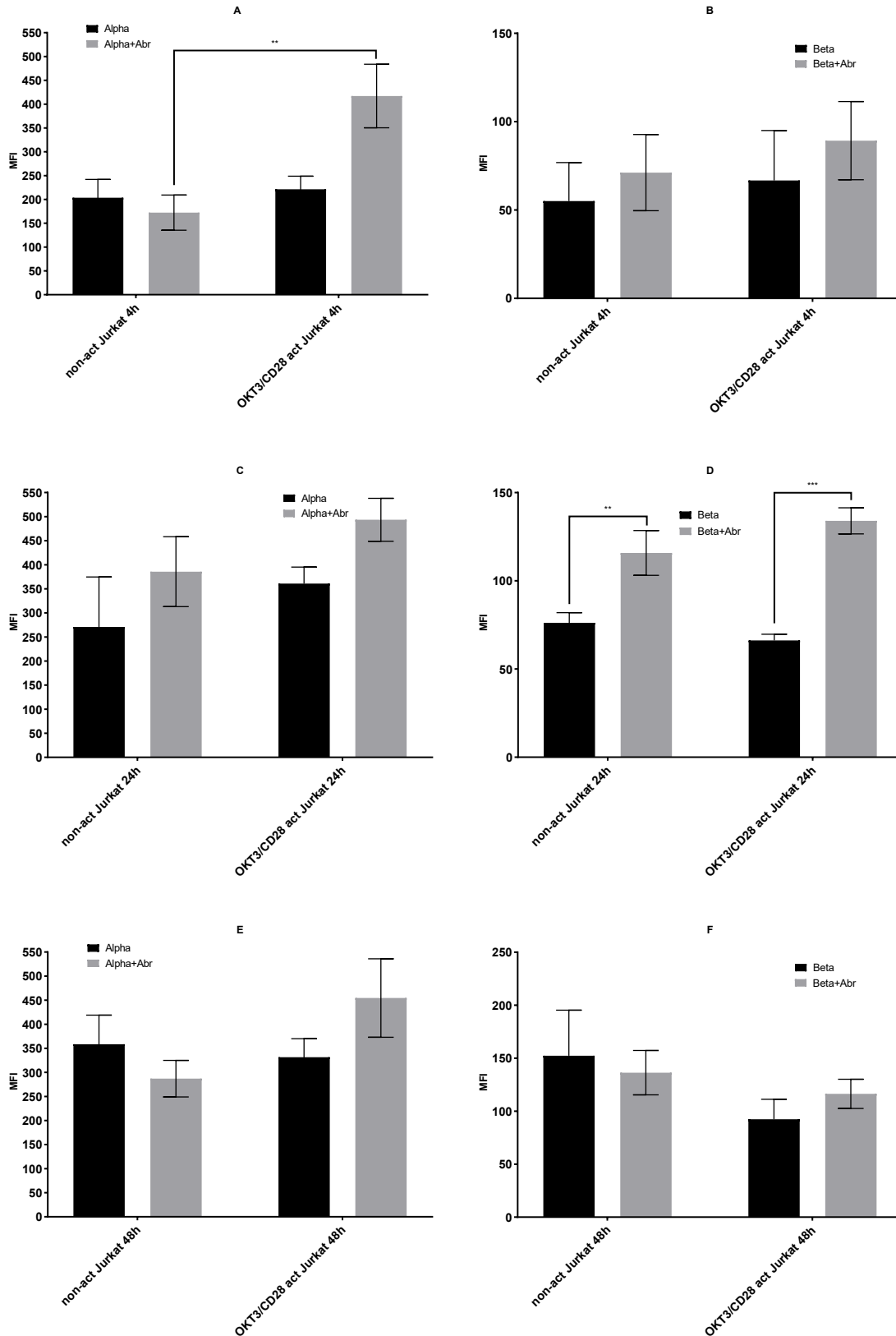
Figure 19. Tubulin mAb MFI values in Jurkat cells resting or activated via CD3 (OKT3)/CD28 and exposed to abraxane or not

Jurkat cells were resting or stimulated with mAbs directed against CD3 (OKT3) and CD28 for 4h (A and B), 24h (C and D) and 48h (E and F). Subsequently they were treated with

abraxane for 2h, followed by staining with mAbs targeting α- or β-tubulin for 20 min. Bar graphs show Geo Mean fluorescence intensities (MFI) (± SEM) of 3 independent experiments.
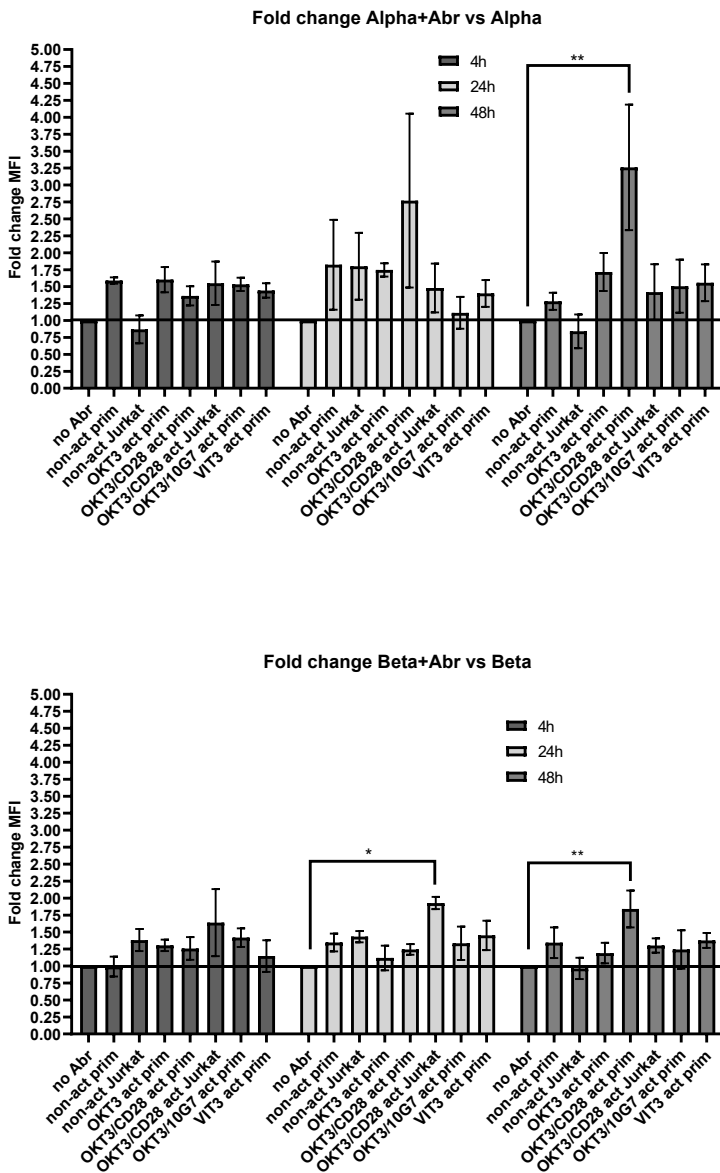
Figure 20. Comparison of the influence of abraxane on tubulin mAb MFI values in differently stimulated T cells
Human peripheral blood T cells were resting or stimulated for 4h, 24h or 48h, using mAbs specific for CD3 (OKT3 or VIT3), CD3 (OKT3) plus CD28 or CD3 (OKT3) plus CD43 (10G7). Jurkat T cells were either stimulated with mAbs directed against CD3 (OKT3) and CD28 for the same periods of time, or resting without stimulus. Subsequently, abraxane was added to the cells for 2h, which was followed by staining with α- or β-tubulin targeting mAbs (A and B, respectively) conjugated to fluorescent dyes, for 20min. Fluorescences were measured by flow cytometry. Each bar shows fold changes of tubulin mAb Geo Mean fluorescence intensities (MFI) (± SEM) of 3 independent experiments, upon abraxane treatment, compared to cells not treated with the drug. Corresponding untreated cells, represented by the first bars in each group, are set to a value of 1.

5. Iron chelators 311, BIP, as well as the combination of both do not influence binding of the used tubulin mAbs to their substrates

To get an idea whether the iron chelators 311 and BIP have an influence on the microtubule cytoskeleton, resting Jurkat cells were administered with each of them alone or with their combination for 2h, followed by α- or β-tubulin staining. Fluorescence intensities were measured by flow cytometry to show if binding capacities of the mAbs to tubulin/microtubules differ from cells not treated with chelators.

Comparing the mean MFI value (of 3 independent experiments) of untreated α-tubulin stained- (121,8) to the one of 311 treated cells (123,8), a 1,02-fold increase was calculated. BIP treatment (leading to a mean MFI of 124,1) had a very similar effect with again a 1,02-fold increase in the mean. When both chelators were used, the value was 1,2 times higher than in untreated cells (144,5).

Looking at cells treated with β-tubulin mAb, a mean MFI value of 65,7 was measured in untreated cells. 311 administration showed a value of 59,4 (0,1-fold lower) and BIP treatment was observed to lead to a mean MFI of 67,9 (1,03-fold increase). When both chelators were added, a value of 63,2 was observed (0,96 times that of untreated cells). All of these differences are statistically not significant. (Figure 21)

α- and β-tubulin stained Jurkat cells ± iron chelators
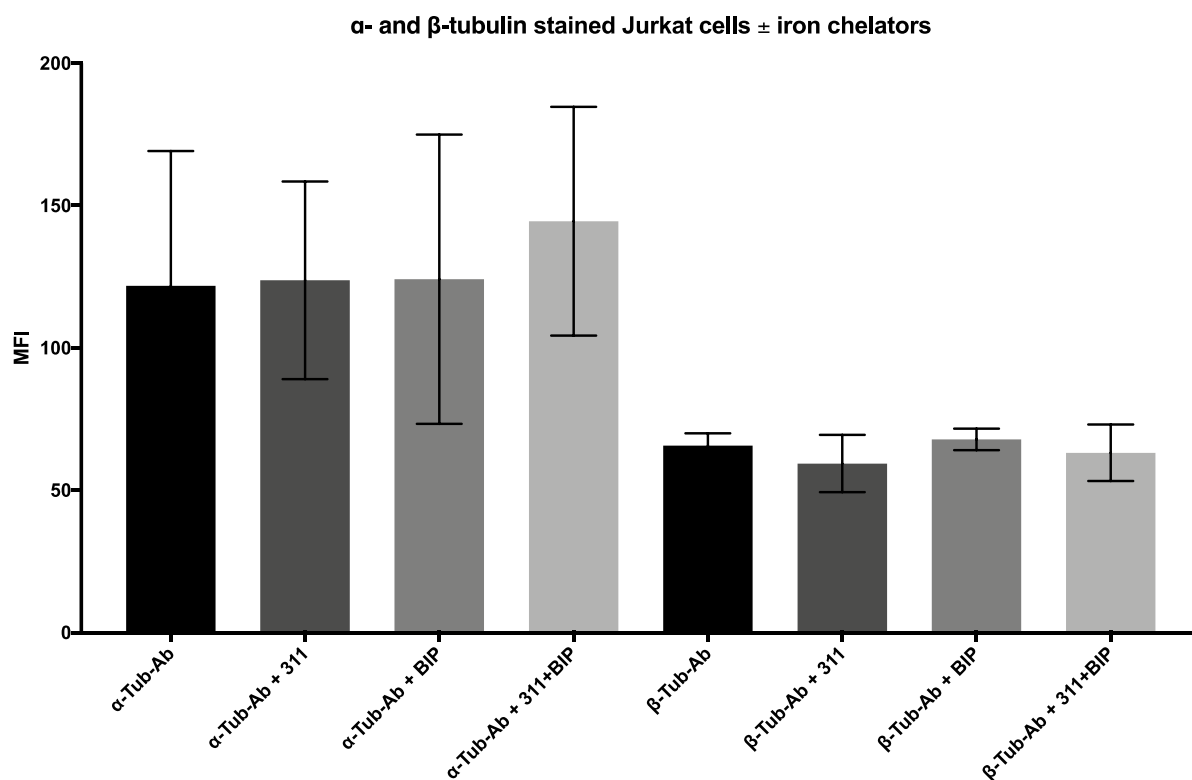
Figure 21. MFI values of 311, BIP and 311+BIP treated Jurkat cells compared to untreated cells, stained for α- or β-tubulin

Jurkat cells were treated with iron chelators for 2h before subjecting them to fluorescent dye conjugated α- or β-tubulin mAbs for 20 min. Fluorescence intensities were measured by flow cytometry. Bars show tubulin mAb Geo Mean fluorescence intensities (MFI) (± SEM) of 3 independent experiments.

6. Discussion

Iron was shown to be necessary for a multitude of cellular processes, comprising DNA replication and cell proliferation.[94] The majority of cytosolic, unmetabolized iron is firmly bound to proteins like ferritin. A tiny fraction of it is only weakly associated with low-molecular weight compounds, making it catalytically active and prone to participate in electron transfer in the Fenton reaction which produces the ROS hydroxyl radical. This radical can cause peroxidation of lipids and protein denaturation leading to damage of organelles and ultimately cell death.[97,119]

Yarosz et al. showed steady downregulation of the LIP in $CD4^+$ and $CD8^+$ murine T cells upon stimulation with mAbs directed against CD3 (plate-bound, 5 μg/ml) and CD28 (soluble, 1 μg/ml) for 1, 2 and 3 days. A downregulation was also observed in $CD4^+$ human peripheral blood T cells activated in the same way, but with a CD28 mAb concentration of 2 μg/ml and

over a period of five days.[103]

To find out whether the LIP is regulated in a comparable way in Jurkat and peripheral blood T cells when stimulated with plate bound CD3 and CD28 specific mAbs, and how further activating stimuli influence labile iron levels in primary T cells, they were seeded in plates coated with the according mAbs for three different periods of time.
Even though there were no significant signal differences detected between chelator treated and untreated resting primary T cells, MFIs were shown to significantly decrease between 4h and 48h of cultivation. This could indicate that the iron concentration in the LIP increases over time of cultivation, leading to dampened calcein signal intensities. Should this be the case, this would mean that primary T cells either increasingly take up iron into the LIP from the extracellular space over time or that intracellular iron gets progressively incorporated into the LIP over time. Longer cultivation without receiving growth stimuli could lead to lower needs for iron and therefore partial transfer of it to the LIP.
4h CD3 (OKT3) stimulated primary T cells treated with 311 in conjunction with BIP, showed a significant 1,4-fold increase compared to untreated cells.
Comparing this increase to the change in resting primary T cells upon 311+BIP administration, shows a further significant 1,42-fold increase, implying a rise in the LIP in CD3 (OKT3) stimulated primary T cells compared to unstimulated cells.

Another statistically significant increase could be observed in the calcein fluorescence values of primary T cells stimulated for 48h with CD3 (OKT3)/CD43 (10G7), when 311+BIP were administered, compared to untreated cells (Figure 15). Here the mean MFI was 2-fold higher (from 37,3 to 74,5). A further significant 2,1-fold rise could be observed at the same time point, upon 311 treatment on its own (Figure 17). This could indicate a stronger contribution of Fe^{3+} to the pool of labile iron than Fe^{2+}, even though iron is normally released from the storage and transport proteins ferritin and transferrin into the cytosolic LIP after it has been reduced from the ferric into the ferrous state.[99] However, oxidation processes could convert ferrous to ferric iron and the oxidized form might accumulate in the cytoplasm after longer times of cultivation where chelators can access it. To test for this indirectly, concentrations of hydroxide radical, a byproduct of the Fenton reaction producing Fe^{3+} from Fe^{2+}, could be determined, e.g. via hydrogen abstraction where the radical can remove an aliphatic α-H from an amine containing fluorescent sensor, converting the amine to an imine and therefore leading to a change in fluorescence.[119] Rising levels could indeed indicate elevated Fe^{3+} levels originating from oxidation of ferrous iron.

Compared to resting primary T cells, the fold increase upon 311 addition in relation to cells not treated with chelators, is significantly higher (1,6-fold) when cells were stimulated via CD3 (OKT3)/CD43 (10G7) for 48h. When both chelators were added, an almost significant (p=0,055) 1,4-fold rise has been detected at the same time point (Figure 17). This finding implies an increase of the LIP in cells exposed to these stimuli for 48h compared to unstimulated cells, with ferric iron probably contributing to the pool to a greater extent than ferrous iron.

In Jurkat cells, significant differences in the MFIs were observed when comparing chelator treatment with no treatment when they were resting for 48h and when they were stimulated via CD3 (OKT3) and CD28 for 4h and 48h.
After 48h of resting, 311 treated cells showed a mean 1,75-fold increase compared to untreated cells. BIP administration led to a 1,53-times elevation and addition of both chelators brought about a 1,59-fold rise.
Stimulation for 4h led to a 0,1 times lower MFI in BIP administered cells, which was not observed in the other conditions. Exposure to the stimuli for 48h led to a mean 1,4-fold MFI increase when 311 was added. Treatment with BIP raised the signal 1,3-fold and addition of both chelators increased it 1,36-fold.
In both cases the signal increase was higher in 311 treated compared to BIP treated samples, which again indicates ferric iron to contribute stronger to the LIP than ferrous iron.

Since Jurkat cells are cancer cells, they receive sustaining proliferative signals, making the here mentioned resting cells actually growth-stimulated ones.[120]
Therefore, their LIP levels cannot be compared to the ones of unstimulated/resting primary T cells.
The increases after stimulation are significantly smaller compared to the ones in resting Jurkat cells (22% smaller in 311 treated-, 13% smaller in BIP administered- and 15% smaller in 311+BIP treated cells), indicating a CD3 (OKT3)/CD28 stimulation dependent reduction of the LIP levels.

This reduction could be explained by CD28 costimulation dependent increased export of intracellular iron into the culture medium as described by Yarosz et al.[103]
Stimulation of primary T cells for 4h via CD3 (OKT3) and for 48h via CD3 (OKT3)/CD43 (10G7) may lead to less iron export out of the cells compared to resting T cells explaining the observed increase in intracellular LIP levels. Levels of extracellular iron in the culture medium could be measured by inductively coupled plasma mass spectrometric analysis of cell supernatants.[103]

Alternatively, such increases might be caused by higher usage of labile iron during cell proliferation initiated under these stimulatory conditions to support the function of factors involved in metabolic activity, followed by its replenishment leading to higher levels compared to the baseline. The decreased levels in CD28 costimulated Jurkat cells may also be explained by higher demands of labile iron upon stimulation, without subsequent replenishment of it or replenishment to levels below baseline after the observed period of time.

During oxidative phosphorylation in mitochondria, which CD4$^+$ and CD8$^+$ T cells rely on for proliferation, multiple iron-sulfur clusters are needed for properly functioning complexes I, II and III of the electron transfer complex.[121,122] Iron for this clusters might be provided by the LIP.

DNA replication, an indispensable prerequisite for cells to proliferate, is also dependent on iron which can be provided by the LIP.[123,122]

Formation of bigger homotypic clusters observed in T cells costimulated with CD43 (10G7) compared to CD28 costimulation and CD3 stimulation alone [43] could lead to higher demands of labile iron.

As an essential part of the eukaryotic cytoskeleton microtubules fulfill structural functions required during processes like cell division, the change of cell shape and intracellular transport via motor proteins of the dynein and kinesin families.[58,59]

Strengthening and maintenance of TCR signaling, as well as its downregulation are dependent on the coordination of signaling component containing microclusters by the microtubule cytoskeleton.[68]

The constant alteration between phases of polymerization and depolymerization in microtubules bestows a highly dynamic nature on them.[61]

This can be counteracted by the cancer drug abraxane which consists of paclitaxel packed into human serum albumin-based nanoparticles and shows a microtubule stabilizing effect, thereby interfering with functions of microtubules which rely on their dynamic nature. In this way, mitosis and multiple other processes including cell motility get inhibited.[84,124]

To investigate the effect of different activating stimuli on the microtubule cytoskeleton of primary and Jurkat T cells and the effect of abraxane on it under these conditions, cells were treated with the drug prior to intracellular staining of α- and β-tubulin.

After 24h of resting and of stimulation with mAbs specific for CD3 (OKT3) and CD28, the β-tubulin MFI was 1,5-fold and twofold higher, respectively in Jurkat cells treated with abraxane compared to untreated cells.

In primary T cells having received the same stimulatory signals for 48h, a 3,3-fold increase of

the α-tubulin MFI value was observed when the drug was added. When they were stained for β-tubulin, a significant 1,84-fold elevation was detected.

These increases imply improved binding of the corresponding tubulin specific mAbs to microtubules/tubulin in abraxane treated T cells compared to untreated cells after the mentioned time points of resting and CD3 (OKT3)/CD28 stimulation. This was not observed in cells stimulated with other mAbs. Furthermore, MFI values after abraxane treatment and tubulin staining in Jurkat (only α-Tubulin) and primary T cells were elevated compared to drug treated resting cells after 4h and 48h of CD28 costimulation, respectively. Taken together, this suggests the tubulin mAbs to bind more effectively to stabilized/polymerized microtubules in resting Jurkat cells, as well as in Jurkat and peripheral blood T cells stimulated via CD3 (OKT3)/CD28, and the stimulation to lead to increased microtubule/tubulin polymerization compared to resting cells.

T cell proliferation is more pronounced after stimulation via this route compared to the other activation conditions.[43,18,125] Therefore, it is likely that more cells in these samples were in the process of mitosis, which would go along with the formation of more mitotic spindles. As mentioned before, microtubules polymerize in the prometaphase of mitosis to push chromatids to the equatorial plate.[66]

Inhibition of their depolymerization by abraxane would lead to a higher count of elongated microtubules compared to samples of resting or differently stimulated cells, resulting in higher binding rates of mAbs and therefore stronger fluorescence signal intensity.

Stimulation of T cells in this way may go along with increased signaling microcluster transport activity along microtubules e.g. to localize signaling molecules to the center of the contact site with the anti-CD3 and CD28 mAbs. When stimulated with an antigen presented by an APC this is what is thought to occur at the immunological synapse.[68]

To provide the microtubule tracks required for that, amplified tubulin polymerization would be needed which would be irreversible after the addition of abraxane, leading to higher MFIs. Such an effect might be less pronounced in resting or differently stimulated primary and Jurkat T cells.

CD3 (OKT3)/CD28 stimulation may also induce changes in cell motility based on microtubule elongation and depolymerization, which could enable the cluster formation observed under the microscope. Stabilization of the elongated microtubules by abraxane could subsequently lead to improved mAb binding, resulting in a higher MFI value.

Even though cluster size was smaller in resting, CD3 (OKT3) and CD3 (VIT3) stimulated cells, it was bigger in CD3 (OKT3)/CD43 (10G7) stimulated primary T cells. However, more clusters almost as big as this size were observed after 48h of CD3 (OKT3)/CD28 stimulation

which could coincide with a bigger need for cell motility and therefore microtubule polymerization.

Resting and CD3 (OKT3)/CD28 stimulated Jurkat cells show a similar cluster size and number after 24h under the microscope (Supplementary Figure 1).

There might also be a cumulative effect of the described possibilities.

CD8$^+$ CTL play an important role in the fight against antigenic cancerous target cells.[126] Since primary T cells seem to be affected by abraxane, which might interfere with their activation, proliferative potential and/or migration, their malignant cell-killing function may be compromised upon exposure to the drug.

Treatment of resting Jurkat cells with the iron chelators 311, BIP or both of them prior to staining of their α- or β-tubulin did not show significant changes in the MFI values compared to untreated cells. This suggests exposure to those chelators to not have an impact on binding of the used tubulin specific mAbs to their substrates and therefore on microtubule polymerization rates.
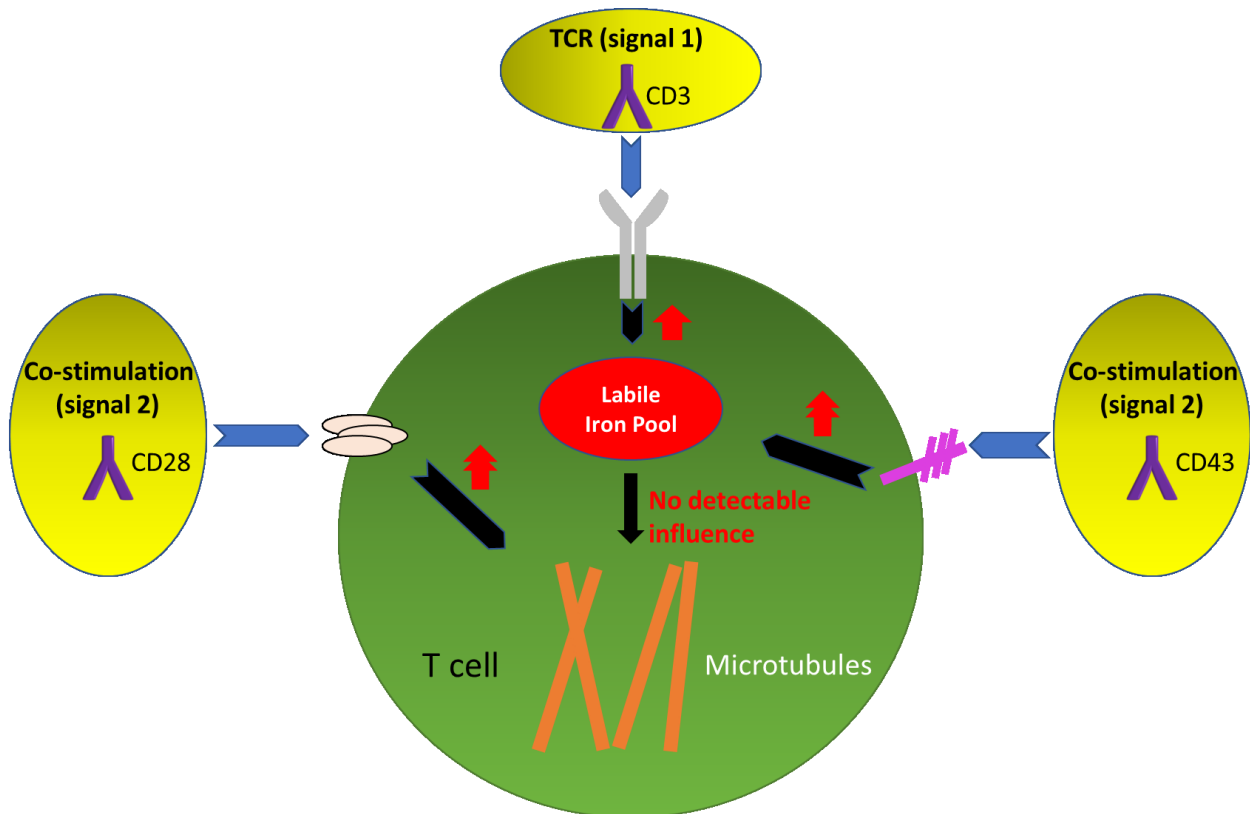
Figure 22. Overview of the conclusion of the study

Labile iron levels are elevated in peripheral blood T cells stimulated via CD3 alone and costimulated via CD43, compared to resting T cells. CD28 costimulation in PB T cells leads to increased microtubule polymerization and additional microtubule-stabilization goes along with enhanced binding of anti-tubulin mAbs.

7. References

1. Abbas AK, Lichtman AH & Pillai S. Cellular and molecular immunology (9th ed.). *Philadelphia: Saunders Elsevier*. 2017

2. Lind EF, Prockop SE, Porritt HE, Petrie HT. Mapping precursor movement through the postnatal thymus reveals specific microenvironments supporting defined stages of early lymphoid development. *J Exp Med*. 2001;194(2):127-134.

3. Alexandropoulos K, Danzl NM. Thymic epithelial cells: antigen presenting cells that regulate T cell repertoire and tolerance development. *Immunol Res*. 2012 Dec;54(1-3):177-90.

4. Klein L, Kyewski B. "Promiscuous" expression of tissue antigens in the thymus: a key to T-cell tolerance and autoimmunity? *J Mol Med* (Berl). 2000;78(9):483-94.

5.   Jordan MS, Boesteanu A, Reed AJ, Petrone AL, Holenbeck AE, Lerman MA, Naji A, Caton AJ. Thymic selection of CD4+CD25+ regulatory T cells induced by an agonist self-peptide. *Nat Immunol*. 2001 Apr;2(4):301-6.

6.   Cosmi L, Maggi L, Santarlasci V, Liotta F, Annunziato F. T helper cells plasticity in inflammation. *Cytometry A*. 2014 Jan;85(1):36-42.

7.   Halle S, Halle O, Förster R. Mechanisms and Dynamics of T Cell-Mediated Cytotoxicity In Vivo. *Trends Immunol*. 2017 Jun;38(6):432-443.

8.   Nagata S, & Golstein, P. The Fas death factor. *Science*. 1995; 267(5203), 1449–1456.

9.   Sakaguchi S, Sakaguchi N, Asano M, Itoh M, Toda M. Immunologic self-tolerance maintained by activated T cells expressing IL-2 receptor alpha-chains (CD25). Breakdown of a single mechanism of self-tolerance causes various autoimmune diseases. *J Immunol*. 1995 Aug 1; 155(3):1151-64.

10.   Acuto O, Michel F. CD28-mediated co-stimulation: a quantitative support for TCR signalling. *Nat Rev Immunol*. 2003 Dec;3(12):939-51.

11.   Kuhns MS, & Badgandi HB. Piecing together the family portrait of TCR-CD3 complexes. *Immunological Reviews*. 2012; 250(1), 120–143.

12.   Brdicka T, Kadlecek TA, Roose JP, Pastuszak AW, Weiss A. Intramolecular regulatory switch in ZAP-70: analogy with receptor tyrosine kinases. *Mol Cell Biol*. 2005;25:4924–4933.

13.   Carreno M, Fuller L, Zucker K, Yang W-C, Burke G, Nery J, … Miller J. Cross-species reactivity of the anti-idiotype anti-OKT3 cascade between mice and humans. *Human Immunology*. 1992; 33(4), 249–258.

14.   Geppert TD, Lipsky PE. Activation of T lymphocytes by immobilized monoclonal antibodies to CD3. Regulatory influences of monoclonal antibodies to additional T cell surface determinants. *J Clin Invest*. 1988;81(5):1497-1505.

15.   Chatenoud L, Baudrihaye MF, Kreis H, Goldstein G, Schindler J, Bach JF. Human in vivo antigenic modulation induced by the anti-T cell OKT3 monoclonal antibody. *Eur J Immunol*. 1982 Nov;12(11):979-82.

16.   Henell KR, Bakke A, Kenny TA, Kimball JA, Barry JM, Norman DJ. Degree of modulation of cell-surface CD3 by anti-lymphocyte therapies. *Transplant Proc*. 1991 Feb;23(1 Pt 2):1070-1.

17.   Caillat-Zucman S, Blumenfeld N, Legendre C, Noel LH, Bach JF, Kreis H, Chatenoud L. The OKT3 immunosuppressive effect. In situ antigenic modulation of human graft-infiltrating T cells. *Transplantation*. 1990 Jan;49(1):156-60.

18. Holter W, Majdic O, Stockinger H, Knapp W. Analysis of T cell activation with a non-mitogenic anti CD3 antibody and the phorbol ester TPA. *Clin Exp Immunol*. 1985;62(3):600-606.

19. Acuto O & Michel F. CD28-mediated co-stimulation: a quantitative support for TCR signalling. *Nature Reviews Immunology*. 2003; 3(12), 939–951.

20. Chen L, Flies DB. Molecular mechanisms of T cell co-stimulation and co-inhibition. *Nat Rev Immunol*. 2013;13(4):227-242.

21. Linsley PS, Greene JL, Brady W, Bajorath J, Ledbetter JA, & Peach R. Human B7-1 (CD80) and B7-2 (CD86) bind with similar avidities but distinct kinetics to CD28 and CTLA-4 receptors. *Immunity*, 1994; 1(9), 793–801.

22. Michel F, Attal-Bonnefoy G, Mangino G, Mise-Omata S & Acuto O. CD28 as a Molecular Amplifier Extending TCR Ligation and Signaling Capabilities. *Immunity*. 2001; 15(6), 935–945.

23. Acuto O, & Cantrell D. T Cell Activation and the Cytoskeleton. *Annual Review of Immunology.* 2000; 18(1), 165–184.

24. Shivanthi P. Manickasingham, Stephen M. Anderton, Christoph Burkhart, David C. Wraith. Qualitative and Quantitative Effects of CD28/B7-Mediated Costimulation on Naive T Cells In Vitro. *The Journal of Immunology*. 1998; 161 (8) 3827-3835

25. Schwartz RH. T CELL ANERGY. *Annual Review of Immunology*. 2003; 21(1), 305–334.

26. Swain SL. T cell subsets and the recognition of MHC class. *Immunol Rev*. 1983;74:129-42

27. Cammarota G, Scheirle A, Takacs B, Doran DM, Knorr R, Bannwarth W, … Sinigaglia F. Identification of a CD4 binding site on the β2 domain of HLA-DR molecules. *Nature*. 1992; 356(6372), 799–801.

28. Salter, R., Norment, A., Chen, B. et al. Polymorphism in the α3 domain of HLA-A molecules affects binding to CD8. *Nature.* 1989; 338, 345–347.

29. Isakov N. Immunoreceptor tyrosine-based activation motif (ITAM), a unique module linking antigen and Fc receptors to their signaling cascades. *Journal of Leukocyte Biology*. 1997; 61(1), 6–16.

30. Wang H, Kadlecek TA, Au-Yeung BB, et al. ZAP-70: an essential kinase in T-cell signaling. *Cold Spring Harb Perspect Biol*. 2010;2(5):a002279.

31. Porciello N, & Tuosto L. CD28 costimulatory signals in T lymphocyte activation: Emerging functions beyond a qualitative and quantitative support to TCR signalling. *Cytokine & Growth Factor Reviews*. 2016; 28, 11–19.

32. Bunnell SC, Kapoor V, Trible RP, Zhang W, Samelson LE. Dynamic actin polymerization drives T cell receptor-induced spreading: a role for the signal transduction adaptor LAT. *Immunity*. 2001 Mar;14(3):315-29.

33. Eferl R, & Wagner EF. AP-1: a double-edged sword in tumorigenesis. *Nature Reviews Cancer*. 2003; 3(11), 859–868.

34. Way KJ, Chou E, King GL. Identification of PKC-isoform-specific biological actions using pharmacological approaches. *Trends Pharmacol Sci*. 2000;21(5):181-187.

35. Park CY, Hoover PJ, Mullins FM, Bachhawat P, Covington ED, Raunser S, Walz T, Garcia KC, Dolmetsch RE, Lewis RS. STIM1 clusters and activates CRAC channels via direct binding of a cytosolic domain to Orai1. *Cell*. 2009 Mar 6;136(5):876-90.

36. Ikura M. Calcium binding and conformational response in E–F hand proteins. *Trends Biochem. Sci*. 1996; 21, 14–17

37. Rhoads AR & Friedberg F. Sequence motifs for calmodulin recognition. *The FASEB Journal*. 1997; 11(5), 331–340.

38. Astoul E. PI 3-K and T-cell activation: limitations of T-leukemic cell lines as signaling models. *Trends in Immunology*. 2001; 22(9), 490–496.

39. Dangelmaier C, Manne BK, Liverani E, Jin J, Bray P, Kunapuli SP. PDK1 selectively phosphorylates Thr(308) on Akt and contributes to human platelet functional responses. *Thromb Haemost*. 2014;111(3):508-517.

40. Abdullah L, Hills LB, Winter EB, Huang YH. Diverse Roles of Akt in T cells. *Immunometabolism*. 2021;3(1):e210007

41. Rosenstein Y, Park JK, Hahn WC, Rosen FS, Bierer BE, Burakoff SJ. CD43, a molecule defective in Wiskott-Aldrich syndrome, binds ICAM-1. *Nature*. 1991; 354:233-5.

42. Stöckl J, Majdic O, Kohl P, Pickl WF, Menzel JE, Knapp W. Leukosialin (CD43)-major histocompatibility class I molecule interactions involved in spontaneous T cell conjugate formation. *J Exp Med*. 1996; 184:1769-79.

43. Modak M, Majdic O, Cejka P, et al. Engagement of distinct epitopes on CD43 induces different co-stimulatory pathways in human T cells. *Immunology*. 2016;149(3):280-296.

44. Remold-O'Donnell E, Zimmerman C, Kenney D, Rosen FS. Expression on blood cells of sialophorin, the surface glycoprotein that is defective in Wiskott-Aldrich syndrome. *Blood*. 1987; 70:104-9.

45. Cyster JG, Shotton DM, Williams AF. The dimensions of the T lymphocyte glycoprotein leukosialin and identification of linear protein epitopes that can be modified by glycosylation. *EMBO J*. 1991; 10:893-902.

46. Clark MC, Baum LG. T cells modulate glycans on CD43 and CD45 during development and activation, signal regulation, and survival. *Ann N Y Acad Sci*. 2012; 1253:58-67.

47. Jones AT, Federsppiel B, Ellies LG, Williams MJ, Burgener R, Duronio V, et al. Characterization of the activation-associated isoform of CD43 on murine T lymphocytes. *J Immunol*. 1994; 153:3426-39.

48. Mattioli I. Comparative analysis of T-cell costimulation and CD43 activation reveals novel signaling pathways and target genes. *Blood*. 2004*;* 104(10), 3302–3304.

49. Manjunath N, Correa M, Ardman M & Ardman B. Negative regulation of T-cell adhesion and activation by CD43. *Nature.* 1995; 377(6549), 535–539.

50. Onami TM, Harrington LE, Williams MA, Galvan M, Larsen CP, Pearson TC, et al. Dynamic regulation of T cell immunity by CD43. *J Immunol.* 2002; 168:6022-31.

51. Zumwalde NA, Domae E, Mescher MF, Shimizu Y. ICAM-1-dependent homotypic aggregates regulate CD8 T cell effector function and differentiation during T cell activation. *J Immunol*. 2013;191(7):3681-3693.

52. de Smet W, Walter H, van Hove L. A new CD43 monoclonal antibody induces homotypic aggregation of human leucocytes through a CD11a/CD18-dependent and -independent mechanism. *Immunology*. 1993; 79:46-54.

53. Santamaría M, López-Beltrán A, Toro M, Peña J, Molina IJ. Specific monoclonal antibodies against leukocyte-restricted cell surface molecule CD43 react with nonhematopoietic tumor cells. *Cancer Res*. 1996 Aug 1;56(15):3526-9.

54. Abraham RT, & Weiss A. Jurkat T cells and development of the T-cell receptor signalling paradigm. *Nature Reviews Immunology.* 2004; 4(4), 301–308.

55. Schneider U, Schwenk HU & Bornkamm G. Characterization of EBV-genome negative "null" and "T" cell lines derived from children with acute lymphoblastic leukemia and leukemic transformed non-Hodgkin lymphoma. *International Journal of Cancer*. 1977; 19(5), 621–626.

56. Montano M. Model systems*. Translational Biology in Medicine*. 2014; 9–33.

57. Lee YR, Chen M, Pandolfi PP. The functions and regulation of the PTEN tumour suppressor: new modes and prospects. *Nat Rev Mol Cell Biol*. 2018 Sep;19(9):547-562.

58. Nogales E. Structural Insights into Microtubule Function. *Annual Review of Biochemistry*. 2000; 69(1), 277–302.

59. Gittes F, Mickey B, Nettleton J & Howard J. Flexural rigidity of microtubules and actin filaments measured from thermal fluctuations in shape. *J. Cell Biol*. 120. 1993; 923–934.

60. Nogales E, Wolf SG, Downing KH. Structure of the alpha beta tubulin dimer by electron crystallography. *Nature*. 1998 Jan 8;391(6663):199-203.

61. Mitchison T & Kirschner M. Dynamic instability of microtubule growth. *Nature*. 1984; 312(5991), 237–242.

62. Mitchison T. Localization of an exchangeable GTP binding site at the plus end of microtubules. *Science*. 1993; 261: 1044-1047.

63. Nogales E, Whittaker M, Milligan RA & Downing KH. High-Resolution Model of the Microtubule. *Cell*. 1999; 96(1), 79–88.

64. Redemann S, Baumgart J, Lindow N. et al. C. elegans chromosomes connect to centrosomes by anchoring into the spindle network. *Nat Commun* 8, 15288 (2017).

65. Melters DP, Paliulis LV, Korf IF & Chan SWL. Holocentric chromosomes: convergent evolution, meiotic adaptations, and genomic analysis. *Chromosome Research*. 2012; 20(5), 579–593.

66. Heald R, Khodjakov A. Thirty years of search and capture: The complex simplicity of mitotic spindle assembly. *J Cell Biol*. 2015;211(6):1103-1111.

67. Martín-Cófreces NB, Sánchez-Madrid F. Sailing to and Docking at the Immune Synapse: Role of Tubulin Dynamics and Molecular Motors. *Front Immunol*. 2018;9:1174.

68. Mastrogiovanni M, Juzans M, Alcover A, Di Bartolo V. Coordinating Cytoskeleton and Molecular Traffic in T Cell Migration, Activation, and Effector Functions. *Front Cell Dev Biol*. 2020;8:591348.

69. Bettencourt-Dias M & Glover DM. Centrosome biogenesis and function: centrosomics brings new understanding. *Nature Reviews Molecular Cell Biology*. 2007; 8(6), 451–463.

70. Lillemeier BF, Mörtelmaier MA, Forstner MB, Huppa JB, Groves JT, Davis MM. TCR and Lat are expressed on separate protein islands on T cell membranes and concatenate during activation. *Nat Immunol*. 2010 Jan;11(1):90-6.

71. Bunnell SC, Hong DI, Kardon JR, Yamazaki T, McGlade CJ, Barr VA, Samelson LE. T cell receptor ligation induces the formation of dynamically regulated signaling assemblies. J Cell Biol. 2002 Sep 30;158(7):1263-75.

72. Hashimoto-Tane A, Yokosuka T, Sakata-Sogawa K, Sakuma M, Ishihara C, Tokunaga M, Saito T. Dynein-driven transport of T cell receptor microclusters regulates immune synapse formation and T cell activation. *Immunity*. 2011 Jun 24;34(6):919-31.

73. Crown J, O'Leary M. The taxanes: an update. *Lancet*. 2000 Apr 1;355(9210):1176-8.

74. Miele E, Spinelli GP, Miele E, Tomao F, Tomao S. Albumin-bound formulation of paclitaxel (Abraxane ABI-007) in the treatment of breast cancer. *Int J Nanomedicine*. 2009; 4:99-105.

75. Amos LA, Löwe J. How Taxol stabilises microtubule structure. *Chem Biol*. 1999 Mar;6(3):R65-9.

76. Giannakakou P, Sackett DL, Kang YK, Zhan Z, Buters JT, Fojo T, Poruchynsky MS. Paclitaxel-resistant human ovarian cancer cells have mutant beta-tubulins that exhibit impaired paclitaxel-driven polymerization. *J Biol Chem*. 1997 Jul 4;272(27):17118-25

77. Kingston DGI, Samranayake G & Ivey CA. The Chemistry of Taxol, a Clinically Useful Anticancer Agent. *Journal of Natural Products*. 1990, 53(1), 1–12.

78. Zhu L, Chen L. Progress in research on paclitaxel and tumor immunotherapy. *Cell Mol Biol Lett*. 2019;24:40.

79. Field JJ, Díaz JF, Miller JH. The binding sites of microtubule-stabilizing agents. *Chem Biol*. 2013 Mar 21;20(3):301-15.

80. Díaz JF, Strobe R, Engelborghs Y, Souto AA, Andreu JM. Molecular recognition of taxol by microtubules. Kinetics and thermodynamics of binding of fluorescent taxol derivatives to an exposed site. *J Biol Chem*. 2000 Aug 25;275(34):26265-76.

81. Díaz JF, Barasoain I, Andreu JM. Fast kinetics of Taxol binding to microtubules. Effects of solution variables and microtubule-associated proteins. *J Biol Chem*. 2003 Mar 7;278(10):8407-19.

82. Nyman DW, Campbell KJ, Hersh E, et al. Phase I and pharmacokinetics trial of ABI-007, a novel nanoparticle formulation of paclitaxel in patients with advanced nonhematologic malignancies. *J Clin Oncol*. 2005; 23(31):7785–7793.

83. ten Tije AJ, Verweij J, Loos WJ, et al. Pharmacological effects of formulation vehicles: Implications for cancer chemotherapy. *Clin Pharmacokinet*. 2003; 42:665–685.

84. Desai N, Trieu V, Yao Z. et al. Increased antitumor activity, intratumor paclitaxel concentrations, and endothelial cell transport of Cremophor-free, albumin-bound paclitaxel, ABI-007, compared with Cremophor-based paclitaxel. *Clin Cancer Res*. 2006; 12:1317–1324.

85. Abraxane®: Prescribing information. Schaumburg, IL, Abraxis Oncology, a Division of American Pharmaceutical Partners, Inc; 2005

86. Parton RG, del Pozo MA. Caveolae as plasma membrane sensors, protectors and organizers. *Nat Rev Mol Cell Biol*. 2013 Feb;14(2):98-112.

87. Gradishar WJ, Tjulandin S, Davidson N, Shaw H, Desai N, Bhar P, Hawkins M, O'Shaughnessy J. Phase III trial of nanoparticle albumin-bound paclitaxel compared with polyethylated castor oil-based paclitaxel in women with breast cancer. *J Clin Oncol*. 2005 Nov 1;23(31):7794-803.

88. Elsadek B, Kratz F. Impact of albumin on drug delivery--new applications on the horizon. *J Control Release*. 2012 Jan 10;157(1):4-28.

89. Zhang L, Marrano P, Kumar S, Leadley M, Elias E, Thorner P, Baruchel S. Nab-paclitaxel is an active drug in preclinical model of pediatric solid tumors. *Clin Cancer Res*. 2013 Nov 1;19(21):5972-83.

90. Jennifer B, Berg V, Modak M, Puck A, Seyerl-Jiresch M, Künig S, Zlabinger GJ, Steinberger P, Chou J, Geha RS, Öhler L, Yachie A, Choe H, Kraller M, Stockinger H, Stöckl J. Transferrin receptor 1 is a cellular receptor for human heme-albumin. *Commun Biol*. 2020 Oct 27;3(1):621.

91. Arezes J, Costa M, Vieira I, Dias V, Kong XL, Fernandes R, Vos M, Carlsson A, Rikers Y, Porto G, Rangel M, Hider RC, Pinto JP. Non-transferrin-bound iron (NTBI) uptake by T lymphocytes: evidence for the selective acquisition of oligomeric ferric citrate species. *PLoS One*. 2013 Nov 21;8(11):e79870.

92. Jhurry ND, Chakrabarti M, McCormick SP, Holmes-Hampton GP, Lindahl PA. Biophysical investigation of the ironome of human jurkat cells and mitochondria. *Biochemistry*. 2012 Jul 3;51(26):5276-84.

93. Gkouvatsos K, Papanikolaou G, Pantopoulos K. Regulation of iron transport and the role of transferrin. *Biochim Biophys Acta*. 2012 Mar;1820(3):188-202.

94. Wang Y, Yu L, Ding J, Chen Y. Iron Metabolism in Cancer. *International Journal of Molecular Sciences*. 2019; 20(1):95.

95. Berg V. Investigating immunomodulatory properties of the transferrin receptor (CD71) in human T cells. 2015

96. Espósito BP, Epsztejn S, Breuer W, Cabantchik ZI. A review of fluorescence methods for assessing labile iron in cells and biological fluids. *Anal Biochem*. 2002 May 1;304(1):1-18.

97. Al-Qenaei A, Yiakouvaki A, Reelfs O, Santambrogio P, Levi S, Hall ND, Tyrrell RM, Pourzand C. Role of intracellular labile iron, ferritin, and antioxidant defence in resistance of chronically adapted Jurkat T cells to hydrogen peroxide. *Free Radic Biol Med*. 2014 Mar;68(100):87-100.

98. Cabantchik ZI. Labile iron in cells and body fluids: physiology, pathology, and pharmacology. *Front Pharmacol*. 2014 Mar 13;5:45.

99. Muir RK, Zhao N, Wei J, Wang YH, Moroz A, Huang Y, Chen YC, Sriram R, Kurhanewicz J, Ruggero D, Renslo AR, Evans MJ. Measuring Dynamic Changes in the Labile Iron Pool in Vivo with a Reactivity-Based Probe for Positron Emission Tomography. *ACS Cent Sci*. 2019 Apr 24;5(4):727-736.

100. Cairo G, Pietrangelo A. Iron regulatory proteins in pathobiology. *Biochem J*. 2000 Dec 1;352 Pt 2(Pt 2):241-50.

101. Muckenthaler M, Gray NK, Hentze MW. IRP-1 binding to ferritin mRNA prevents the recruitment of the small ribosomal subunit by the cap-binding complex eIF4F. *Mol Cell*. 1998 Sep;2(3):383-8.

102. Pinto JP, Arezes J, Dias V, Oliveira S, Vieira I, Costa M, Vos M, Carlsson A, Rikers Y, Rangel M, Porto G. Physiological implications of NTBI uptake by T lymphocytes. *Front Pharmacol*. 2014 Feb 26;5:24.

103. Yarosz EL, Ye C, Kumar A, Black C, Choi EK, Seo YA, Chang CH. Cutting Edge: Activation-Induced Iron Flux Controls CD4 T Cell Proliferation by Promoting Proper IL-2R Signaling and Mitochondrial Function. *J Immunol*. 2020 Apr 1;204(7):1708-1713.

104. Porto G, De Sousa M. Iron overload and immunity. *World J Gastroenterol*. 2007 Sep 21;13(35):4707-15.

105. Cabantchik ZI, Glickstein H, Milgram P, Breuer W. A fluorescence assay for assessing chelation of intracellular iron in a membrane model system and in mammalian cells. *Anal Biochem*. 1996 Jan 15;233(2):221-7.

106. Debebe Z, Ammosova T, Jerebtsova M, Kurantsin-Mills J, Niu X, Charles S, Richardson DR, Ray PE, Gordeuk VR, Nekhai S. Iron chelators ICL670 and 311 inhibit HIV-1 transcription. *Virology*. 2007 Oct 25;367(2):324-33.

107. Lui GY, Kovacevic Z, Richardson V, Merlot AM, Kalinowski DS, Richardson DR. Targeting cancer by binding iron: Dissecting cellular signaling pathways. *Oncotarget*. 2015 Aug 7;6(22):18748-79.

108. Constable EC, Housecroft CE. The Early Years of 2,2'-Bipyridine-A Ligand in Its Own Lifetime. *Molecules*. 2019 Oct 31;24(21):3951.

109. Petrat F, de Groot H, Sustmann R, Rauen U. The chelatable iron pool in living cells: a methodically defined quantity. *Biol Chem*. 2002 Mar-Apr;383(3-4):489-502.

110. Miles FL, Lynch JE, Sikes RA. Cell-based assays using calcein acetoxymethyl ester show variation in fluorescence with treatment conditions. *J Biol Methods*. 2015;2(3):e29.

111. Lipson BK, Yannuzzi LA. Complications of intravenous fluorescein injections. *Int Ophthalmol Clin*. 1989 Fall;29(3):200-5.

112. Sahoo S, Ur Rehman J, Shah MR, De P, Tecilla P. Cholate Conjugated Polymeric Amphiphiles as Efficient Artificial Ionophores. *ACS Appl Polym Mater*. 2021 Feb 12;3(2):588-593.

113. Epsztejn S, Kakhlon O, Glickstein H, Breuer W, Cabantchik I. Fluorescence analysis of the labile iron pool of mammalian cells. *Anal Biochem*. 1997 May 15;248(1):31-40.

114. Prus E, Fibach E. Flow cytometry measurement of the labile iron pool in human hematopoietic cells. *Cytometry A*. 2008 Jan;73(1):22-7.

115. De Domenico I, Vaughn MB, Li L, Bagley D, Musci G, Ward DM, Kaplan J. Ferroportin-mediated mobilization of ferritin iron precedes ferritin degradation by the proteasome. *EMBO J*. 2006 Nov 15;25(22):5396-404.

116. Tenopoulou M, Kurz T, Doulias PT, Galaris D, Brunk UT. Does the calcein-AM method assay the total cellular 'labile iron pool' or only a fraction of it? *Biochem J*. 2007 Apr 15;403(2):261-6.

117. Mimori-Kiyosue Y, Grigoriev I, Sasaki H, Matsui C, Akhmanova A, Tsukita S, Vorobjev I. Mammalian CLASPs are required for mitotic spindle organization and kinetochore alignment. *Genes Cells*. 2006 Aug;11(8):845-57.

118. Chutvanichkul B, Vattanaviboon P, Mas-Oodi S, U-Pratya Y, Wanachiwanawin W. Labile iron pool as a parameter to monitor iron overload and oxidative stress status in β-thalassemic erythrocytes. *Cytometry B Clin Cytom*. 2018 Jul;94(4):631-636.

119. Hou JT, Zhang M, Liu Y, Ma X, Duan R, Cao X, Yuan F, Liao Y, Wang S, Ren WX. Fluorescent detectors for hydroxyl radical and their applications in bioimaging: A review. *Coordination Chemistry Reviews*. 2020; 421, 213457

120. Pui CH, Relling MV, Downing JR. Acute lymphoblastic leukemia. *N Engl J Med*. 2004 Apr 8;350(15):1535-48.

121. Geltink RIK, Kyle RL, Pearce EL. Unraveling the Complex Interplay Between T Cell Metabolism and Function. *Annu Rev Immunol*. 2018 Apr 26;36:461-488.

122. Cronin SJF, Woolf CJ, Weiss G, Penninger JM. The Role of Iron Regulation in Immunometabolism and Immune-Related Disease. *Front Mol Biosci*. 2019 Nov 22;6:116.

123. Chaudhry R, Khaddour K. Biochemistry, DNA Replication. *StatPearls Publishing*. 2020 [Updated 2021 May 9].

124. Rowinsky EK, Donehower RC. Paclitaxel (taxol). *N Engl J Med*. 1995 Apr 13;332(15):1004-14.

125. Waclavicek M, Majdic O, Stulnig T, Berger M, Sunder-Plassmann R, Zlabinger GJ, Baumruker T, Stöckl J, Ebner C, Knapp W, Pickl WF. CD99 engagement on human peripheral blood T cells results in TCR/CD3-dependent cellular activation and allows for Th1-restricted cytokine production. *J Immunol*. 1998 Nov 1;161(9):4671-

126. Weigelin B, den Boer AT, Wagena E, Broen K, Dolstra H, de Boer RJ, Figdor CG, Textor J, Friedl P. Cytotoxic T cells are able to efficiently eliminate cancer cells by additive cytotoxicity. *Nat Commun*. 2021 Sep 1;12(1):5217.

8. Supplementary Material

Time in medium	MFI prim. TC, CA	MFI prim. TC, CA+311	ΔMFIs
4h	165,4	189	23,6
24h	91,1	106,7	15,6
48h	38,1	47,4	9,3

Time in medium	MFI prim. TC, CA	MFI prim. TC, CA+BIP	ΔMFIs
4h	165,4	171,7	6,3
24h	91,1	100,9	9,8
48h	38,1	47,4	9,3

Time in medium	MFI prim. TC, CA	MFI prim. TC, CA+311+BIP	ΔMFIs
4h	165,4	154,7	-10,7
24h	91,1	86,2	-4,9
48h	38,1	51,5	13,4

Time in medium	MFI Jurkat TC, CA	MFI Jurkat TC, CA+311	ΔMFIs
4h	238	224,2	-13,8
24h	195,9	215,7	19,8
48h	213,8	373,7	159,9

Time in medium	MFI Jurkat TC, CA	MFI Jurkat TC, CA+BIP	ΔMFIs
4h	238	202,8	-35,2
24h	195,9	171,2	-24,7
48h	213,8	326,9	113,1

Time in medium	MFI Jurkat TC, CA	MFI Jurkat TC, CA+311+BIP	ΔMFIs
4h	238	192,8	-45,2
24h	195,9	218,5	22,6
48h	213,8	339,5	125,7

Supplementary Table 4. MFIs and ΔMFIs of non-activated primary and Jurkat T cells treated with calcein (CA) only or with CA+311 and/or BIP

MFIs of cells cultured for 4h, 24h or 48h in RPMI medium without activating stimuli represent the arithmetic mean of three experiments. ΔMFI values were calculated by subtracting the MFI of cells not treated with chelators from the MFI of cells exposed to them.

Activation time	MFI prim. TC, CA	MFI prim. TC, CA+311	ΔMFIs
4h	135,2	124,5	-10,7
24h	96,7	129,5	32,8
48h	65,2	98,3	33,1

Activation time	MFI prim. TC, CA	MFI prim. TC, CA+BIP	ΔMFIs
4h	135,2	155	19,8
24h	96,7	114,7	18
48h	65,2	89,4	24,2

Activation time	MFI prim. TC, CA	MFI prim. TC, CA+311+BIP	ΔMFIs
4h	135,2	154,7	19,5
24h	96,7	131,2	34,5
48h	65,2	99,9	34,7

Activation time	MFI Jurkat TC, CA	MFI Jurkat TC, CA+311	ΔMFIs
4h	207,5	226,1	18,6
24h	127,8	166	38,2
48h	289,8	413,9	124,1

Activation time	MFI Jurkat TC, CA	MFI Jurkat TC, CA+BIP	ΔMFIs
4h	207,5	190,7	16,8
24h	127,8	145,9	18,1
48h	289,8	378,4	88,6

Activation time	MFI Jurkat TC, CA	MFI Jurkat TC, CA+311+BIP	ΔMFIs
4h	207,5	228,4	20,9
24h	127,8	183	55,2
48h	289,8	394,9	105,1

Supplementary Table 5. MFIs and ΔMFIs of CD3 (OKT3)/CD28-activated primary and Jurkat T cells treated with calcein (CA) only or with CA+311 and/or BIP

MFIs of cells incubated for 4h, 24h or 48h with the CD3 mAb OKT3 and a CD28 mAb represent the arithmetic mean of three experiments. ΔMFI values were calculated by subtracting the MFI of cells not treated with chelators from the MFI of cells exposed to them.

Condition	Time exposed to stimulus/medium	ΔMFIs non-activated cells	ΔMFIs CD3 (OKT3)/CD28	Difference between ΔMFIs
Primary TC, CA+311	4h	23,6	-10,7	34,3
	24h	15,6	32,8	17,2
	48h	9,3	33,1	23,8

Primary TC, CA+BIP	4h	6,3	19,8	13,5
	24h	9,8	18	8,2
	48h	9,3	24,2	14,9
Primary TC, CA+311+BIP	4h	-10,7	19,5	30,2
	24h	-4,9	34,5	39,4
	48h	13,4	34,7	21,3
Jurkat TC, CA+311	4h	-13,8	18,6	32,4
	24h	19,8	38,2	18,4
	48h	159,9	124,1	35,8
Jurkat TC, CA+BIP	4h	-35,2	16,8	52
	24h	-24,7	18,1	42,8
	48h	113,1	88,6	24,5
Jurkat TC, CA+311+BIP	4h	-45,2	20,9	66,1
	24h	22,6	55,2	32,6
	48h	125,7	105,1	20,6

Supplementary Table 6. Comparison between ΔMFI values of non-activated and CD3 (OKT3)/CD28 activated T cells

Differences between ΔMFIs of primary and Jurkat T cells, unstimulated or stimulated with CD3 (OKT3) and CD28 specific mAbs for 4h, 24h or 48h. They were calculated by subtracting the values of unstimulated cells from the ones of stimulated cells. This was done for ΔMFIs obtained by comparing MFIs of cells administered with 311, BIP or the combination of both chelators to untreated cells.

Activation time	MFI prim. TC, CA	MFI prim. TC, CA+311	ΔMFIs
4h	121,9	146,7	24,8
24h	89,3	114,8	25,5
48h	41,2	54,6	13,4

Activation time	MFI prim. TC, CA	MFI prim. TC, CA+BIP	ΔMFIs
4h	121,9	156,3	34,4

	24h	89,3	101,6	12,3
	48h	41,2	45,5	4,3

Activation time	MFI prim. TC, CA	MFI prim. TC, CA+311+BIP	∆MFIs
4h	121,9	176	54,1
24h	89,3	112,3	23
48h	41,2	55,5	14,3

Supplementary Table 7. MFIs and ∆MFIs of CD3 (OKT3)-activated primary T cells treated with calcein (CA) only or with CA+311 and/or BIP

The table depicts the arithmetic means of the calcein MFIs of three experiments in cells stimulated with the CD3 mAb OKT3 for 4h, 24h or 48h. ∆MFI values were calculated by subtracting the MFI of cells not exposed to chelators from the one of cells administered with them.

Condition	Time exposed to stimulus/medium	∆MFIs non-activated cells	∆MFIs CD3 (OKT3)	Difference between ∆MFIs
Primary TC, CA+311	4h	23,6	24,8	1,2
	24h	15,6	25,5	9,9
	48h	9,3	13,4	4,1
Primary TC, CA+BIP	4h	6,3	34,4	28,1
	24h	9,8	12,3	2,5
	48h	9,3	4,3	-5
Primary TC, CA+311+BIP	4h	-10,7	54,1	64,8
	24h	-4,9	23	27,9
	48h	13,4	14,3	0,9

Supplementary Table 8. Juxtaposition between ∆MFI values of non-activated and CD3 (OKT3) activated T cells

∆MFIs of primary T cells, unstimulated or stimulated for 4h, 24h or 48h with a mAb specific for CD3 (OKT3), were compared. The differences between the ∆MFIs were calculated by subtracting the ones of non-activated cells from the ones of cells stimulated with the mAb. This was done with ∆MFIs derived from subtracting MFIs of untreated cells from the ones of cells administered with 311, BIP or the combination of both chelators.

Activation time	MFI prim. TC, CA	MFI prim. TC, CA+311	∆MFIs
4h	130,2	165	34,8
24h	114,2	148,1	33,9

	48h	37,3	78,5	41,2

Activation time	MFI prim. TC, CA	MFI prim. TC, CA+BIP	ΔMFIs
4h	130,2	150,7	20,5
24h	114,2	115,3	1,1
48h	37,3	57,9	20,6

Activation time	MFI prim. TC, CA	MFI prim. TC, CA+311+BIP	ΔMFIs
4h	130,2	162,7	32,5
24h	114,2	118,9	4,7
48h	37,3	74,5	37,2

Supplementary Table 9. MFIs and ΔMFIs of CD3 (OKT3)/CD43 (10G7)-activated primary T cells treated with calcein (CA) only or with CA+311 and/or BIP

Arithmetic means of the calcein signal MFIs of three independent experiments in cells stimulated with mAb targeting CD3 (OKT3) and CD43 (10G7) for 4h, 24h or 48h, are shown. ΔMFI values were derived by detraction of the MFI of cells not administered with chelators from the one of cells treated with them.

Condition	Time exposed to stimulus/medium	ΔMFIs non-activated cells	ΔMFIs CD3 (OKT3)/10G7	Difference between ΔMFIs
Primary TC, CA+311	4h	23,6	34,8	11,2
	24h	15,6	33,9	18,3
	48h	9,3	41,2	31,9
Primary TC, CA+BIP	4h	6,3	20,5	14,2
	24h	9,8	1,1	8,7
	48h	9,3	20,6	11,3
Primary TC, CA+311+BIP	4h	-10,7	32,5	43,2
	24h	-4,9	4,7	9,6
	48h	13,4	37,2	23,8

Supplementary Table 10. Comparison between ΔMFI values of non-activated and CD3 (OKT3)/CD43 (10G7)-activated primary T cells

The table shows ΔMFI values of primary T cells, non-activated or stimulated for 4h, 24h or 48h with mAbs targeting CD3 (OKT3) and CD43 (10G7). The differences between their ΔMFIs were obtained by detracting the ones of non-activated cells from the ones of mAb-stimulated cells. This was done with ΔMFIs derived from subtracting MFIs of untreated cells from the ones of cells treated with 311, BIP or 311+BIP.

Activation time	MFI prim. TC, CA	MFI prim. TC, CA+311	ΔMFIs
4h	121,5	153,3	31,8
24h	107	113,2	6,1
48h	43,8	50,9	7,1

Activation time	MFI prim. TC, CA	MFI prim. TC, CA+BIP	ΔMFIs
4h	121,5	133,7	12,2
24h	107	101,1	-5,9
48h	43,8	46,1	2,3

Activation time	MFI prim. TC, CA	MFI prim. TC, CA+311+BIP	ΔMFIs
4h	121,5	152	30,5
24h	107	101,5	-5,6
48h	43,8	62,6	18,8

Supplementary Table 11. MFIs and ΔMFIs of CD3 (VIT3)-activated primary T cells treated with calcein (CA) or with CA+311 and/or BIP

The table represents arithmetic means of calcein MFIs of three experiments in cells

stimulated with the CD3 mAb VIT3 for 4h, 24h or 48h. ∆MFI values were calculated by detracting the MFI of cells not exposed to chelators from the one of cells administered with 311, BIP or 311+BIP.

Condition	Time exposed to stimulus/medium	∆MFIs non-activated cells	∆MFIs CD3 (VIT3)	Difference between ∆MFIs
Primary TC, CA+311	4h	23,6	31,8	8,2
	24h	15,6	6,1	-9,5
	48h	9,3	7,1	-2,2
Primary TC, CA+BIP	4h	6,3	12,2	5,9
	24h	9,8	-5,9	-15,7
	48h	9,3	2,3	-7
Primary TC, CA+311+BIP	4h	-10,7	30,5	41,2
	24h	-4,9	-5,6	-0,7
	48h	13,4	18,8	5,4

Supplementary Table 12. Juxtaposition of ∆MFI values of non-activated and CD3 (VIT3) activated T cells

∆MFIs of primary T cells, unstimulated or stimulated for 4h, 24h or 48h with a mAb specific for CD3 (VIT3), were compared. The differences between the ∆MFIs were calculated by subtracting the ones of non-activated cells from the ones of cells stimulated with the mAb. This was done with ∆MFIs derived from subtracting MFIs of untreated cells from the ones of cells administered with 311, BIP or the combination of both chelators.

Time in medium	α-Tub mAb MFI	α-Tub mAb + Abr MFI	α-Tub ∆MFIs	β-Tub mAb MFI	β-Tub mAb + Abr MFI	β -Tub ∆MFIs
4h	22,6	36,1	13,5	12,6	12,5	-0,1
24h	17,3	36	18,7	8,7	11,6	2,9
48h	24,7	33,7	9	7,9	10,5	2,6

Supplementary table 13. MFI and ∆MFI values of resting primary T cells, treated with abraxane or not, and stained with α- or β-tubulin specific mAbs

Depiction of Arithmetic means of tubulin specific mAb MFI values of three experiments in primary T cells resting in RPMI medium for 4h, 24h and 48h. ∆MFI values were obtained by deduction the MFI of cells not exposed to abraxane from the one of cells administered with it.

Time in medium	α-Tub mAb MFI	α-Tub mAb + Abr MFI	α-Tub ΔMFIs	β-Tub mAb MFI	β-Tub mAb + Abr MFI	β -Tub ΔMFIs
4h	203,7	172,3	-31,3	55,1	71,2	16,1
24h	270,8	385,7	114,9	76,2	115,8	39,6
48h	358,5	287	-71,5	152,3	136,3	-16

Supplementary table 14. MFIs and ΔMFIs of resting Jurkat T cells, untreated or treated with abraxane and stained with α- or β-tubulin specific mAbs

Arithmetic means of tubulin binding mAb MFI values of three experiments in Jurkat cells resting in RPMI medium for 4h, 24h and 48h are shown. ΔMFI values were obtained by subtracting the MFI of cells not exposed to abraxane from the one of cells administered with it.

Activation time	α-Tub mAb MFI	α-Tub mAb + Abr MFI	α-Tub ΔMFIs	β-Tub mAb MFI	β-Tub mAb + Abr MFI	β -Tub ΔMFIs
4h	51	73,9	22,9	15,3	19	3,7
24h	73,3	149,4	76,1	22,6	28,1	5,5
48h	63,3	173,3	110	19,6	37	17,3

Supplementary table 15. MFIs and ΔMFIs of CD3 (OKT3)/CD28 stimulated primary T cells, administered with abraxane or not, and stained with α- or β-tubulin targeting mAbs

The table shows arithmetic means of MFI values of tubulin binding mAb of three experiments in primary T cells stimulated by mAbs directed against CD3 (OKT3) and CD28 for 4h, 24h and 48h. ΔMFI values were attained by detracting the MFI of unexposed cells from the MFI of cells exposed to abraxane.

Activation time	α-Tub mAb MFI	α-Tub mAb + Abr MFI	α-Tub ΔMFIs	β-Tub mAb MFI	β-Tub mAb + Abr MFI	β -Tub ΔMFIs
4h	221,3	417	195,7	66,8	89,3	22,5
24h	361	493,5	132,5	66,2	134	67,8
48h	331,5	454,5	123	92,3	116,3	24

Supplementary table 16. MFIs and ΔMFIs of Jurkat T cells stimulated via CD3 (OKT3)/CD28, untreated or treated with abraxane and stained with mAbs specific for α- or β-tubulin

Arithmetic means of MFI values of tubulin binding mAbs of three experiments in Jurkat cells stimulated via CD3 (OKT3) and CD28 for 4h, 24h and 48h are portrayed. ΔMFI values were calculated by subtracting the MFI of cells not exposed to abraxane from the one of cells administered with it.

Activation time	α-Tub mAb MFI	α-Tub mAb + Abr MFI	α-Tub ΔMFIs	β-Tub mAb MFI	β-Tub mAb + Abr MFI	β -Tub ΔMFIs
4h	47,4	81,3	33,9	13,7	30,2	16,5
24h	55,6	95,7	40,1	16,3	19,5	3,2
48h	31,8	52,4	20,6	15,2	18,1	2,9

Supplementary table 17. MFIs and ΔMFIs of CD3 (OKT3) stimulated primary T cells, exposed to abraxane or not, and stained with α- or β-tubulin specific mAbs

Here the arithmetic means of tubulin binding mAb MFI values of three experiments in primary T cells stimulated via CD3 (OKT3) for 4h, 24h and 48h are depicted. ΔMFI values were obtained by deducting the MFI of cells not administered with abraxane from the one of cells administered with the drug.

Activation time	α-Tub mAb MFI	α-Tub mAb + Abr MFI	α-Tub ΔMFIs	β-Tub mAb MFI	β-Tub mAb + Abr MFI	β -Tub ΔMFIs
4h	39	56,4	17,4	14,4	20,7	6,3
24h	98,1	94	-4,1	26,5	32,1	5,6
48h	65	98,7	33,6	26,4	30,1	3,7

Supplementary table 18. MFIs and ΔMFIs of primary T cells stimulated via CD3 (OKT3)/CD43 (10G7), untreated or treated with abraxane and stained with α- or β-tubulin binding mAbs

Arithmetic means of tubulin specific mAb MFI values gathered from three experiments in primary T cells stimulated with mAbs targeting CD3 (OKT3) and CD43 (10G7) for 4h, 24h and 48h are presented. ΔMFI values were obtained by subtracting the MFI of cells not exposed to abraxane from the one of cells administered with it.

Activation time	α-Tub mAb MFI	α-Tub mAb + Abr MFI	α-Tub ΔMFIs	β-Tub mAb MFI	β-Tub mAb + Abr MFI	β -Tub ΔMFIs
4h	44,5	60,8	16,3	10,9	16,5	5,6
24h	58,1	88,1	30	15,9	21,4	5,5
48h	31,6	49,8	18,2	11	14,9	3,9

Supplementary table 19. MFIs and ΔMFIs of CD3 (VIT3) stimulated primary T cells, exposed to abraxane or not and stained with α- or β-tubulin specific mAbs

Representation of arithmetic means of MFI values of tubulin targeting mAb of three experiments in Jurkat cells stimulated via CD3 (VIT3) for 4h, 24h and 48h. ΔMFI values were obtained by subtracting the MFI of cells not treated with abraxane from the one of cells exposed to it.

Time exposed to stimulus/ medium	α-Tub ΔMFIs resting cells	α-Tub ΔMFIs CD3 (OKT3)/ CD28 stimulation	Difference between ΔMFIs α-Tub	β-Tub ΔMFIs resting cells	β-Tub ΔMFIs CD3 (OKT3)/ CD28 stimulation	Difference between ΔMFIs β -Tub
4h	13,5	22,9	9,4	-0,1	3,7	3,8
24h	18,7	76,1	57,4	2,9	5,5	2,6
48h	9	110	101	2,6	17,3	14,7

Supplementary table 20. Comparison between ΔMFIs of resting and CD3 (OKT3)/CD28 stimulated primary T cells stained with α- or β-tubulin specific mAbs

ΔMFI values obtained by subtracting the arithmetic mean (of 3 experiments) of MFIs of α- or β-tubulin stained primary T cells not treated with abraxane from the ones of drug treated cells, are shown. Differences between ΔMFI values of CD3 (OKT3)/CD28 stimulated and resting cells were attained by detracting the latter one from the first.

Time exposed to stimulus/ medium	α-Tub ΔMFIs resting cells	α-Tub ΔMFIs CD3 (OKT3)/ CD28 stimulation	Difference between ΔMFIs α-Tub	β-Tub ΔMFIs resting cells	β-Tub ΔMFIs CD3 (OKT3)/ CD28 stimulation	Difference between ΔMFIs β -Tub
4h	-31,3	195,7	227	16,1	22,5	6,4
24h	114,9	132,5	17,6	39,6	67,8	28,2
48h	-71,5	123	194,5	-16	24	40

Supplementary table 21. Comparison between ΔMFIs of resting and CD3 (OKT3)/CD28 stimulated Jurkat T cells stained with α- or β-tubulin specific mAbs

Depiction of ΔMFI values calculated by subtracting the arithmetic mean (of 3 experiments) of MFIs of α- or β-tubulin stained Jurkat cells not treated with abraxane from the ones of drug treated cells. The difference between the ΔMFI values of CD3 (OKT3)/CD28 stimulated and resting cells was obtained by detracting the latter one from the first.

Time exposed to stimulus/ medium	α-Tub ΔMFIs resting cells	α-Tub ΔMFIs CD3 (OKT3) stimulation	Difference between ΔMFIs α-Tub	β-Tub ΔMFIs resting cells	β-Tub ΔMFIs CD3 (OKT3) stimulation	Difference between ΔMFIs β -Tub
4h	13,5	33,9	20,4	-0,1	16,5	16,6
24h	18,7	40,1	21,4	2,9	3,2	0,3
48h	9	20,6	11,6	2,6	2,9	0,3

Supplementary table 22. Comparison between ΔMFIs of resting and CD3 (OKT3) stimulated primary T cells stained with α- or β-tubulin specific mAbs

Representation of ΔMFI values calculated by subtracting the arithmetic mean (of 3 experiments) of MFIs of α- or β-tubulin stained primary T cells not treated with abraxane from the ones of cells exposed to the drug. The difference between ΔMFI values of CD3 (OKT3) stimulated and resting cells was calculated by deducting the latter one from the first.

| Time exposed to stimulus/ medium	α-Tub ΔMFIs resting cells	α-Tub ΔMFIs CD3 (OKT3)/ CD43 (10G7) stimulation	Difference between ΔMFIs α-Tub	β-Tub ΔMFIs resting cells	β-Tub ΔMFIs CD3 (OKT3)/ CD43 (10G7) stimulation	Difference between ΔMFIs β -Tub
4h	13,5	17,4	3,9	-0,1	6,3	6,4
24h	18,7	-4,1	-22,8	2,9	5,6	2,7
48h	9	33,6	24,6	2,6	3,7	1,1

Supplementary table 23. Comparison between ΔMFIs of resting and CD3 (OKT3)/CD43 (10G7) primary T cells stained with α- or β-tubulin specific mAbs

ΔMFI values were calculated by detracting the arithmetic mean (of 3 experiments) of MFIs of α- or β-tubulin stained primary T cells not treated with abraxane from the ones of drug treated cells. Disparities between ΔMFI values of CD3 (OKT3)/CD43 (10G7) stimulated and resting cells were obtained by subtraction of the latter one from the first.

Time exposed to stimulus/ medium	α-Tub ΔMFIs resting cells	α-Tub ΔMFIs CD3 (VIT3) stimulation	Difference between ΔMFIs α-Tub	β-Tub ΔMFIs resting cells	β-Tub ΔMFIs CD3 (VIT3) stimulation	Difference between ΔMFIs β -Tub
4h	13,5	16,3	2,8	-0,1	5,6	5,7
24h	18,7	30	11,3	2,9	5,5	2,6
48h	9	18,2	9,2	2,6	3,9	1,3

Supplementary table 24. Comparison between ΔMFIs of resting and CD3 (VIT3) primary T cells stained with α- or β-tubulin specific mAbs

ΔMFI values calculated by subtracting the arithmetic mean (of 3 experiments) of MFIs of α- or β-tubulin stained primary T cells not treated with abraxane from the ones of drug treated cells, are depicted. The difference between the ΔMFIs of CD3 (VIT3) stimulated and resting cells was obtained by deducting the latter one from the first.

4h time p...

24h time p...

48h time p...
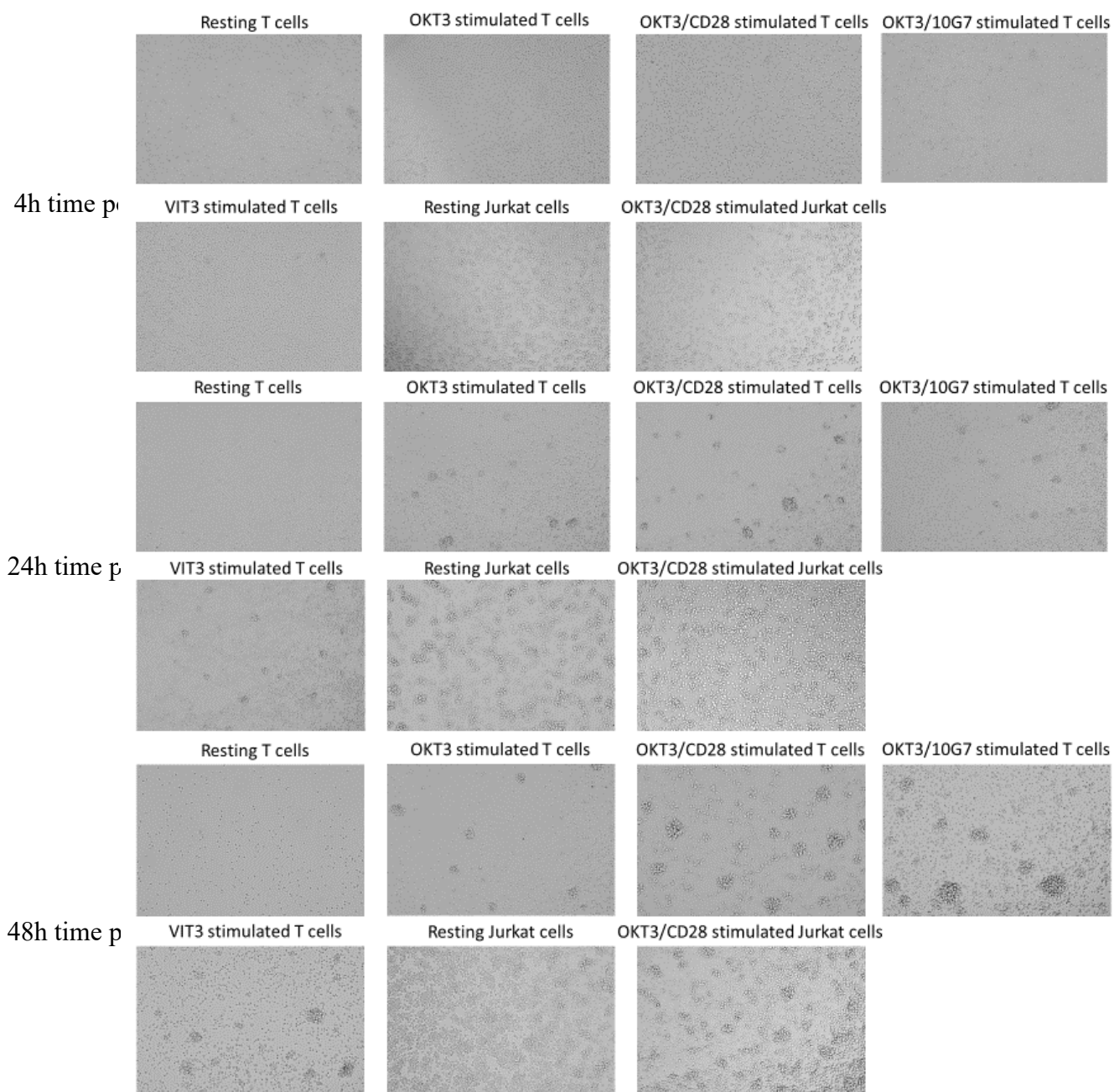
Supplementary Figure 1. Morphology of peripheral blood and Jurkat T cells

Jurkat and primary T cells exposed to RPMI medium alone (resting) or to above described stimulating mAbs for 4h, 24h or 48h. Images were taken by an inverted Nikon Diaphot tissue culture microscope at 10x magnification.